GSF-Forschungszentrum für Umwelt und Gesundheit
Institut für Entwicklungsgenetik

The role of MAP-Kinases in anxiety disorders and depression - studies with knockout and knockdown mouse models

Christiane Hitz

Vollständiger Abdruck der von der Fakultät Wissenschaftszentrum Weihenstephan für Ernährung, Landnutzung und Umwelt der Technischen Universität München zur Erlangung des akademischen Grades eines

Doktors der Naturwissenschaften

genehmigten Dissertation.

Vorsitzender:	Univ.-Prof. Dr. Erwin Grill
Prüfer der Dissertation:	1. Univ.-Prof. Dr. Wolfgang Wurst 2. Univ.-Prof. Angelika Schnieke, Ph.D. (Univ. of Edinburgh/UK)

Die Dissertation wurde am 06. Juni 2007 bei der Technischen Universität München eingereicht und durch die Fakultät Wissenschaftszentrum Weihenstephan für Ernährung, Landnutzung und Umwelt am 10. September 2007 angenommen.

Danksagung

Ich danke Herrn Prof. Dr. Wolfgang Wurst für die Möglichkeit, meine Promotionsarbeit an seinem Institut durchzuführen. Sein Interesse an meiner Arbeit, sein Ideenreichtum und seine konstruktive Kritik in zahlreichen Diskussionen haben meine Begeisterung an der Wissenschaft gefördert und wesentlich zu meiner Motivation beigetragen. Herrn Dr. Ralf Kühn danke ich für seine hervorragende Betreuung in allen wissenschaftlichen Fragen während meiner Promotion. Sowohl praktisch wie auch theoretisch konnte ich viel von ihm lernen, wobei vor allem seine kritische, analytische Denkweise und sein fundiertes Wissen mein wissenschaftliches Verständnis und meine Argumentationsfähigkeit geschärft haben. Ebenso dankbar bin ich für die Freiräume in der Gestaltung und Durchführung der Forschungsarbeit, die mir gewährt wurden und die mein selbstständiges Denken und Handeln sowie meine Kreativität gefördert haben.

Mein Dank geht auch an Frau Prof. Dr. Schnieke und Herrn Prof. Dr. Grill für ihre Bereitschaft, meine Dissertation zu beurteilen und die Promotionsprüfung durchzuführen. Weiterhin danke ich Frau Dr. Daniela Vogt Weisenhorn für ihre exzellente Beratung in histologischen und morphologischen Analysen, sowie für ihre tatkräftige Unterstützung bei der Publikation der Expressionsanalyse. Mein ganz besonderer Dank gilt Barbara Di Benedetto für die tolle Zusammenarbeit bei der anstrengenden, aber sehr lohnenswerten Expressionsanalyse. Frau Dr. Sabine Hölter-Koch und ihrem Team danke ich für die unzähligen Verhaltensanalysen mit den Mäusen.

Patricia Steuber-Buchberger, Sabit Delic, Florian Giesert und Magdalena Kallnik danke ich für zahlreiche anregende Diskussionen und ihre Unterstützung im Labor. Patricia Steuber-Buchberger bin ich zusätzlich zu großem Dank verpflichtet für ihr gewissenhaftes und kritisches Korrekturlesen des Manuskripts.

Den technischen Angestellten des Instituts, allen voran Regina Kneuttinger („Da muss noch was gerechnet werden ...“), Adrianne Tasdemir („Hilfe, ich muss perfundieren!“), Conny Schneider, Annerose Kurz-Drexler und Katrin Angermüller („Was, die Schwänze sind schon fertig?!“) danke ich für ihre Unterstützung und Hilfsbereitschaft bei zahlreichen Experimenten im Labor und Tierstall. Ohne die exzellente Arbeit des Injektionsteams um Susi Weidemann und Adrianne Tasdemir wären aus meinen ES-Zellen nie Mäuse geworden - dafür auch ein großes Dankeschön.

Mein besonderer Dank gilt auch allen Tierpflegerinnen, vor allem Claudia, Monika und Julia, ohne deren Engagement und Hilfsbereitschaft diese Arbeit nicht möglich gewesen wäre. Allen Praktikanten, die während meiner Anwesenheit im Labor tätig

waren, danke ich für ihre praktische Hilfe. Ich danke außerdem allen Mitgliedern unseres Instituts für die kollegiale und freundschaftliche Atmosphäre, die den Arbeitsalltag wesentlich erleichtert hat.

Ein ganz dickes Dankeschön geht an Anneli Nau für ihre selbstlose Hilfe bei einigen Grafiken, damit auch die Optik nicht zu kurz kommt. Meiner Familie, meinen Freunden und ganz besonders Matthias Nau danke ich für die liebevolle Unterstützung, den Zuspruch und die Geduld, die sie mir während meines Studiums und meiner Promotion entgegengebracht haben. Ihr habt mir alle sehr geholfen, diesen Weg erfolgreich zu beschreiten.

In der Wissenschaft gleichen wir alle nur den Kindern,
die am Rande des Wissens hier und da einen Kiesel aufheben,
während sich der weite Ozean des Unbekannten
vor unseren Augen erstreckt.
ISAAC NEWTON

Content

1 Abstract

In genetics a variety of tools are available to dissect the function of genes and signaling pathways. In the last years, RNA interference (RNAi)-mediated gene knockdown has developed into a routine method to assess gene function in cultured mammalian cells in a fast and easy manner. This technique can also be used to generate mouse models similar like knockout mice but in a faster and easier way. For this approach, short hairpin (sh)RNA vectors are expressed stably from the genome and mediate gene knockdown in the entire organism. In this study, an advanced strategy for conditional gene knockdown in mice has been established. With the use of the Cre/loxP system RNAi can be activated in a time and tissue dependent manner in the adult mouse brain. By placing conditional RNAi constructs into the defined genomic *Rosa26* locus and by using recombinase mediated cassette exchange (RMCE) instead of laborious homologous recombination, a fast, easy, and reproducible approach to assess gene function in adult mice has been developed. This technique, together with a conditional knockout mouse model, was used to dissect the function of a prominent signaling cascade in depression and anxiety disorders.

The mitogen-activated protein kinases (MAPKs), also called extracellular signal-regulated kinases (ERKs), are a group of serine/threonine terminal protein kinases, which are activated downstream of a variety of transmembrane receptors. Main intracellular components of the MAPK signaling pathway are the RAF, MEK and ERK proteins, which work in a cascade of activator and effector proteins. They regulate many fundamental cellular functions including proliferation, cell survival and differentiation by transducing extracellular signals to cytoplasmic and nuclear effectors. Besides their essential function in learning and memory processes, MAPKs are also supposed to play an important role in depression and anxiety disorders.

A detailed expression analysis of the mRNA of *Braf*, *Mek1*, *Mek2*, and *Mek5* gave some hints for possible interaction and activation processes within these molecules in distinct regions of the adult mouse brain. Furthermore, the conditional inactivation of *Braf* or *Mek1* and *Mek2* in the adult mouse brain with the knockout and knockdown technique, respectively, revealed an essential role for *Braf* in anxiety and emotional behavior.

2 Introduction

2.1 RNA interference

A few years ago, the complete sequencing of the human genome revealed that we carry only 25,000 different genes in our cells (Consortium, 2004). Compared to some lower organisms, e.g. plants and worms, with a similar number of genes, it is amazing that also such a complex organism like the human body does not need more genes as building plan (Consortium, 1998; Initiative, 2000). One reason for this is a elaborated regulation of gene expression. With different mechanisms to regulate gene activity, also complex organisms like mammals can be built up and develop with a small set of genes. Many of these regulatory mechanisms are known, on the chromatin level as well as on the transcriptional and translational level or by posttranslational modifications (Knippers, 2001). One of these mechanisms is RNA interference (RNAi), first known in plants as posttranscriptional gene silencing (PTGS) or co-suppression (Metzlaff et al., 1997). In general, it describes the degradation of an mRNA by a second specific RNA with complementary sequence, naturally used as defense mechanism against infections from RNA viruses (Waterhouse et al., 2001).

2.1.1 RNAi - from worms towards a genetic tool for all organisms

Less than one decade ago, Craig Mello and Andrew Fire discovered the mechanism of RNAi in the nematode *C.elegans*, named it, and made it popular all around the scientific world. They were the first to use this new technique in order to silence individual genes in the worm (Fire et al., 1998). In the following years, it could be shown that also in many other organisms this novel genetic tool is applicable. Now, the mechanism behind this newly discovered regulatory system is roughly known (Fig. 1; for review see Dykxhoorn et al., 2003). A double stranded (ds)RNA entering the cell is first recognized by an RNase III-like enzyme called Dicer, which cuts the long RNA strand in shorter pieces. These short dsRNAs have a characteristic structure, i.e. 21-23 nt in length with 2-3 nt symmetric 3' overhangs on both ends, and are called short interfering (si)RNAs. A multiprotein RNA-inducing silencing complex (RISC) incorporates the siRNA, unwinds the double strand, and removes the sense strand of the bound siRNA. The antisense strand directs the loaded RISC to its homologous target mRNA. Once bound to it, RISC induces the endonucleolytic cleavage of the mRNA at a single site within the duplex. The cleaved mRNA is not functional any more and is subsequently degraded by RNases in the exosome.

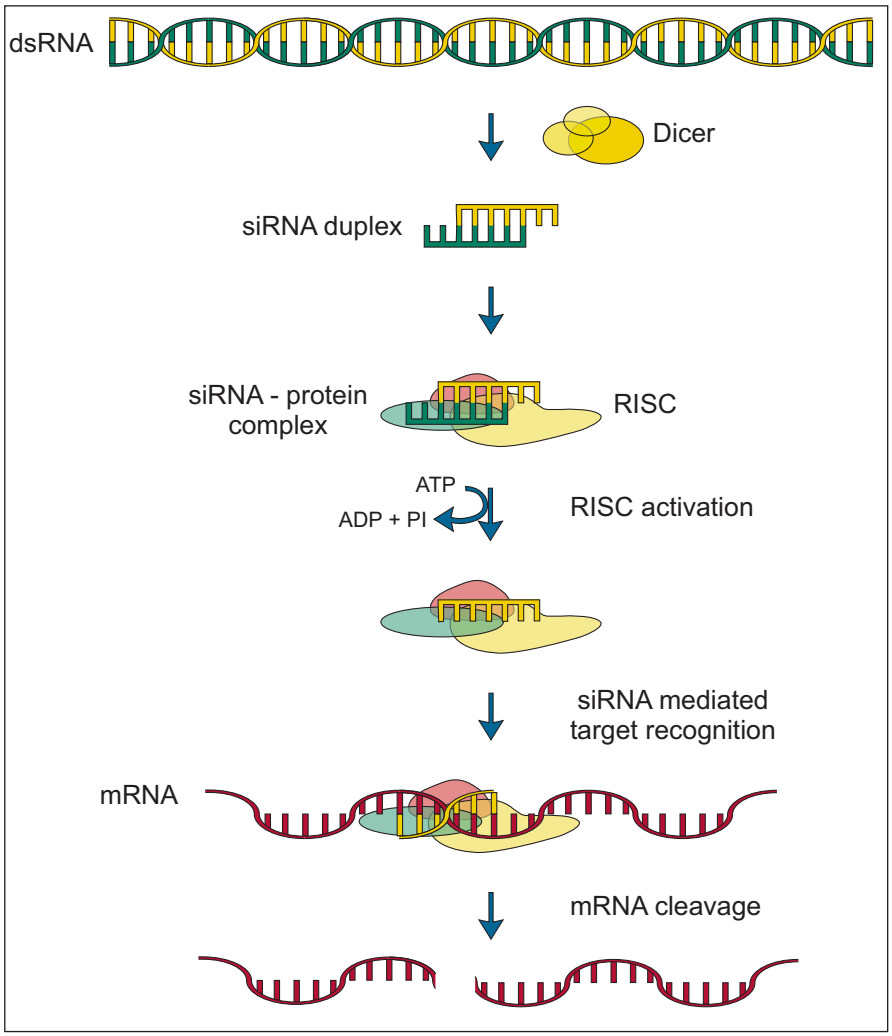

Fig. 1: Illustration of the RNAi mechanism.

Using RNAi as a genetic tool to inhibit the expression of specific genes, long dsRNAs or siRNAs, similar to the product of Dicer, can be used as a trigger (Fig. 2A and C). These molecules can be delivered to the worms via the food or the medium as it has been performed by Fire and Mello in C.elegans (Tabara et al., 1998; Timmons and Fire, 1998). For studies in cell culture, dsRNAs or siRNAs can be transfected or virally transduced into the cells. Since RNA molecules just remain temporarily in the cell, DNA vectors can be used to produce constantly short hairpin (sh)RNAs (Fig. 2B). From these vectors a short RNA sequence consisting of an antisense and sense strand connected by a loop sequence is transcribed. This transcript forms a double stranded secondary structure, similar to a hairpin. As long dsRNAs, also shRNAs are processed by Dicer to produce active siRNAs (Dykxhoorn et al., 2003; Vermeulen et al., 2005).

The event of specific mRNA reduction was termed knockdown, according to knockout describing the complete loss of gene expression. Depending on the

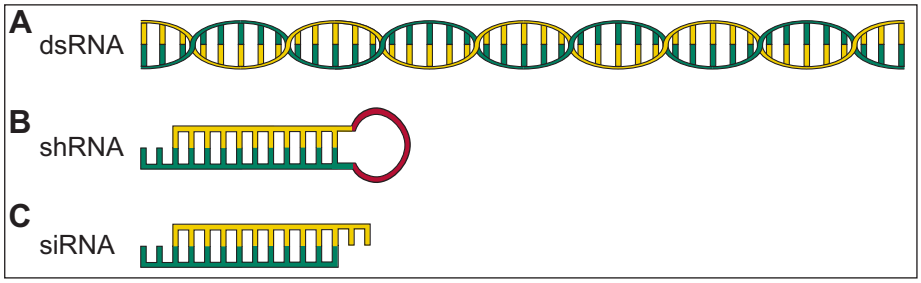

Fig. 2: Different trigger molecules can induce RNAi. Long dsRNAs (**A**) and shRNAs (**B**) produced from a DNA vector are processed by Dicer to get siRNAs, which can also be introduced into the cell directly (**C**).

efficiency of the siRNA used, the level of knockdown can vary. Together with the fast and easy application, this gradually regulation of gene activity is one of the main advantages of RNAi compared to conventional genetic or pharmacologic gene or protein inhibition.

2.1.2 RNAi in mammals

In the beginnings, RNAi was mainly used in lower organisms, but not in mammalian cells or organisms. First, there is no natural mechanism of RNAi in vertebrates. In these higher organisms only a similar, but also quite distinct, mechanism using micro (mi)RNAs to block the translation of the target mRNA occurs (for review see He and Hannon, 2004). So it was doubtful if RNAi functions here in the same way as in worms and flies. Second, dsRNAs longer than 30 nt induce an interferon response in mammalian cells. This antiviral mechanism leads to global mRNA cleavage and shut down of all translational processes. Only with the discovery of the short siRNAs to trigger RNAi, it has been shown that the same mechanism as in lower organisms can also be used in mammalian cells for specific gene inactivation (Elbashir et al., 2001). Since then, RNAi has been applied to many organisms, including the mammalian model organism number one, the mouse.

With these tools fast and easy analyses of the function of specific genes by transient gene silencing in cultured cells and specific tissues of mice upon local administration are possible (for reviews see Lieberman et al., 2003; Fountaine et al., 2005). Also in humans it is intended to use siRNAs as new therapeutic agents (for review see Racz and Hamar, 2006). However, more knowledge of the RNAi mechanism itself and its chances and risks has to be achieved before it can be applied to patients. All these examples show the high potential of this new Nobel prize awarded technique.

2.1.3 Stable RNAi in mice - constitutive and conditional

The application of siRNAs results only in transient knockdown effects. For more detailed studies in animals, for which a long and stable reduction of a specific gene is desired, shRNA vector transgenic mice can be used. The DNA vector, from which the shRNA is transcribed, is integrated into the genome resulting in mice with shRNA expression in each cell of the body. These mice produce an all-over knockdown phenotype, similar to conventional knockout mice (Kunath et al., 2003). As the complete knockout of many genes leads to an embryonic lethal phenotype, also a knockdown can cause developmental defects, so that investigation of the specific gene in adult tissue and processes is not possible. To overcome these early phenotypes and to activate RNAi in specific tissues or in a time dependent manner, conditional shRNA vectors are used.

ShRNA expression can either be regulated by an inducing compound like doxycycline acting on artificial regulatory sequences in the promoter (Gossen et al., 1995) or shRNA production is blocked by a transcriptional stop element, which can be deleted through Cre mediated recombination. Cre is a site specific recombinase naturally occurring in the bacteriophage P1 and catalyzes DNA recombination between a pair of so called loxP sites (Sternberg et al., 1986). A loxP site is a 34 bp sequence with two binding sites for Cre recombination. Upon recombination Cre cuts out the loxP flanked sequence and releases it as a closed circle leaving one loxP site in place. The Cre/loxP system has been widely used in gene targeting and conditional knockout strategies. Also for conditional RNAi various vector designs have been described (Kasim et al., 2004; Tiscornia et al., 2004). The combination of RNAi with the Cre/loxP system is a versatile tool, which can be applied to a huge variety of biological questions. Since there is a large collection of mouse strains that express Cre recombinase in specific cell types, it is possible to activate conditional shRNA vectors at different developmental stages and in selected tissues of mice (Nagy and Mar, 2001).

2.2 Anxiety and mood disorders: disturbed signaling in the brain

Mental disorders represent some of the most common health problems worldwide. One third of the German population suffers from one or several mental diseases and only 36% of the affected persons are under medical treatment (Wittchen and Jacobi, 2001). But medical treatment is not an equivalent of cure or even relief because the pharmacologic compounds available are not effective in every patient and are also not free of side effects. So it is important to obtain more knowledge about

the molecular basis of mental disorders in order to develop novel drugs for better adapted therapies.

2.2.1 Anxiety and depression

Affective mood disorders, including major depression (also known as unipolar disorder) and bipolar disorder (characterized by manic and depressive episodes), and anxiety disorders are the most common diagnoses among psychiatric afflictions. These diseases are strongly influenced by environmental factors, as stress or emotional disturbances, but are also based on genetic predisposition (Hettema et al., 2001; Sklar, 2002). So, it is possible to study the genetic basis of these diseases with appropriate genetic models, e.g. in mice (for review see Cryan and Holmes, 2005). For generalized anxiety it may still be conceivable to give a diagnosis for the mouse, but for a "depressed" mouse it becomes more complicated, because the complete phenotype of mood disorders is quite complex. Regarding this heterogeneity of the disease pattern, it is not only difficult to give the right diagnosis (in man and mouse), but also to find the right treatment and to investigate the biochemistry behind. Thus, analysis and modeling of single behavioral, physiological, or neurochemical aspects - so called endophenotypes - is necessary (Hasler et al., 2004).

Anxiety is a natural emotional reaction to danger and becomes pathological, when the anxious state is persistent and unreasonable as no real danger is present. Clinicians distinguish between different subtypes of anxiety disorders, which are mainly generalized anxiety disorder, panic disorder, phobia (specifically or socially), obsessive-compulsive disorder, and post-traumatic stress disorder (Association, 2000). All these subtypes vary mainly in the nature of the stimulus inducing the anxiety and are therefore easily to distinguish. More heterogeneous are mood disorders, where first major depression and bipolar disorder have to be distinguished. For major depression and the depressive episodes of bipolar disorders several endophenotypes have been described, as e.g. anhedonia, changes in appetite, insomnia, loss of energy, feelings of worthlessness, and thoughts of suicide (Association, 2000). Although anxiety and depression being defined as two distinct disorders, comorbidity between both of them is very high, i.e. patients diagnosed with one of these diseases are very likely to exhibit also symptoms of the other one during their lifetime, and drugs often act on both diseases simultaneously (Williamson et al., 2005). This effect is even more often observed in women than in men. In fact, women are in general more often affected by anxiety and mood disorders than men and respond differently to some medications (Gorman, 2006). This may be an indication for sex specific neural circuits involved in

anxiety and depression. Thus, it is important to distinguish between sexes also in animal models in order to develop well adapted gender specific treatments in addition to the conventional drugs.

2.2.2 Lithium & Co.

Many antidepressant, mood stabilizing, and anxiolytic components are available, but their mode of action is often unknown. One of the first drugs of this type is lithium (Li), which is used for more than 50 years in the treatment of bipolar disorder since it acts as mood stabilizer (Cade, 1949). The use of lithium for manic-depressed patients was not based on any neurochemical knowledge, and also today its exact function is still under analysis. Best investigated direct target of lithium may be glycogen synthase kinase 3 (GSK3, a downstream effector of the Wnt pathway), but also inositol monophosphatase (IMP) and other phosphomonoesterases are known to be directly inhibited by lithium. In the brain, lithium acts indirectly on a variety of transcription factors and phosphoproteins, mediates neuroprotection against excitotoxic neurotransmitters, and enhances synaptic and axonal remodeling (for reviews see Manji et al., 1995; Phiel and Klein, 2001). However, it is unlikely that all these effects contribute to the mood stabilizing effect of lithium and it is the aim of many current studies to figure out the relevant target molecules and pathways.

Besides lithium, other agents are used as mood stabilizers or antidepressants. Valproic acid (VPA) for example mediates neuroprotection and axonal remodeling, similar to lithium, but molecularly it increases the concentration of γ-aminobutyric acid (GABA) in the brain, modulates sodium channels, and induces transcriptional activity by the inhibition of histone deacetylases (HDAC; for review see Gurvich and Klein, 2002). A recently discovered target of VPA are mitogen activated protein kinases (MAPK) often acting downstream of neurotrophins and being activated during long-term treatment with VPA independently of HDAC-related transcriptional activity (Yuan et al., 2001; Hao et al., 2004). Other antidepressant medications increase the serotonin concentration in the brain (selective serotonin reuptake inhibitors, SSRI), inhibit monoamine oxidases, or increase the concentration of other signaling molecules, like dopamine and norepinephrine. All these agents, in general, act as antidepressants, but are not effective in all patients and often cause side effects.

For the treatment of anxiety disorders, anxiolytic drugs are used. Some antidepressant agents act also as anxiolytics, like SSRIs and some other recently predicted therapeutics (Holmes et al., 2003). A huge group of pure anxiolytics are the benzodiazepines (BDZ), which act as GABA agonists but exhibit also sedative side effects

(Atack, 2005). Buspirone is a serotonin 1A agonist with less side effects than BDZ (Davids and Lesch, 1996). Although some target proteins for these molecules are known, the real neurochemical basis of anxiety disorders is still under investigation.

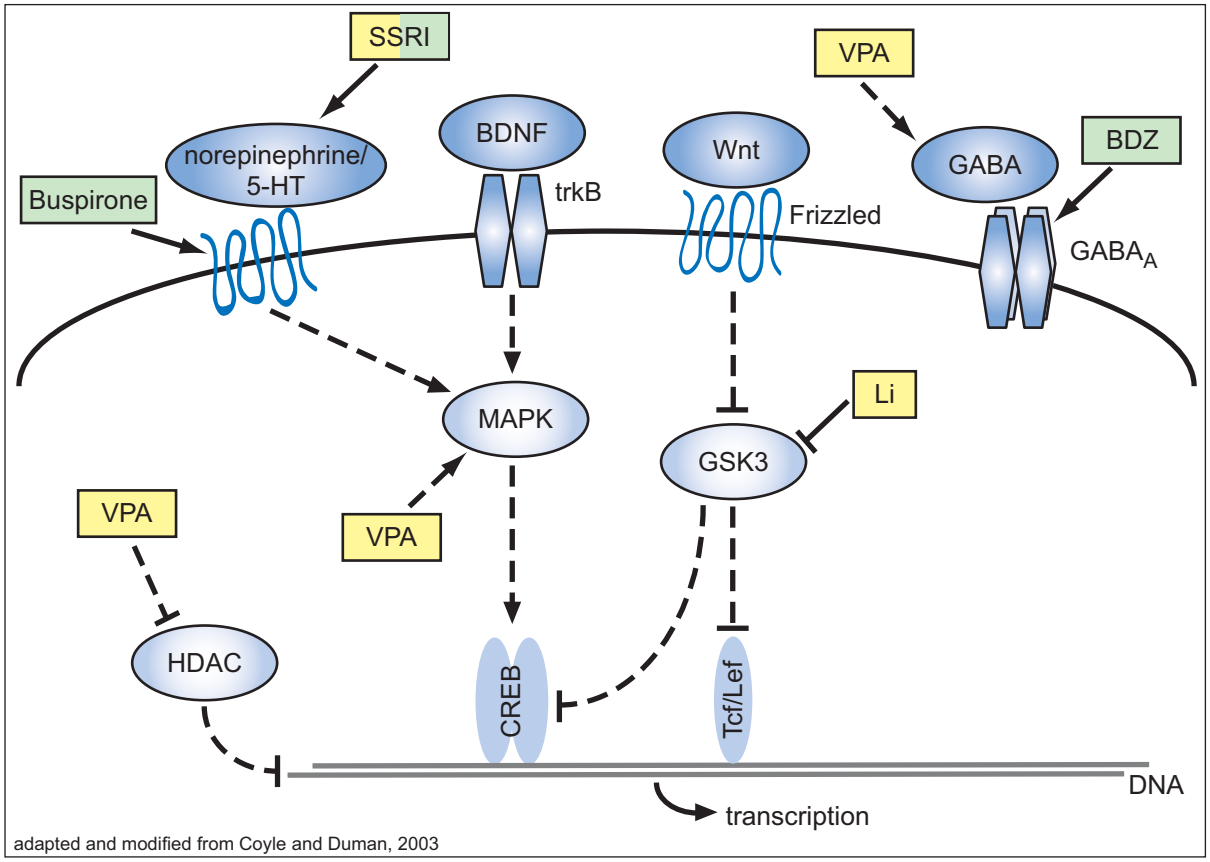

Fig. 3: Examples of some intracellular pathways known to be involved in the mode of action of antidepressant (yellow) and anxiolytic (green) drugs. Dashed lines indicate indirect activation via several molecules in between (known and unknown).

Taken together, for mood disorders as well as for anxiety, a variety of drugs are available. But the actual therapeutic options are not satisfactory, since they can not give relief to all patients and exhibit numerous side effects. However, also the neurochemical mechanisms affected in these diseases are not sufficiently understood. Some of the signaling pathways already known to be involved are shown in Fig. 3. Since various systems, like serotonin, GABA, Wnt, and neurotrophins, seem to be involved, further efforts are necessary to provide deeper insight into these complex diseases.

2.2.3 The MAPK cascade

Mitogen-activated protein kinases (MAPKs), also called extracellular signal-regulated kinases (ERKs), are a group of serine/threonine terminal protein kinases evolutionarily conserved from yeast to human. They are activated by a signaling cascade -

known as the ERK/MAPK signaling pathway - which mediates the transduction of extracellular signals to cytoplasmic and nuclear effectors. ERKs regulate a variety of cellular functions, like cell growth, proliferation, differentiation, and cellular stress responses (Pages et al., 1993; Kyriakis and Avruch, 1996; Weber et al., 1997; Refojo et al., 2005; Werry et al., 2005). Eight different ERK isoforms were described, among which only ERK1, ERK2, ERK3, ERK4, ERK5 and ERK7 were found to be expressed in the adult rodent brain. Among these eight proteins ERK1, ERK2, ERK3 and ERK5 belong to the canonical MAPK signaling pathway (Fig. 4). The activation of these ERKs is mediated by their phosphorylation on tyrosine and threonine residues via the action of MEKs (MAPK/ERK kinases). The atypical MAPKs ERK4 and ERK7 are not activated by MEKs and are therefore not considered within the classical canonical MAPK cascade (Bogoyevitch and Court, 2004). Regarding the MEK proteins, MEK1 and MEK2 were identified as specific activators of ERK1 and ERK2, while MEK5 was described as the specific upstream activator of ERK5 (Zhou et al., 1995). As activators of the MEKs, RAF kinases were identified (Catling et al., 1994; for review see Wellbrock et al., 2004). Among the RAF proteins, BRAF and CRAF are expressed in the adult rodent brain. BRAF expression is mainly restricted to the brain in adult tissue and is described as the main activator of MEK1/2 (Storm et al., 1990; Papin et al., 1996; Morice et al., 1999). For MEK5, however, no interaction with any RAF protein could be shown, indicating a RAF-independent activation of the MEK5→ERK5 cascade (Zhou et al., 1995).

Up to now the activation of the MAPK signaling pathway has been implicated in a variety of processes in the adult brain. Most of the studies analyzing the functions of MAPKs use pharmacological inhibitors, which block the kinase activity of MEK1 and MEK2. Since it has been shown that these inhibitors are not specific for MEK1/2 only, but inhibit also MEK5 mediated ERK activation, it is sometimes difficult to assign one possible function to the right MEK/ERK signaling pathway (Kamakura et al., 1999). Nevertheless, the best-known function of ERK1/2 is in the refinement of synaptic connections based on neural activity, mostly driven by the function of N-methyl-D-aspartate (NMDA) receptors. In this process the activation of ERK1 and ERK2 seems to be essential (for reviews see Constantine-Paton et al., 1990; Shatz, 1990). Moreover, experimental evidence revealed additional roles of ERK1 and ERK2 activation to mediate adaptive responses of mature neurons, like long-term potentiation, as well as memory formation (English and Sweatt, 1997; Atkins et al., 1998; Impey et al., 1998; Impey et al., 1999; Schafe et al., 1999; Arendt et al., 2004). However, recently MAPKs have also been shown to be critically involved in the process of neuroprotection. The

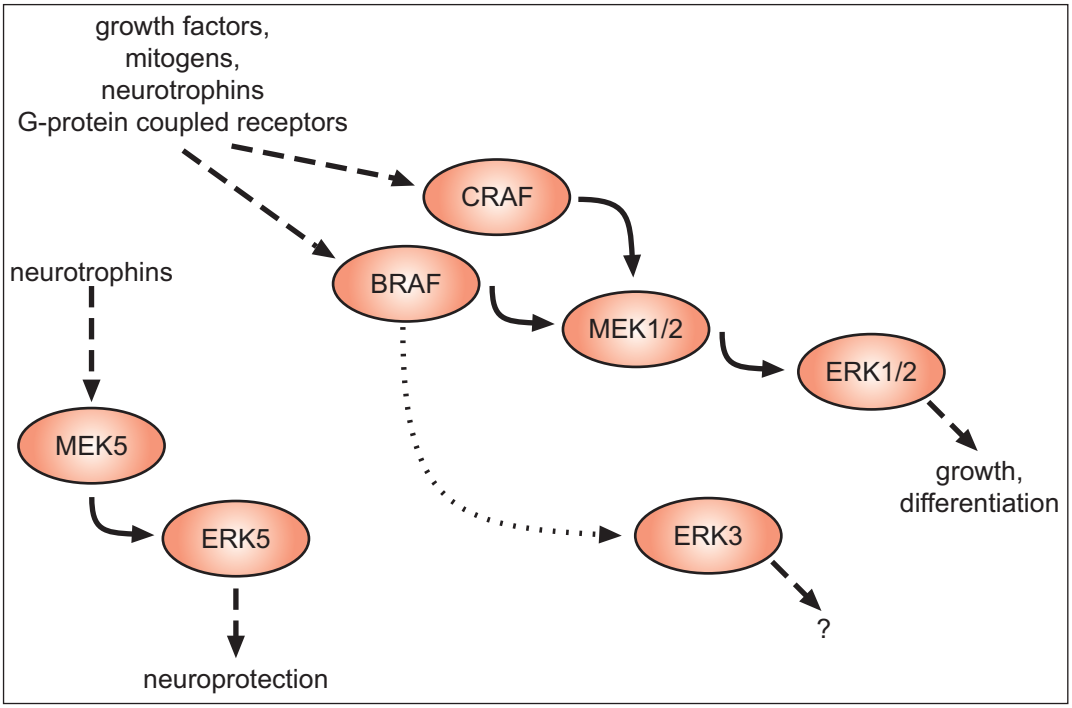

Fig. 4: Schematic representation of the MAPK cascade. Dashed lines indicate indirect activation via several molecules in between, the dotted line indicates a suggested pathway.

activation of ERK5 after cerebral ischemic insult exerts neuroprotective effects for granule cells in the hippocampus (Wang et al., 2005). Furthermore Cavanaugh et al. (2001) reported that the MEK5-dependent activation of ERK5 in primary cortical neurons is mediated by neurotrophins, but not by neuronal activity. In dopaminergic neurons neuroprotective effects upon oxidative stress are not only mediated by ERK5 but also by ERK1/2 signaling (Cavanaugh et al., 2006). This suggests an alternative role for the MEK5→ERK5 and the MEK1/2→ERK1/2 signaling pathway in neuroprotection, additionally to that for ERK1/2 in activity-dependent synaptic plasticity.

Finally, a regulatory function of MAPK signaling for anxiety and depression related behavior has been proposed but not yet tested with genetic models *in vivo* (Coyle and Duman, 2003). Accordingly, it has been shown that the mood stabilizers lithium and VPA activates MAPK signaling especially in the hippocampus to induce neuronal outgrowth and neurogenesis (Yuan et al., 2001; Einat et al., 2003). In line with this, in the hippocampus and prefrontal cortex of brains of human suicide victims, who often suffered from mood disorders in their life, BRAF and activated ERK1/2 protein was reduced (Dwivedi et al., 2006). In contrast to this, Casu et al. (2007) showed that activation of ERK1/2 in the amygdala was decreased after chronic treatment with VPA. All these studies show clearly an involvement of MAPKs in mood disorders, but their exact function is still obscure and is also suggested to vary in different brain regions.

2.3 Objective of this thesis

The present study has two aspects, a technical and a neurobiological one. First, the novel technique of RNA interference should be used to generate knockdown mice. Therefore, applicable tools and methods had to be found and tested to establish a fast and easy tool for the generation of RNAi mice. These mice were supposed to harbor an shRNA construct in a specified locus of their genome. In order to regulate shRNA expression in a time and tissue dependent manner *in vivo*, the construct had to be designed conditionally with the Cre/loxP system. Thus, effective and specific shRNAs had to be found, which are not active before but exhibit a high knockdown efficiency after Cre recombination. Moreover, the system had to be effective with only one copy of the shRNA construct in the genome in ES cells as well as in the adult brain.

For the neurobiological part of this thesis, the newly generated knockdown mouse models together with a conventional knockout model should be used to investigate the role of MAPK signaling in the adult brain in anxiety and mood disorders. As basis for all further analyses, first the expression pattern of different members of the MAPK signaling pathway in the adult murine brain was investigated. Next, a conditional Braf knockout mouse was analyzed histologically and in a battery of behavior tests, which aimed to reveal alterations in depression and anxiety related behavior due to the loss of BRAF in adult forebrain neurons. Additionally, conditional knockdown mice with shRNAs against *Braf* or *Mek1* and *Mek2* were analyzed as far as possible within the given time-frame.

As I succeeded to establish the new technique of RNAi knockdown mice, it is possible to generate genetic mouse models in a fast and easy way. With these models further insights into the role of the MAPK signaling pathway in anxiety and depression can be given.

3 Results

3.1 Expression analysis of MAPKs in the adult mouse brain

To get a more detailed view of the in situ expression of the different members of the MAPK signaling cascade in the adult mouse brain than previously reported in the literature, radioactive in situ hybridizations (ISH) were performed with probes for the mRNA of *Braf*, *Mek1*, *Mek2*, and *Mek5* (Di Benedetto et al., 2007). The aim of this study was also to suggest possible functional interactions among activator and effector proteins in this signaling pathway.

The expression study was performed on adjacent paraffin sections of adult mouse brains, in order to be able to compare the expression of the different genes in different regions of the brain. Since the ISH is rather a qualitative than a quantitative method, signal intensities were compared only among different brain regions with one probe and not among different probes. The spatial distribution of the signals was evaluated on coronal sections and confirmed on sagittal and horizontal sections. A detailed schematic overview of the expression of all the genes analyzed is given at the end of this section in Fig. 9 and Tab. 1.

3.1.1 Cloning of ISH probes

To generate plasmids containing the template for *in vitro* transcription of ISH probes, first cDNA was transcribed from total RNA extracted from adult brains of wildtype C57BL/6J mice (ten weeks of age). By PCR reactions, the probe DNA was amplified with specific primers for each ISH probe. Primers covered the following regions on the cDNA: nt 434-1278 of *Braf* gene (NCBI acc #XM_355754), nt 1303-2151 of *Mek1* gene (NCBI acc #BC051137), nt 1522-1965 of *Mek2* gene (NCBI acc #NM_023138), and nt 487-1291 of *Mek5* gene (NCBI acc #NM_011840). PCR products were purified with agarose gel extraction and cloned into a TOPO TA vector (pCRII). Plasmids containing the cDNA fragments coding for the probes were isolated and the sequence was verified by sequencing the inserted fragment with primers T3 and T7.

3.1.2 Expression of *Braf* in the adult mouse brain

The hybridization signal for *Braf* mRNA (Fig. 5) was absent from the olfactory bulbs, except of a weak signal in the anterior olfactory nucleus. More posterior the distribution of the signal became variegated, with weak-to-moderate labeling in the cortical fields (cerebral and piriform cortices) and a weak hybridization signal in most

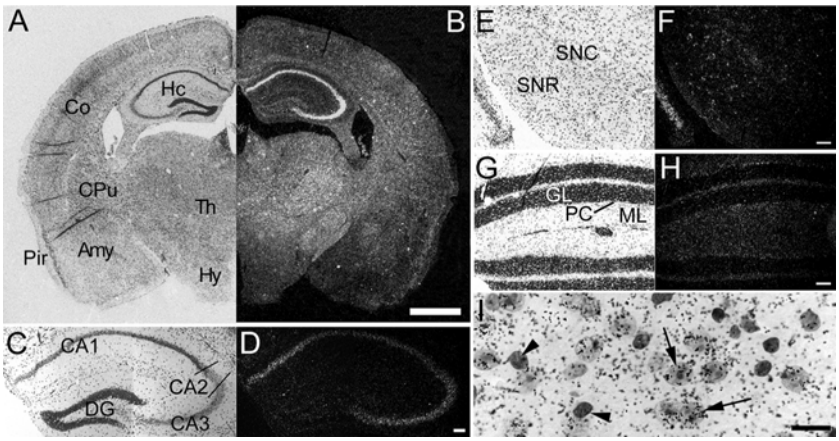

Fig. 5: Coronal sections of adult mouse brain hybridized with the *Braf* ISH probe. Darkfield photomicrographs (**B**, **D**, **F**, **H**) and corresponding brightfield images of Nissl stained sections (**A**, **C**, **E**, **G**) are displayed. B shows the weak but widespread expression of *Braf* mRNA. Magnifications of the hippocampus (C, D), the substantia nigra (E, F), and the cerebellum (G, H) present more details and views from more posterior parts of the brain. In the brightfield image of a high magnification of thalamic cells (I) expression signal is only visible in large neuron-like cells (arrows) and not in smaller, darker Nissl stained glia-like cells (arrowheads). Scale bar = 1 mm in B; 0.1 mm in D, F, H; 0.016 mm in I. For abbreviations see section 8.1.2, p. 144.

regions of the basal ganglia, such as the nucleus accumbens and adjacent regions. However, in the caudate putamen a slightly stronger signal could be seen, especially in the medial parts of this region. In the septum, only the lateral septum showed weak-to-moderate labeling for *Braf*, while the signal was completely absent from other septal nuclei. Hybridization signals were present in all amygdalar nuclei, with a moderate signal in the central nucleus, weak-to-moderate labeling in the lateral nucleus and a weak signal in the basal nucleus. The hippocampus was the region where the signal for *Braf* was most prominent, with strong hybridization reactions in the pyramidal neurons of all the CA (Cornu Ammoni) regions. Most conspicuously the only part devoid of any expression was the dentate gyrus (Fig. 5D). Other subcortical regions that showed low levels of *Braf* mRNA were the medial and lateral habenulae and the thalamus, which showed variable expression in different nuclei. On this anterior-posterior level, the only region without any detectable *Braf* mRNA was the hypothalamus. In contrary, the lateral geniculate nucleus showed a moderate but clearly present signal. In the midbrain the substantia nigra exhibited expression of *Braf*. While the substantia nigra pars compacta was weakly labeled, the substantia nigra pars reticulata showed only a very weak labeling accumulated in some groups of cells (Fig. 5F). Very weak or weak signals were present in the superior and inferior colliculi, in the pretectal nucleus, the pontine nuclei, the raphe nuclei, the ventrotegmental area, and the mammillary bodies. No labeling for *Braf* was observed in the red nucleus, in the periaqueductal gray, and in the oculomotor nucleus. But various nuclei of the brainstem

showed low expression. A weak hybridization signal could be seen in the tegmental nuclei, in the formatio reticularis, in the olivary nuclei, and in the locus coeruleus. Also in the cerebellum *Braf* mRNA was present. In granule cells it was only very weakly and in Purkinje cells it was weakly expressed (Fig. 5H).

On the cellular level, silvergrains indicating the presence of *Braf* mRNA could be seen mostly overlaying neurons which were identified by their size and pale Nissl-staining (arrows in Fig. 5I). However, not every neuron showed expression. The silvergrains seemed to be completely absent from the smaller and darker stained glia cells (arrowhead in Fig. 5I).

3.1.3 Expression of *Mek1* in the adult mouse brain

The expression of *Mek1* mRNA (Fig. 6) in the olfactory bulb showed moderate signals in the anterior olfactory nucleus and in granule cells. Also the mitral cell layer of the bulbs showed the signals, at weak-to-moderate levels (Fig. 6B). The cerebral as well as the piriform cortex expressed *Mek1* mRNA at moderate-to-strong and strong levels, respectively. Also some regions of the basal ganglia showed strong signals for *Mek1* mRNA, as the claustrum and the endopiriform nucleus. All the other parts of the basal ganglia were only weakly to moderately labeled; with exception of the zona incerta, showing only very weak signals, and the pars reticulata of the substantia nigra since this region was completely devoid of any *Mek1* labeling (Fig. 6H). Also the lateral habenula did not show any signals for *Mek1*, while the medial part did at weak levels.

In the hippocampal formation signals were quite prominent, as in the dentate gyrus granule cells were moderately labeled, as well as the CA1 and CA2 regions. The CA3 region showed even a very strong *Mek1* expression. These differences in the intensity of the signals could be detected at a closer view. Fig. 6D shows the very strong labeling in CA3 in contrast to the slightly weaker signals in CA1 and CA2 (that is not readily distinguishable on the highly exposed picture in the overview of Fig. 6B). Also in the amygdala high levels of *Mek1* mRNA were expressed, particularly the lateral and central parts showed strong signals, whereas the basal nuclei showed only moderate labeling (Fig. 6F).

Furthermore, the hypothalamus was moderately labeled with the *Mek1* probe, while the thalamus showed only a weak expression. In more posterior areas *Mek1* mRNA was not so prominent any more. Only the locus coeruleus and the VII cranial nerve showed moderate signals whereas other regions in the posterior parts of the brain expressed *Mek1* only at weak or even very weak levels. Moreover the red and

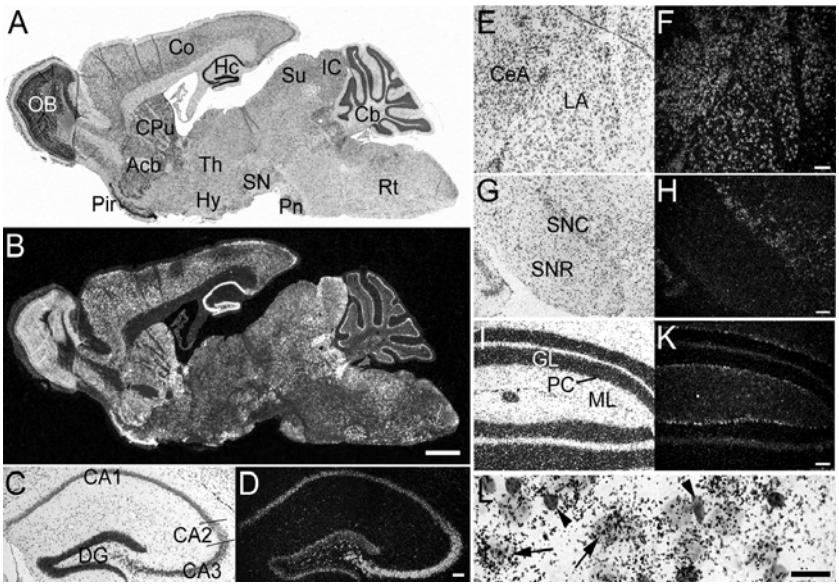

Fig. 6: Sections of adult mouse brain hybridized with the *Mek1* ISH probe. Darkfield photomicrographs (**B**, **D**, **F**, **H**, **K**) and corresponding brightfield images of Nissl stained sections (**A**, **C**, **E**, **G**, **I**) are displayed. A and B show a high exposed complete sagittal section at a glance. Magnifications of the hippocampus (C, D), the amygdala (E, F), the substantia nigra (G, H), and the cerebellum (I, K) from coronal sections present the expression pattern of *Mek1* mRNA in more details and with more graduations (especially in D). In the brightfield image of a high magnification of striatal cells (L) expression signal is visible mostly in large neuron-like cells (arrows) and only weak, but well detectable, in some smaller, darker Nissl stained glia-like cells (arrowheads). Scale bar = 1 mm in B; 0.1 mm in D, F, H, K; 0.016 mm in L. For abbreviations see section 8.1.2, p. 144.

cochlear nuclei and the trapezoid body did not express it at all. In the cerebellum only Purkinje cells showed moderate signals (Fig. 6 K).

Mek1 expression in the brain is not restricted to one specific cell type. Although strong signals for *Mek1* mRNA were visible on almost all neurons, also some glia cells, identified by the smaller size and dark Nissl-staining, showed weak expression (arrowhead in Fig. 6L).

3.1.4 Expression of *Mek2* in the adult mouse brain

In line with previous reports (Brott et al., 1993) showing Northern blot analyses, in which very low levels of *Mek2* mRNA were present in the adult murine brain, the probe for the in situ detection of *Mek2* mRNA showed barely detectable levels of the hybridization signal in sections of adult brains (Fig. 7). The very weak signal was confined to CA2 and CA3 hippocampal regions (Fig. 7B, barely visible). More posterior very weak signals were present in the locus coeruleus, in the pontine reticular nuclei, in the inferior olive, in the formatio reticularis, and in the X and XII cranial nerves. In the cerebellum a weak labeling of Purkinje cells was visible (Fig. 7D).

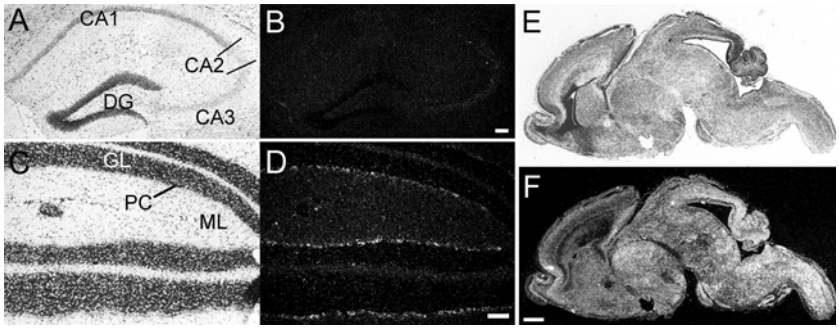

Fig. 7: Sections of adult mouse brain hybridized with the *Mek2* ISH probe. Darkfield photomicrographs (**B**, **D**, **F**) and corresponding brightfield images of Nissl stained coronal sections (**A**, **C**, **E**) are displayed. Since the expression is very weak and restricted only the magnifications of the hippocampus (A, B) and the cerebellum (C, D) visualize these signals. A strong signal in the brain of newborn mice confirms the functionality of the probe (E, F). Scale bar = 1 mm in B; 0.1 mm in D; 0.5 mm in F. For abbreviations see section 8.1.2, p. 144.

Due to the weakness of the signal, it was not possible to get an impression of the cell types expressing *Mek2*. But to confirm the functionality of the probe, I performed an ISH on slices cut from the brain of newborn mice, known to express high levels of *Mek2*, where I could observe a widespread labeling signal (Fig. 7F). Thus, the expression level of *Mek2* mRNA in adult mouse brain is in fact very low.

3.1.5 Expression of *Mek5* in the adult mouse brain

The probe for *Mek5* mRNA (Fig. 8) hybridized weakly in the mitral cells of the olfactory bulbs and showed a moderate signal in the anterior olfactory nucleus. More posterior the neurons of the cortical regions labeled for *Mek5*. The cerebral cortex showed a moderate labeling signal with slight variations in intensity through different layers and parts (Fig. 8B), whereas the piriform cortex was only very weakly labeled. Cells of the basal ganglia showed expression of *Mek5* mRNA mostly at low levels and not in all regions. Only in the globus pallidus and in the endopiriform nucleus weak-to-moderate and moderate signals, respectively, could be seen, but no signal was detectable in the nucleus accumbens and in the olfactory tubercle. In the hippocampus, the hybridization signal for *Mek5* was weak in the dentate gyrus, but moderate-to-strong in all the CA regions (Fig. 8B; weak signal barely visible in Fig. 8D). Not many differences in the expression level could be seen in the amygdala, where all the nuclei showed very weak signals with only slightly elevated levels in cells of the lateral nuclei (Fig. 8F).

In the thalamic area, the hypothalamus as well as the thalamus showed signals for expression of *Mek5*, namely at weak and weak-to-moderate levels (Fig. 8B). More posterior, *Mek5* mRNA was expressed in many regions, but only very weakly or weakly and some parts, as the red and tegmental nuclei and the superior olive, were

devoid of any signal. In the cerebellum only the cells of the Purkinje layer hybridized very weakly with the probe for *Mek5* mRNA, in addition to some signals in the white matter (Fig. 8H).

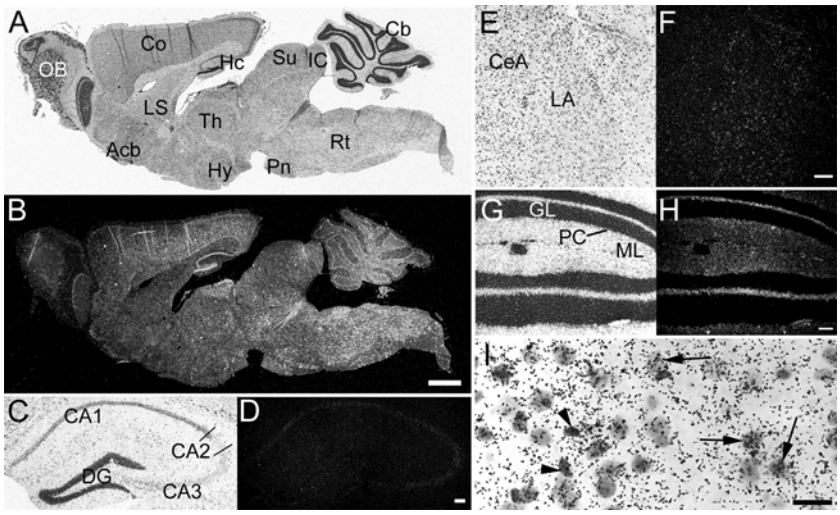

Fig. 8: Sections of adult mouse brain hybridized with the *Mek5* ISH probe. Darkfield photomicrographs (**B**, **D**, **F**, **H**) and corresponding brightfield images of Nissl stained sections (**A**, **C**, **E**, **G**) are displayed. A and B show a complete sagittal section at a glance. Magnifications of the hippocampus (C, D), the amygdala (E, F), and the cerebellum (G, H) from coronal sections present the expression pattern of *Mek5* mRNA in more detail. In the brightfield image of a high magnification of cortical cells (I) expression signal is visible as well in large neuron-like cells (arrows) as in smaller, darker Nissl stained glia-like cells (arrowheads). Scale bar = 1 mm in B; 0.1 mm in D, F, H; 0.016 mm in I. For abbreviations see section 8.1.2, p. 144.

On the cellular level, labeling for *Mek5* mRNA could be observed in all cell types distinguishable by Nissl staining (Fig. 8I). Thus, Mek5 appears not to be specific for neurons.

3.1.6 Comparison of expression patterns

Although most of the genes described here could be found abundantly throughout the adult murine brain, a comparison of the detailed distribution patterns is useful (Fig. 9 and Tab. 1).

	Braf	***Mek1***	***Mek2***	***Mek5***
Olfactory bulb				
Periglomerular layer	-	-	-	-
External plexiform layer	-	-	-	-
Mitral cells	-	+ / ++	-	+
Granule cells	-	++	-	-
Anterior olfactory nucleus	+	++	-	++
Cerebral cortex	+/++	++/+++	-	++
Piriform cortex	+/++	+++	-	-/+
Hippocampus				
CA1 pyramidal cells	+++	++	-	++/+++

	Braf	***Mek1***	***Mek2***	***Mek5***
CA2 pyramidal cells	+++	++	-/+	++/+++
CA3 pyramidal cells	+++	++++	-/+	++/+++
Dentate gyrus	-	++	-	+
Tenia tecta	+	++	-	++
Nucleus of olfactory tract	-	+	-	-/+
Ventral tegmental area	+	-/+	-	-/+
Amygdala				
Basal amygdaloid nuclei	+	++	-	-/+
Lateral amygdaloid nuclei	+/++	+++	-	+
Central amygdaloid nucleus	++	+++	-	-/+
Basal ganglia				
Caudate putamen	++	++	-	+
Lateral striatal stripe	-	++	-	-
Nucleus accumbens	+	++	-	-
Olfactory tubercle	+	++	-	-
Globus pallidus	-	+	-	+ / ++
Endopiriform nucleus	+	+++	-	++
Claustrum	+	+++	-	+
Zona incerta	-/+	-/+	-	-/+
Substantia nigra, pars reticulata	-/+	-	-	-/+
Substantia nigra, pars compacta	+	++	-	+
Septum				
Bed nucleus stria terminalis	-	++	-	+
Lateral septum	+/++	++	-	-
Medial septum	-	-	-	+
Diagonal band	-/+	-	-	+
Habenula, medial part	+	+	-	+
Habenula, lateral part	+	-	-	-/+
Thalamus (general)	+/++	+	-	+/++
Pretectal nucleus	-/+	-/+	-	-/+
Lateral geniculate nucleus	++	+	-	+
Hypothalamus (general)	-	++	-	+
Mammillary nuclei	+	-/+	-	-/+
Mid- and hindbrain				
Superior colliculus	-/+	-/+	-	-/+
Inferior colliculus	+	-/+	-	+
Periaqueductal gray	-	+	-	-/+
Oculomotor nucleus	-	-/+	-	-
Red nucleus	-	-	-	-
Cerebellum				
Molecular cell layer	-	-	-	-
Purkinje cell layer	+	++	+	-/+
Granule cell layer	-/+	-	-	-
Raphe nuclei	-/+	+	-	+

	Braf	***Mek1***	***Mek2***	***Mek5***
Locus coeruleus	-/+	++	-/+	-/+
Pontine reticular nucleus	-/+	-/+	-/+	+
Pontine nuclei	-/+	+	-	+
Tegmental nuclei	-/+	-/+	-	-
Cochlear nucleus	-/+	-	-	-/+
Superior olive	+	-/+	-	-
Inferior olive	-	-/+	-/+	-/+
Trapezoid body	+	-	-	-
Formatio reticularis	-/+	-/+	-/+	-/+
Nuclei of cranial nerves (5, 7, 10, 12)	-/+ to ++	-/+ to ++	- to -/+	-/+ to +

Tab. 1: Expression levels of the MAPKs in all analyzed regions in the adult mouse brain. Regions are listed in the left column. Expression levels for *Braf*, *Mek1*, *Mek2*, and *Mek5* are listed in the following columns. "-" means no expression detectable, "-/+" indicates a faint expression, up to "++++" for a strikingly high expression; referred to the background signal. When the distribution of expression signal throughout one region was not uniform, the intensity depicted here corresponds to an estimated overall mean in this region. The 5th, 7th, 10th and 12th nucleus of cranial nerve were analyzed individually but pooled in this table. For a graphic representation of these data see Fig. 9.

In the olfactory bulb, *Braf* and *Mek2* were not expressed at all. *Mek1* and *Mek5* showed signals in mitral cells, but only *Mek1* was expressed in granule cells.

Mek5 was absent in the nucleus accumbens and the lateral septum. In the hippocampus, expression in the CA3 region was common for all the genes, but signals in the CA1 region were absent for *Mek2*. Additionally, the dentate gyrus was missing signals for *Braf* and *Mek2*. In the amygdala all the genes (except for *Mek2*) were expressed.

In the thalamus, signals for all the genes were present (except for *Mek2*), but *Braf* and *Mek2* were absent in the hypothalamus. In the habenula, *Mek1* and *Mek2* were not expressed. Another interesting region is the substantia nigra, where all the genes except *Mek2* were expressed in the pars compacta, but only *Braf* and *Mek5* gave signals in the pars reticulata in addition. In the periaqueductal gray, *Braf* and *Mek2* were absent. Strikingly, in the red nucleus neither *Braf* nor any *Mek* gene was expressed, although for the *Erk*s, as downstream genes of the *Mek*s, high expression levels could be found there (Di Benedetto et al., 2007). Expression in the raphe nuclei was absent for *Braf* and *Mek2*.

Regarding the nuclei of the cranial nerves, except *Mek2*, all genes are expressed in the V, VII, X, and XII nerve. Also in the cerebellum, all genes are at least present in Purkinje cells and *Braf* - but no *Meks* - also in granule cells.

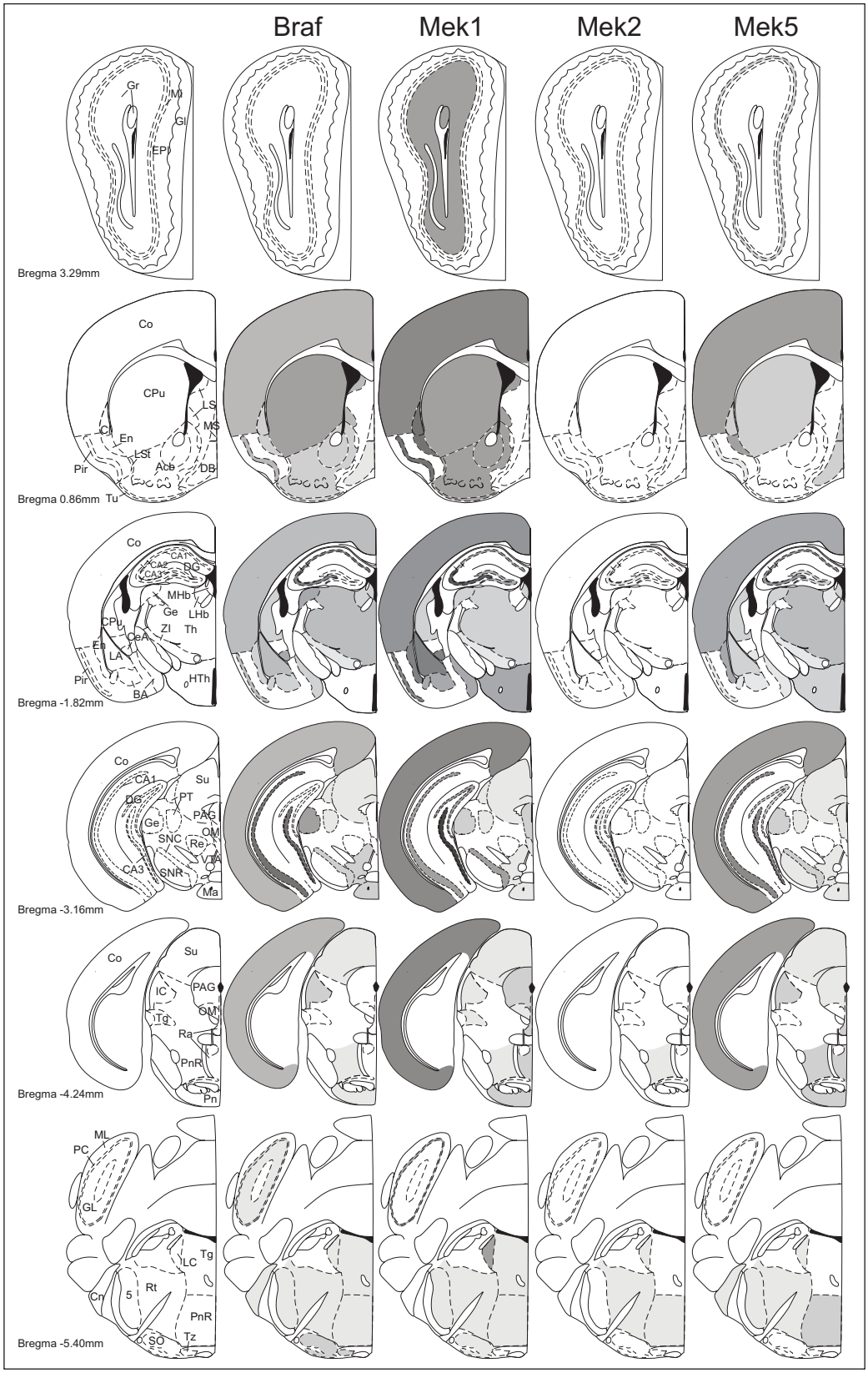

Fig. 9: Schematic representation of expression levels of the MAPKs in adult mouse brain. Drawings of coronal sections at the indicated Bregma levels (adapted from Franklin and Paxinos, 1997) are shown for all MAPKs analyzed, i.e. *Braf*, *Mek1*, *Mek2*, and *Mek5*. Darker grey shades indicate higher RNA levels in the corresponding regions. All regions investigated are labeled in the first section of each line; for abbreviations see section 8.1.2, p. 144.

3.2 Inactivation of *Braf* in adult forebrain neurons

Among the three different *Raf* genes, *Braf* is the only one whose expression in adult mice is almost restricted to the brain (Storm et al., 1990), as shown in this expression study (section 3.1.2, p. 12), it is quite abundant in all brain regions, and therefore it is the best candidate to activate MAPK signaling in brain functions. Since *Braf* plays an essential role in embryonic development, mice with complete knockout of this gene, generated by Wojnowski et al. (1997), die during mid-gestation and are of no use for the analysis of processes in adulthood.

3.2.1 The Braf mouse

Chen et al. (2006) generated a conditional knockout mouse to circumvent the embryonic lethality of the complete knockout and to study the loss of *Braf* in forebrain neurons. They provided me with the floxed mouse for my own studies. In this mouse line exon 12 of the *Braf* gene, which is the first exon encoding the kinase domain of *Braf*, is flanked by loxP sites (Fig. 10A). For this modification, a targeting vector, containing a 1.2 kb fragment flanking exon 12, the loxP sites, and a neomycin selection marker, was inserted into one *Braf* allele by homologous recombination in ES cells. The neomycin selection marker was deleted in a late stage of ES cell culture. After the modification, the allele encodes the active BRAF protein, but can be inactivated by Cre recombinase mediated deletion of the sequence between the two loxP sites. The deletion of the floxed exon by Cre recombination resulted in a shift in the open reading frame and therefore in a null mutation of *Braf* (Fig. 10B and C).

For genotyping, PCR with the primers 9, 11, and 17 was performed to distinguish the wildtype allele from the floxed and deleted alleles. In the wildtype, primer 9 and 11 amplified a 357 bp fragment in intron 11. Due to one of the inserted loxP sites in the floxed allele, the fragment enlarged to 413 bp in this case. After Cre mediated deletion of exon 12, the binding site of primer 11 was lost, but primer 9 and 17 amplified a 282 bp fragment (Fig. 10D).

3.2.2 Expression of Cre recombinase under the CamKIIα promoter

To express Cre recombinase in the forebrain of adult mice, the Cre transgene was controlled by the CamKIIα promoter. This CamKII-cre mouse line was generated by Minichiello et al. (1999) via random integration of an expression vector into zygotes. The construct consisted of the 8.5 kb CaMKIIα promoter and a hybrid intron in front of the Cre coding region with a nuclear localization sequence and a SV40 poly-adenylation signal. Mice were kept on a C57Bl/6J background for all breeding purposes.

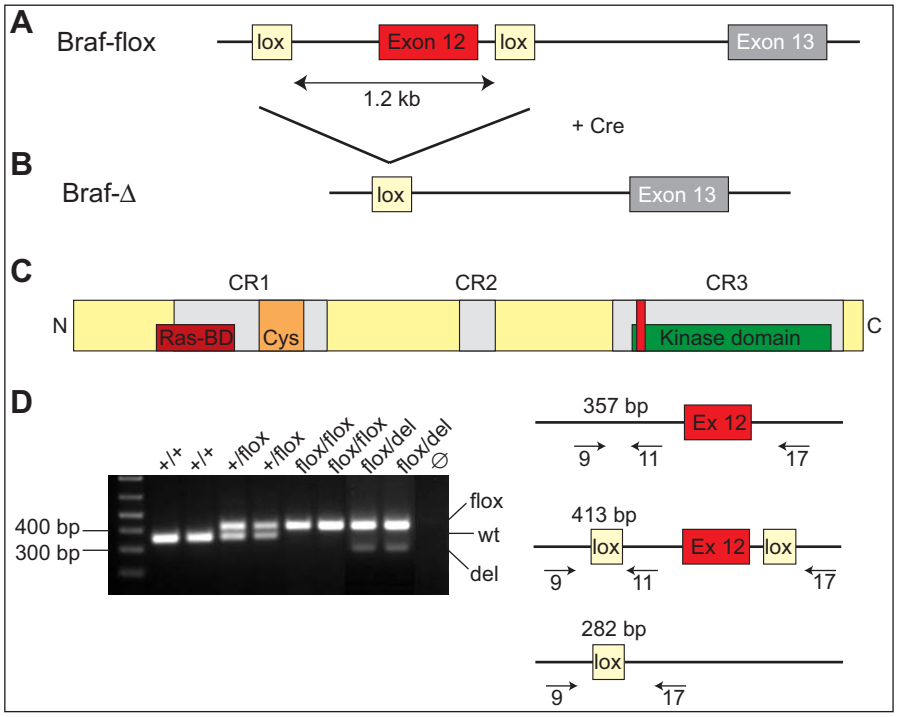

Fig. 10: Scheme of the floxed *Braf* allele before (**A**) and after Cre recombination (**B**). Exon 12 is flanked by loxP sites (lox) and excised by Cre recombinase (Cre), resulting in a null mutation. The protein structure (**C**) shows Exon 12 (red) at the start of the kinase domain. **D**: PCR-genotyping with the primers 9, 11, and 17 was used to determine wildtype (wt, 357 bp), floxed (flox, 413 bp), and deleted (del, 282 bp) alleles. Ras-BD: Ras-binding domain; Cys: cystein-rich domain; CR1-3: conserved regions of RAF proteins; N: amino terminus; C: carboxyl terminus; Ø: negative control.

Cre recombinase is expressed in excitatory neurons of the adult forebrain starting at postnatal day 20 (Minichiello et al., 1999). So, expression of Cre recombinase is expected in the following regions of adult mouse brain: olfactory bulb, hippocampus, striatum, cortex, thalamus and hypothalamus, and slightly in the midbrain.

3.2.3 Breeding of the conditional Braf CamKII-cre mice

I have got four heterozygous floxed Braf mice ($Braf^{+/flox}$) from Dr. Sylvain Provot, Boston. These mice were on a mixed background of 129/SvEms and FVB with backcrossing to FVB for five generations. The males were mated to wildtype females of the strain C57Bl/6J to get more floxed offspring (F1). According to the mendelian ratio 25% of these offspring were $Braf^{+/flox}$ whereas 75% were wildtype mice. $Braf^{+/flox}$ from the F1 generation were again crossed with C57Bl/6J mice to get $Braf^{+/flox}$ mice of the F2 generation, which were intercrossed with each other to get homozygous $Braf^{flox/flox}$ mice. To inactivate the *Braf* gene in adult forebrain neurons, homozygous floxed mice were crossed to CamKII-cre mice (on C57Bl/6J background). According to the mendelian ratio 50% of the offspring were heterozygous floxed with Cre ($Braf^{+/flox}$ CamKII-cre) and 50% without Cre ($Braf^{+/flox}$). Female $Braf^{+/flox}$ CamKII-cre mice were mated

to male Braf$^{flox/flox}$ mice to generate Braf$^{flox/flox}$ CamKII-cre mice, which represented the mutant mice for analysis, since both alleles of *Braf* were knocked out in the adult forebrain. Since it is known that the Cre recombinase driven by the CamKIIα promoter may be expressed already in male germ cells (personal communication by Dr. Ralf Kühn), it was avoided to combine Cre and the floxed allele in male germline, and female Braf$^{+/flox}$ CamKII-cre mice were used for breeding.

In total, Braf mice were backcrossed to C57Bl/6J mice for three generations to enrich the C57Bl/6J background as much as possible in the given time-frame. So, the ratio of C57Bl/6J genome in the genetic background of the Braf mice for analysis averaged to 87%.

For breeding of large cohorts of mutant and control animals for behavior analyses, female Braf$^{+/flox}$ CamKII-cre mice were mated to male Braf$^{flox/flox}$ mice to obtain 25% Braf$^{flox/flox}$ CamKII-cre mice (mutants) and 25% Braf$^{flox/flox}$ mice (controls). Breeding with higher efficiency for mutant and control animals was hampered by a lack of maternal care of Braf$^{flox/flox}$ CamKII-cre mothers about their pups. So breeding with these mothers was only possible in double matings with Braf$^{+/flox}$ CamKII-cre mice as second females, which then served as foster mothers.

3.2.4 Deletion of *Braf* exon 12

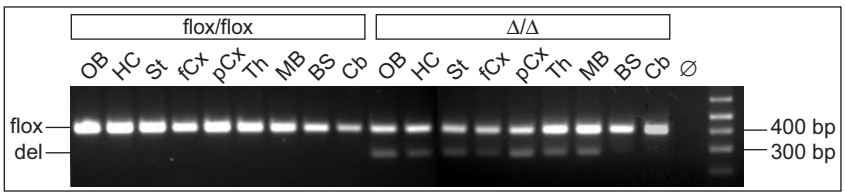

Fig. 11: PCR detection of floxed (flox) and excised (del) Exon 12 from Braf mice. No recombination occurred in Braf$^{flox/flox}$ (flox/flox) mice, whereas the deleted allele is visible mainly in forebrain regions of Braf$^{flox/flo}$ CamKII-cre (Δ/Δ) mice. OB: olfactory bulb; HC: hippocampus; St: striatum; fCx: Cortex, frontal part; pCx: Cortex, posterior part; Th: thalamus; MB: midbrain; Cb: cerebellum; BS: brainstem; Ø: negative control.

To check the regions in the adult brain, where *Braf* exon 12 was deleted by Cre recombinase, a PCR with DNA from different brain regions was performed. The olfactory bulb, hippocampus, striatum, cortex (divided into an anterior and a posterior part), thalamus, midbrain (containing the superior and inferior colliculi amongst others), brainstem (including parts of the spinal chord), and cerebellum were dissected and DNA was isolated from these tissues. Upon PCR amplification, the deleted allele (282 bp) was detected in all these regions except brainstem and cerebellum (Fig. 11). But also in the regions, where deletion of exon 12 took place, the band from the floxed

allele (413 bp) was still present, since Cre recombinase was active only in excitatory neurons and not in other cells present in the brain, like glia cells for example.

3.2.5 Loss of BRAF protein in adult forebrain

In accordance with the pattern of deletion of exon 12 in the adult forebrain, the loss of BRAF protein in the same brain regions as described in section 3.2.4, p. 23 could be shown on a Western blot (Fig. 12). BRAF protein was lost completely in hippocampus, striatum, and cortex of mutant $Braf^{flox/flox}$ CamKII-cre mice. In the olfactory bulb, thalamus, and midbrain of these mutants BRAF expression was reduced, whereas in brainstem and cerebellum it was not altered.

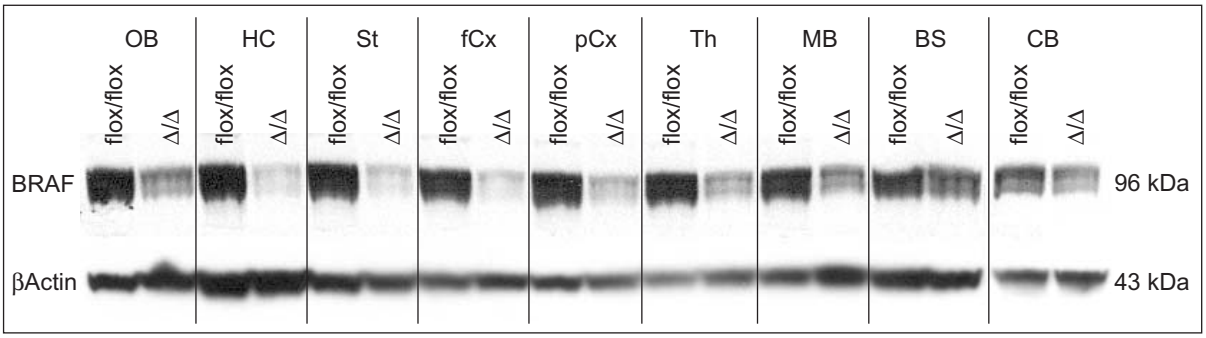

Fig. 12: Western blot against BRAF protein on brain regions of mutant $Braf^{flox/flox}$ CamKII-cre mice (Δ/Δ) and control $Braf^{flox/flox}$ mice (flox/flox). An antibody against β-ACTIN was used as loading control. OB: olfactory bulb; HC: hippocampus; St: striatum; fCx: Cortex, frontal part; pCx: Cortex, posterior part; Th: thalamus; MB: midbrain; Cb: cerebellum; BS: brainstem.

3.3 RNA interference for the generation of conditional knockdown mice

As faster alternative to knockout studies RNAi interference for the generation of knockdown mice is a new tool for inactivation of specific genes *in vivo*. Thereby an expression cassette consisting of an RNA polymerase III promoter, which produces short RNA fragments that form hairpin structures is integrated into the mouse genome. These short hairpin (sh) RNAs are processed by the RNAi machinery such that sequence-specific gene silencing occurs (Dykxhoorn et al., 2003). Mice transgenic for shRNA vectors produce an all-over knockdown phenotype, similar to conventional knockout mice (Kunath et al., 2003). But the complete knockdown, as well as the complete knockout, of developmentally essential genes may cause embryonic lethality. To overcome this embryonic phenotype and to investigate gene functions in specific tissues and/or in a time dependent manner, conditional vectors have to be used. With the strategy used here, shRNA expression was blocked by a transcriptio-

nal stop element that can be deleted via the Cre/loxP system, similar as in conditional knockout mice (see section 3.2.1, p. 21).

3.3.1 Construction of U6-shRNA vectors

To drive the expression of the shRNA construct, RNA polymerase III promoters like the human U6 or H1 promoter have been described predominately (Brummelkamp et al., 2002; Paddison et al., 2004). Previous experiments showed that for my purposes the U6 promoter is the most efficient variant (Hitz et al., 2007).

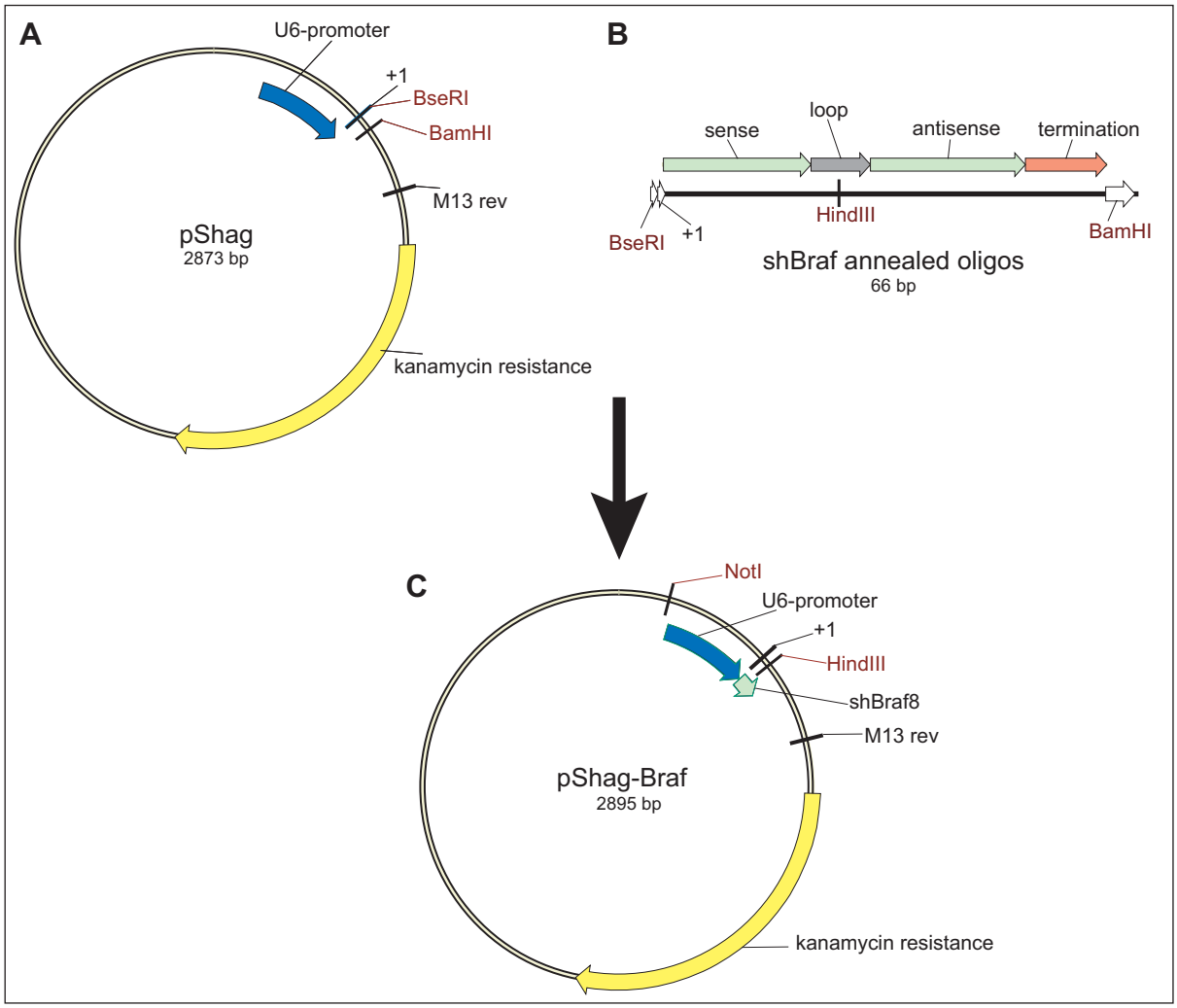

Fig. 13: Cloning strategy for the U6-shRNA vector. pShag (**A**) was opened with BseRI and BamHI and ligated with a fragment of annealed oligonucleotides containing the shRNA sequence (**B**). The correct plasmid after ligation was checked by NotI / HindIII digestion (**C**). +1: transcriptional start site; M13rev: primer M13rev for sequencing.

A vector containing the human U6 promoter followed by a BseRI restriction site within the transcriptional start was used for cloning the shRNA sequences (pShag; Paddison et al., 2004). Targeting sequences were chosen by prediction programs

available online (e.g. https://rnaidesigner.invitrogen.com/sirna/) and, as far as not done by the prediction program itself, modified according to efficiency rules published previously (Schwarz et al., 2003). Two oligonucleotides for each targeting sequence were designed in a way that, upon annealing of both molecules, a double stranded DNA fragment with sticky ends was formed (Fig. 13B). The vector pShag was opened with BseRI and BamHI, 5' ends were dephosphorylated, a fragment of double stranded oligonucleotides was ligated to the vector, and plasmids were transformed into DH5α competent bacteria (Fig. 13). Kanamycin resistant clones were screened by digestion of the plasmids with NotI and HindIII restriction enzymes, where the vector with shRNA insert showed two fragments (289 bp and 2.6 kb) due to the newly introduced HindIII site in the loop sequence and the empty vector showed only one fragment (2.8 kb).

Against *Braf* seven different shRNA sequences were cloned into pShag. For targeting *Mek1* and *Mek2* with one shRNA sequence, three different targeting sequences were chosen. For shRNA constructs against *Mek1* and *Mek2* with separate hairpins, two sequences for each gene were cloned (Tab. 2 and Fig. 14).

Gene	Vector name	Targeting sequence	Oligonucleotides
Braf	pShag-Braf1	gca atc agt ttg ggc aac gag a	shBraf1-A, shBraf1-B
	pShag-Braf4	gcc tca tta cct ggc tca ctc act a	shBraf4-A, shBraf4-B
	pShag-Braf5	ggt cct cag cgg gaa agg aag tca t	shBraf5-A, shBraf5-B
	pShag-Braf6	gct ctg cat caa tgg aca ccg tta	shBraf6-A, shBraf6-B
	pShag-Braf7	gga gat tcc tga tgg aca gat	shBraf7-A, shBraf7-B
	pShag-Braf8	gga gag gag tta cat gtt gaa	shBraf8-A, shBraf8-B
	pShag-Braf9	gct tac tgg aga gga gtt aca	shBraf9-A, shBraf9-B
Mek1&2	pShag-Mek1	gcc ttc tac agc gac ggc gag atc a	shMek1-A, shMek1-B
	pShag-Mek2	gcg acg gcg aga tca gca tct gca	shMek2-A, shMek2-B
	pShag-Mek3	gac ggc gag atc agc atc tgc at	shMek3-A, shMek3-B
Mek1	pbs-U6-Mek1-1	gca gcta att gac tct atg gcc aac	shMek1-1-A, shMek1-1-B
	pbs-U6-Mek1-2	gcc aaa ttg tac ttg tgt cat	shMek1-2-A, shMek1-2-B
Mek2	pbs-U6-Mek2-1	gtt acc ggc act cac tat caa ccc t	shMek2-1-A, shMek2-1-B
	pbs-U6-Mek2-2	ggc taa ggt cgg tga gct caa	shMek2-2-A, shMek2-2-B

Tab. 2: shRNAs against *Braf*, *Mek1*, and *Mek2*. For each gene the names of the shRNA vectors, the shRNA targeting sequence, and the names of the oligonucleotides used for cloning are listed. For the sequences of the oligonucleotides see section 5.19.3, p. 102.

The sequence of shMek1 obviously formed a very tight secondary structure making it impossible to clone it into pShag. Also after a number of attempts with varying cloning conditions and strategies, it was not possible to get positive clones with the oligonucleotides for the shMek1 sequence in pShag. So this targeting sequence had to be omitted in further experiments.

The shRNA constructs for singly targeting *Mek1* or *Mek2*, respectively, were cloned into the vector pbs-U6 in the same way as all the other constructs with pShag. Pbs-U6 consists of the pBluescript vector backbone with the U6 promoter and the cloning sites from pShag (data not shown). For screening of positive vectors, plasmids were digested with HindIII and PstI (instead of NotI) and the two fragments of correct clones were of 300 bp and 3 kb.

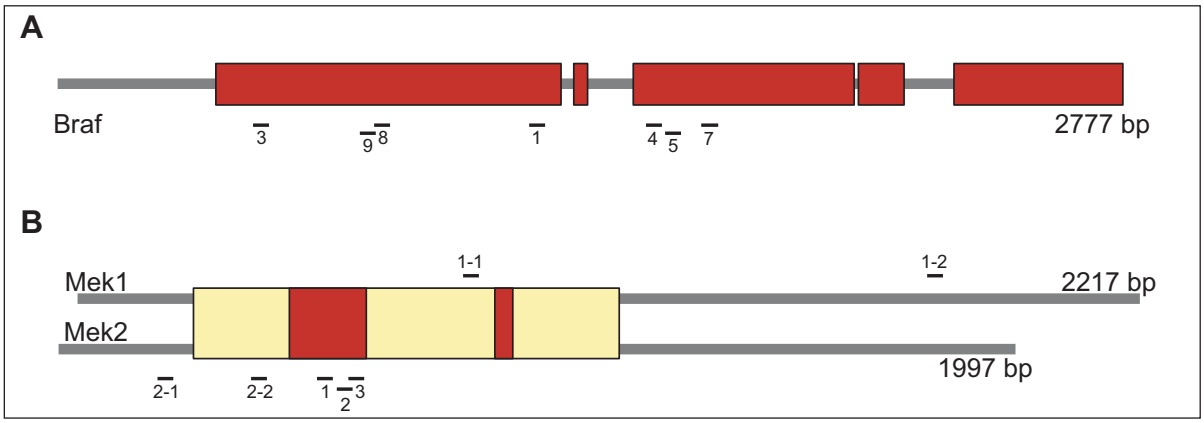

Fig. 14: shRNAs against *Braf*, *Mek1*, and *Mek2*. The positions of the different shRNA targeting sequences on the mRNA are shown for *Braf* (**A**) and *Mek1* and *Mek2* (**B**). The red boxes in A represent not alternative spliced exons, where the targeting sequences are positioned to target all splice forms of *Braf*. The yellow box in B shows regions with high homology between *Mek1* and *Mek2* mRNA. ShRNA sequences targeting both, *Mek1* and *Mek2*, are positioned in the regions (red) with 100% identical sequences for both mRNAs.

3.3.2 Testing for shRNA efficiency

The targeting sequences for the shRNA vectors were chosen in silico by prediction rules that are not yet very precise. So it was very important to validate the efficiency of the different shRNAs *in vitro* and to determine the construct with the strongest knockdown efficiency. First, a screening system commercially available by Invitrogen was used, and later on or additionally electroporation experiments followed by Western blotting were performed.

- Cloning of pScreenIt expression vectors

The original pScreenIt vector was modified in a way that some nonessential features were deleted by digestion with PmeI and XhoI and this 1.7 kb fragment was

replaced by a 102 bp fragment from the pBluescript vector (digested with SacI and KpnI) containing a multiple cloning site (MCS) with restriction sites for various commonly used restriction enzymes (Fig. 15A and B). The whole cDNA or only fragments of the cDNA of the targeted genes were cloned into the new pScreenIt-MCS. So upon transfection of this vector into cells, a CMV promoter drove the expression of a fusion transcript of lacZ and the cloned cDNA (Fig. 15C).

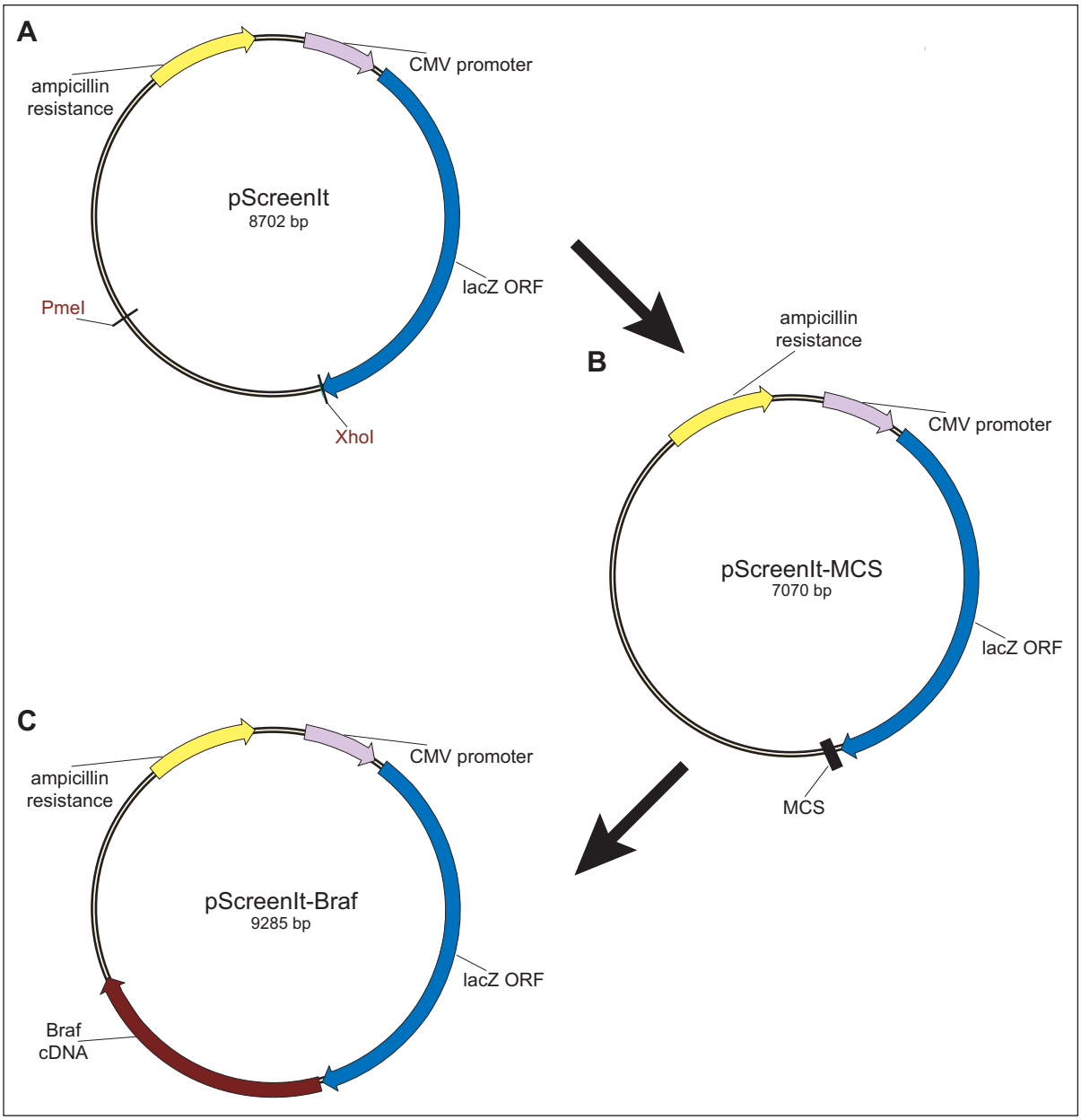

Fig. 15: pScreenIt vectors. The parental pScreenIt vector from Invitrogen (**A**) was equipped with a multiple cloning site (MCS, **B**) for an easier subcloning of the cDNA of the targeted genes (here shown with *Braf*, **C**). The CMV promoter of pScreenIt drives the expression of a fusion transcript of lacZ and the subcloned cDNA. ORF: open reading frame.

Braf cDNA was generated by PCR amplification of different cDNA fragments from adult mouse brain cDNA. Each of these fragments was cloned into one TOPO TA vector and then all the fragments were assembled into one vector (data not shown). From this expression vector the *Braf* fragment was purified by digestion with XbaI and SpeI, whereas the SpeI generated sticky ends were filled in with Klenow fragment of DNA polymerase I, and recloned into the XbaI and SmaI digested pScreenIt-MCS. For *Mek1* and *Mek2* only parts of the cDNA were amplified by PCR and cloned into the TOPO TA vector (data not shown). The cDNA vectors were digested to obtain the cDNA fragments (with PstI and BamHI for *Mek1*, and with EcoRV and SpeI for *Mek2*), which were recloned into pScreenIt-MCS (digested with PstI and BamHI for *Mek1* cDNA, and with SmaI and XbaI for *Mek2* cDNA).

- Screening with pScreenIt

Each shRNA vector was co-transfected with the corresponding pScreenIt-cDNA vector into mouse ES cells to assess the efficiency of shRNAs *in vitro*. While the fusion mRNA of lacZ and the cDNA was transcribed from pScreenIt-cDNA, the shRNA was produced from the shRNA plasmid and mediated knockdown of the entire fusion mRNA by binding the targeting sequence on the mRNA derived from the cDNA. Two days after transfection, the cells were lysed and β-Galactosidase (β-Gal) activity was measured in a luminometer. The reduction in β-Gal activity in cells transfected with an shRNA vector in comparison to cells not transfected with an shRNA vector should correspond directly with the knockdown of the cDNA. To take varying cell numbers or transfection efficiencies into account, a third plasmid, expressing firefly-Luciferase (Luc), was co-transfected, and β-Gal activity was normalized to Luc activity, which was also measured in the cell lysate.

Each transfection was performed in duplicate and was repeated several times. The results for all shRNA constructs are shown in Fig. 16. For the knockdown of *Braf*, shBraf1, 7, 8, and 9 reached the highest efficiency with 5%, 14%, 3%, and 5% remaining β-Gal activity, respectively. The vector with the sequence shBraf4 did not give rise to any knockdown effect at all, but showed a very high variability between the different transfection experiments as visualized by the huge error bar. For knocking down *Mek1* and *Mek2* with one shRNA sequence, shMek2 and 3 showed similar knockdown levels for both genes (14% to 17%). For further work the most efficient shRNA vectors were chosen, i.e. shBraf1, 7, 8, 9, and shMek2 and 3.

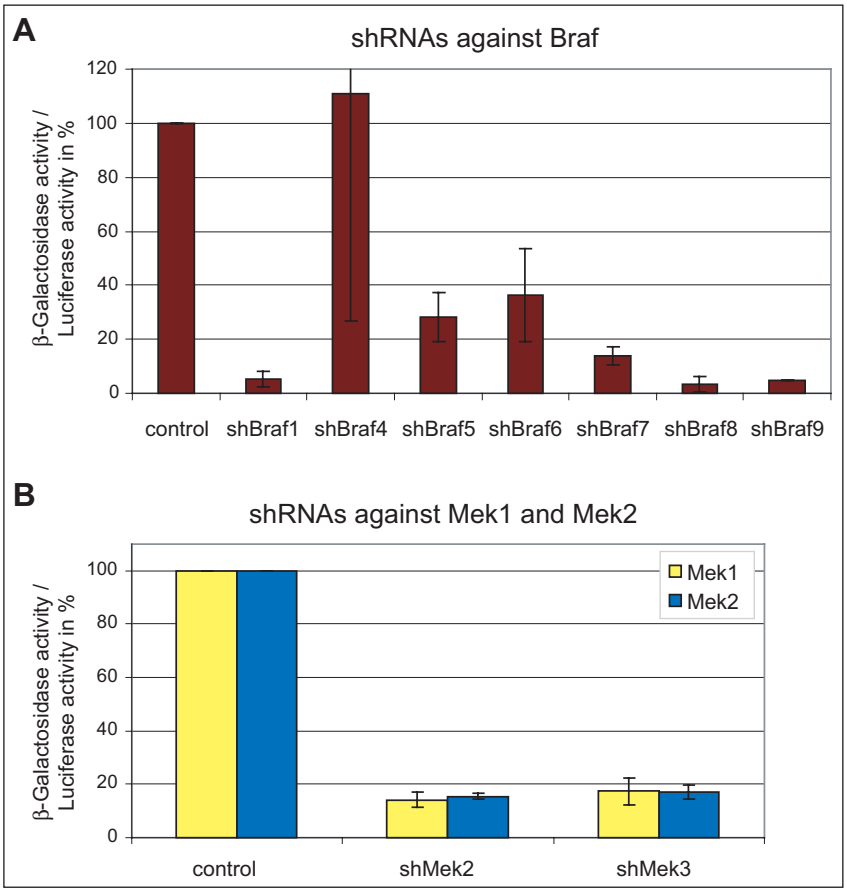

Fig. 16: Efficiency of shRNA constructs tested with the pScreenIt system. β-Gal activity normalized with Luc activity is shown as percentage, 100% being β-Gal activity without shRNA vector transfected (control). ShRNAs against *Braf* - shBraf1, 4, 5, 6, 7, 8, 9 - are presented in **A**. shRNAs against *Mek1* (yellow bars) and *Mek2* (blue bars) - shMek2 and shMek3 - are shown in **B**.

- Screening with Western blotting

Since doubts on the reliability of the results, which have been assessed with the pScreenIt system, arose, for screening of the shMek1-1, 1-2, 2-1, and 2-2 shRNAs Western blotting was used. For this, shRNA expression vectors were electroporated into mouse ES cells and conditions were used so that a transfection efficiency of at least 90% were achieved (tested previously with reporter genes, data not shown). Assuming that most of the cells had been transfected with the shRNA plasmid, knock-down of the endogenous gene activity of all the cells could have been analyzed. So, two days after electroporation the cells were harvested, protein was extracted, and western blots for the corresponding proteins were performed. Since a small number of cells remained non-transfected, the shRNA efficiency determined with this assay was slightly lower than the real knockdown, but it was unaffected of artificial mRNA structures that were used in the pScreenIt system and may alter the results.

As shown in Fig. 17, shMek1-1 gave rise to a much better knockdown of MEK1 protein than shMek1-2. For MEK2 no knockdown could be observed with these two shRNA constructs, showing their specificity for *Mek1*. Against *Mek2*, both constructs tested - shMek2-1 and shMek2-2 - showed quite high knockdown efficiencies, with shMek2-2 giving an even higher knockdown than shMek2-1. As expected, the latter two constructs did not affect expression of MEK1.

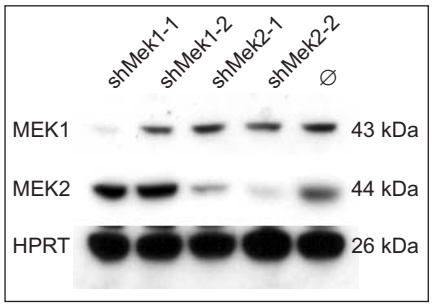

Fig. 17:
Western blotting after transient electroporation of the shRNA constructs. ShRNAs against *Mek1* and *Mek2*, respectively, have been transfected into ES cells and Western blotting against MEK1 and MEK2 protein is shown. HPRT antibody was used as loading control. Ø: protein from non-transfected control cells.

3.3.3 Construction of U6-shRNA-flox vectors

The shRNA vectors that were chosen for further work - i.e. shBraf1, 7, 8, 9, shMek2 and 3, shMek1-1, 1-2, 2-1, and 2-2 - were modified with a stop element that blocks transcription of the intact shRNA. By flanking this stop cassette with loxP elements, it could be eliminated upon Cre mediated recombination and the entire shRNA could be transcribed. With this Cre/loxP system the shRNA activity could be regulated in a time and tissue dependent manner similar to conditional knockout approaches (see section 3.2.1, p. 21). As evaluated previously (Hitz et al., 2007), the best position for inserting the stop element was the loop region of the shRNA. Before Cre mediated recombination only the sense strand of the shRNA was transcribed so that no active hairpin could form, and after deletion of the stop cassette, the remaining 34 bp of one loxP site were located in the loop region, which resulted in a bigger loop but no altered activity of the shRNA (Fig. 18A). Using the HindIII restriction site in the loop of the parental shRNA vector, the 338 bp stop element (isolated as MlyI fragment from pNEB-lox-RLuc-lox) was cloned blunt-ended into the loop of the shRNA constructs. This stop element consisted of a 19 bp Renilla-Luciferase antisense, serving as stuffer DNA, and two polythymidine sequences, serving as termination signals, between two loxP sequences (Hitz et al., 2007). In the constructs shMek2-1 and shMek2-2, a 863 bp fragment from the vector pbs-lox2272-neo-lox2272 was inserted as stop element (blunt ended as well). This alternative stop cassette was flanked by the lox2272 sites instead of the classical loxP sites. The lox2272 sites recombine with each other in the same way as loxP sites upon Cre recombination, but they can not interact with the

loxP sites. For using two different conditional shRNA cassettes on one construct it was essential to use these different lox sites to control deletion of each stop element. In addition, this alternative stop cassette is larger than the one from the plasmid pNEB-lox-RLuc-lox due to an additional 679 bp fragment from the neomycin resistance gene to enlarge the stop element and therefore possibly increase its efficiency to block transcription.

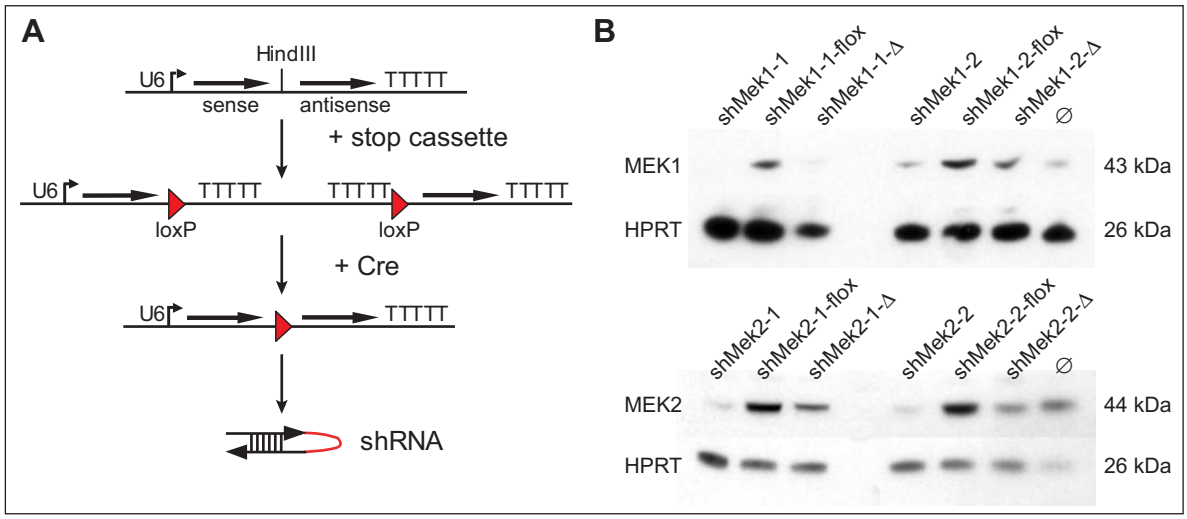

Fig. 18: Conditional U6-shRNA-flox vectors. **A**: Insertion of a loxP-flanked stop element resulted in blocking of shRNA transcription. Upon Cre mediated deletion of the stop cassette, the remaining loxP site enlarged the loop region but allowed the transcription of an active and efficient shRNA. **B**: Knockdown efficiencies of the shRNAs against *Mek1* and *Mek2*, respectively, were assessed by Western blotting. Constructs before insertion of the stop element, with the stop cassette (-flox), and after deletion of the stop cassette (-Δ) have been transfected into ES cells and western blotting against MEK1 and MEK2 protein, respectively, is shown. HPRT antibody was used as loading control. Ø: protein from non-transfected control cells.

For the shBraf9 sequence it was not possible to clone the stop element into the HindIII site in the loop region, since an additional HindIII site was present in the antisense sequence. So, this construct could not be followed up for the conditional RNAi studies.

The knockdown efficiencies of these modified constructs were assessed with the pScreenIt system or Western blotting. ShRNA constructs with the stop element were supposed not to alter gene activity, and shRNA constructs after deletion of the stop cassette were supposed to give a knockdown as high as possible. This did not hold true for all the constructs tested, as shown in Fig. 18B and Fig. 19. Whereas the floxed construct with shBraf1 seemed to increase the β-Gal activity compared to control expression, after deletion of the stop element shBraf1 showed only a knockdown of 63% (Fig. 19A). Before inserting the stop cassette, the same hairpin showed knockdown of 95% (Fig. 16A), indicating that for this specific sequence the elongated loop

sequence altered knockdown efficiency. On the other hand, shBraf8 gave still 91% knockdown after deletion of the stop cassette.

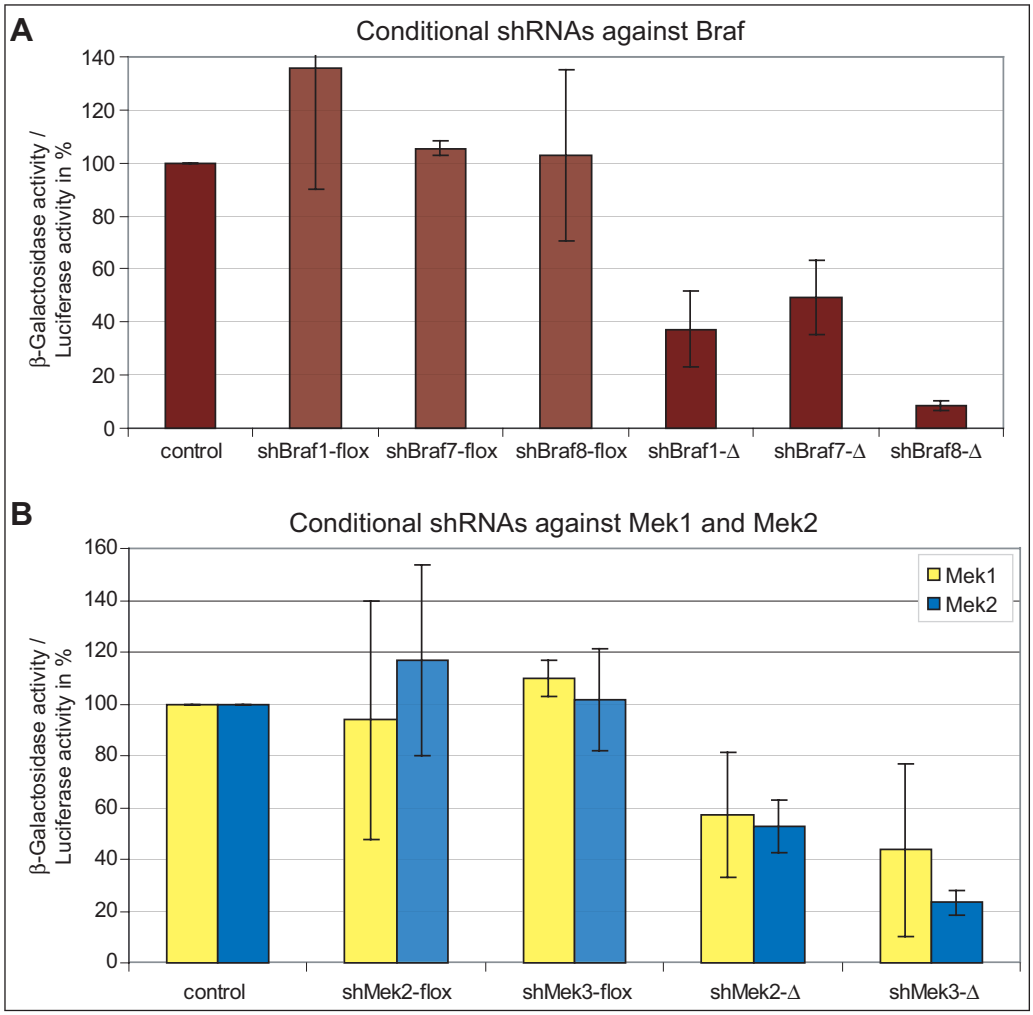

Fig. 19: Conditional U6-shRNA-flox vectors. Efficiency of shRNA constructs tested with the pScreenIt system. β-Gal activity normalized with Luc activity is shown as percentage, 100% being β-Gal activity without shRNA vector transfected (control). ShRNAs against *Braf* - shBraf1, 7, 8, with stop cassette (-flox) and after deletion of the stop cassette (-Δ) - are presented in **A**. shRNAs against *Mek1* (yellow bars) and *Mek2* (blue bars) - shMek2 and shMek3, with stop cassette (-flox) and after deletion of the stop cassette (-Δ) - are shown in **B**.

For *Mek1* and *2*, the stop element blocked shRNA transcription in the expected manner so that no knockdown was measured with all the floxed constructs. But after Cre recombination only shMek3 gave a similar knockdown against *Mek2* as the same non-conditional construct (Fig. 16B and Fig. 19B). shMek2 showed a strongly diminished knockdown efficiency against *Mek1* and *Mek2*. The efficiencies of the shRNAs singly targeting *Mek1* or *Mek2* were assessed by Western blotting after electroporation (see section 3.3.2, p. 27). Here, shMek1-1-flox showed a better knockdown of *Mek1* than shMek1-2-flox after Cre recombination. For *Mek2*, both hairpin constructs showed a significantly reduced knockdown after deletion of the stop cassette compa-

red to the parental non-conditional vector (Fig. 18B). This could be due to the lox2272 site, which may disturb shRNA efficiency compared to the loxP sites, or for these specific shRNA sequences the elongated loop affects knockdown efficiency. So, for mouse production I used the shMek2-2 in a non-conditional way. The knockdown of this shRNA was much better and a conditional construct for *Mek2* knockdown was not essential, since *Mek2* complete knockout mice are viable and show no obvious phenotype (Belanger et al., 2003).

For the generation of shRNA mice the most efficient conditional shRNA constructs were chosen. So, for *Braf* knockdown mice shBraf8-flox was used. For the knockdown of *Mek1* and *2* with one shRNA construct, shMek3-flox was chosen. ShMek1-1-flox and shMek2-2 were used for singly targeting *Mek1* and *Mek2*, respectively.

3.3.4 Recombinase mediated cassette exchange

For the genomic integration of the conditional shRNA vectors a single copy approach is preferable since multicopy integrations in the genome could undergo unpredictable and non-functional rearrangements upon Cre mediated recombination. As shown previously with reporter genes (Hitz et al., 2007), one single copy of an shRNA construct in the *Rosa26* locus of the mouse genome is sufficient to achieve strong knockdown. The *Rosa26* gene is located on mouse chromosome 6 and its locus has been frequently used for the genomic integration of expression vectors, including RNAi constructs (Soriano, 1999; Seibler et al., 2005; Yu and McMahon, 2006). Since also a double targeting of both *Rosa26* alleles does not give rise to any phenotype, homozygote mice with two modified alleles are possible within this locus.

To facilitate the insertion of shRNA vectors into the *Rosa26* locus of ES cells for the fast and easy generation of knockdown mouse lines, I used the technique of recombinase mediated cassette exchange (RMCE) with the integrase of phage ϕC31 (C31Int). RMCE is based on two pairs of attachment sites (attB and attP), which can recombine with each other via C31Int. So the sequence between two attP sites is exchanged by an attB-flanked fragment. To use this system for the generation of shRNA mice, ES cells with a *Rosa26* acceptor allele were generated. These cells harbored a pgk promoter driven hygromycin resistance gene, of which the coding and polyA region was flanked by attP recognition sites, in the *Rosa26* locus (Fig. 20C). The acceptor allele was designed such that the attP-flanked segment could be replaced by an attB-flanked construct from a donor plasmid (pRMCE) upon transfection of ES cells together with a C31Int expression plasmid (Fig. 20B). The donor vector con-

tained a promoterless neomycin resistance coding and polyA region and the shRNA expression cassette between the attB recognition sites. With a shift from hygromycin to neomycin resistance in ES cells selection for RMCE events was possible (Fig. 20D), such that correct cassette exchange occurred at a frequency of 40 to 60% among the neomycin resistant ES cell colonies.

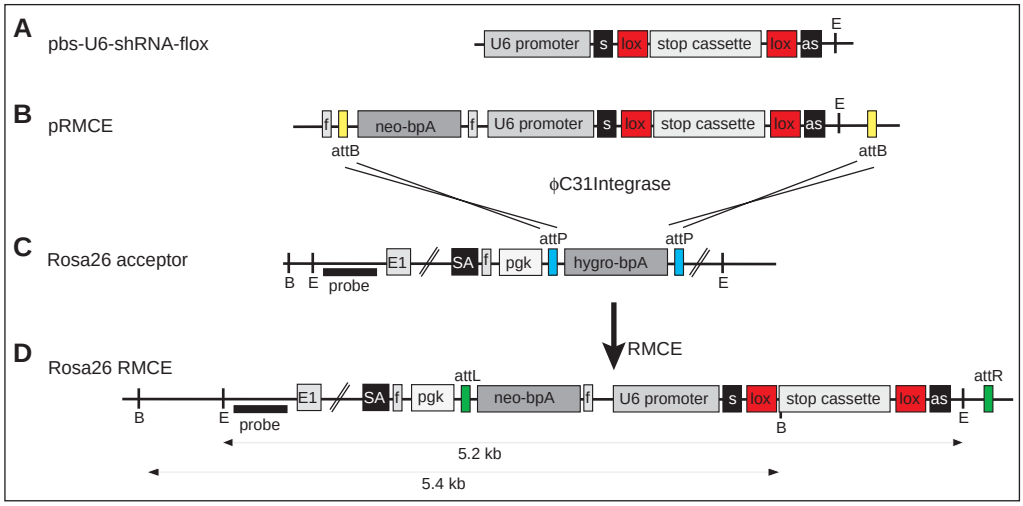

Fig. 20: Vector construction and RMCE for the generation of shBraf and shMek-flox mice. **A**: The conditional shRNA expression cassette from the vector pbs-U6-shRNA-flox (or pShag-shRNA-flox, respectively) contained the U6 promoter in front of the sense (s) sequence of the shRNA, the loxP (lox) flanked stop cassette in the loop region and the antisense (as) shRNA sequence. **B**: For RMCE, the shRNA expression cassette was cloned into the RMCE donor vector pRMCE behind the promoterless neomycin selection marker (neo-bpA) so that the two attB sites from pRMCE flanked the selection marker as well as the shRNA expression cassette. **C**: Acceptor ES cells for RMCE harbored a *Rosa26* allele where in intron 1 a splice acceptor (SA) was inserted followed by a pgk promoter (pgk) driving a hygromycin selection marker (hygro-bpA) which was flanked by attP sites. **D**: Upon RMCE with C31Int, the attP-flanked cassette in the acceptor ES cells from C was replaced by the attB-flanked cassette from the donor vector in B. FRT (f) sites allowed to excise the pgk promoter and the neomycin marker in recombined ES cells or in mice. E: EcoRV; B: BamHI; probe: 5'-Rosa26 probe; E1: exon 1.

For the generation of pRMCE-U6-shRNA-flox, pRMCE was digested with NotI and EcoRV, and the opened vector (4.4 kb) was ligated with a 800 bp fragment from pShag-shRNA-flox digested with the same restriction enzymes. For pbs-U6-shMek1-1-flox, pRMCE was opened with AsiSI and EcoRV, and pbs-U6-shMek1-1-flox was first digested with SpeI, sticky ends were filled in with Klenow fragment of DNA polymerase I, and then digested with AsiSI to obtain compatible ends. The 4.4 kb vector and the 722 bp fragment containing the shRNA expression cassette were ligated.

As additional construct for the generation of double knockdown mice with two independent shRNA sequences against *Mek1* and *Mek2*, U6-shMek2-2 was cloned in tandem to shMek1-1-flox. For this plasmid, pRMCE-U6-shMek1-1-flox was opened

with SpeI 3' to the shRNA sequence and a XbaI fragment from pbs-U6-shMek2-2, containing the U6-promoter and the shMek2-2 hairpin, was inserted (Fig. 21).

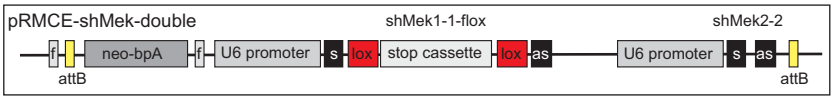

Fig. 21: Double knockdown construct for *Mek1* and *Mek2* with two independent shRNAs. 3' to the shRNA of pRMCE-U6-shMek1-1-flox the non-conditional hairpin construct U6-shMek2-2 against *Mek2* was cloned. f: FRT site; attB, attP: attB / attP recognition sites for C31Int; s: sense sequence of the shRNA; as: antisense sequence of the shRNA.

3.3.5 Generation of shRNA-flox ES cells

Using the RMCE system described in section 3.3.4, p. 34, genetically modified ES cells were generated, which harbored the conditional shRNA construct in their *Rosa26* locus. For this, the pRMCE plasmid with the shRNA expression cassette between two attB recognition sites was electroporated together with a C31Int expression plasmid into mouse F1 ES cells. For each electroporation, 24 neomycin resistant clones were analyzed by PCR and verified by Southern blotting for correct cassette exchange. For PCR analysis, genomic DNA of the cells was amplified with the primers pgk3 and exneo2 to screen for integration of the neomycin gene 3' to the pgk promoter (280 bp band). By amplification with the primers hygro1 and hygro2 the loss of the hygromycin gene from the RMCE acceptor allele was confirmed (absence of 552 bp band). Clones positive for the neo band and negative for the hygro band were supposed to have correct cassette exchange (Fig. 22A) and this was confirmed by Southern blotting. An alternative PCR strategy used the primers U6_for and Rosa3'HA_rev2, amplifying the shRNA expression cassette from the U6 promoter to the *Rosa26* intron 3' of the integration site. All clones giving rise to this 941 bp band were supposed to be positive for correct cassette exchange (Fig. 22B).

Confirmation of positive clones by Southern blotting was performed by ScaI or EcoRV digestion of genomic DNA from ES cells followed by detection with the Rosa5'probe (448 bp fragment from plasmid pCRII-Rosa5'probe digested with EcoRI). For constructs based on the pShag vector (shBraf8 and shMek3), upon ScaI digestion, the wildtype *Rosa26* allele gave rise to a 6.1 kb band, the RMCE acceptor allele before cassette exchange showed a 7.6 kb band, and after correct cassette exchange the band shifted to 9.2 kb (Fig. 22C). For constructs based on the pbs-U6 vector (shMek1-1, shMek2-2), upon EcoRV digestion, the wildtype *Rosa26* allele gave rise to a 11.5 kb band, the RMCE acceptor allele before cassette exchange showed a 4.5 kb

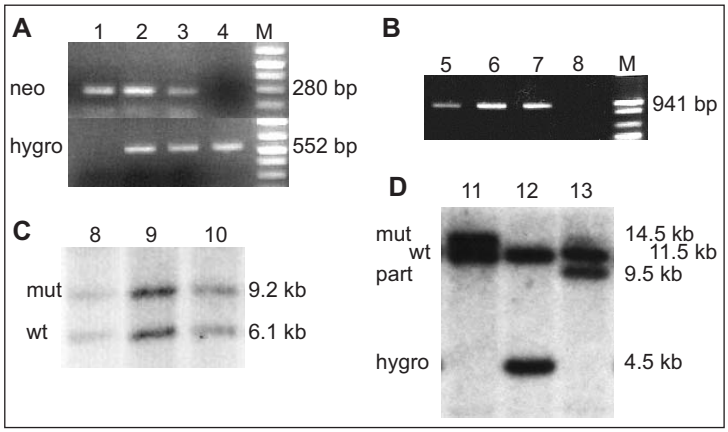

Fig. 22: Screening of ES cells for correct cassette exchange by PCR (A and B) and Southern blotting (C and D). **A**: PCR amplification of genomic DNA with primers pgk3 and exneo2 showed a 280 bp band (neo) after integration of the pRMCE vector (lane 1). Primers hygro1 and hygro2 amplified a 552 bp fragment from the *Rosa26* acceptor allele (hygro, lane 4). Detection of both bands (lanes 2 and 3) indicated a partial cassette exchange with recombination only at the 5' attP site, where the hygromycin resistance gene was still present after exchange. **B**: Alternative PCR screening with primers U6_for and Rosa3'HA_rev2 showed the 941 bp band only upon correct exchange (lanes 5-7). **C**: Southern blotting of ScaI digested genomic DNA confirmed the correct cassette exchange with a 6.1 kb band for the wildtype *Rosa26* allele (wt) and a 9.2 kb band for the correctly exchanged cassette (mut, lanes 8-10). **D**: Southern blotting of EcoRV digested genomic DNA confirmed the correct cassette exchange with a 11.5 kb band for the wildtype *Rosa26* allele (wt) and a 14.5 kb band for the correctly exchanged cassette (mut, lane 11). A 4.5 kb band indicated the *Rosa26* acceptor allele (hygro) without cassette exchange (lane 12) and a 9.5 kb band was visible upon partial cassette exchange (part, lane 13).

band, and after correct cassette exchange the band shifted to 14.5 kb and 14.9 kb in case of the shMek1-1-flox-Mek2-2 double construct (Fig. 22D).

For each transfection several confirmed positive clones were identified as listed in Tab. 3.

Gene targeted	Construct	Positive clones
Braf	pShag-Braf8-flox	89B3, 89B4, 89B6, 89C2, 89C4, 89D1
Mek1&2	pShag-Mek3	81C5, 81F1, 81F2, 81F9
	pbs-U6-Mek1-1-flox-Mek2-2	971-7, 971-11, 971-17, 972-2, 972-7, 972-8, 972-9, 972-11, 972-17, 972-19, 972-21, 972-22, 972-23
Mek1	pbs-U6-Mek1-1	961-1, 961-2, 962-5, 962-13, 962-14, 962-15, 962-16, 962-19, 962-22, 962-23

Tab. 3: Positive clones for all shRNA expression cassettes transfected into ES cells. Underlinede clones were used for mouse production.

3.3.6 Generation of shRNA-flox mice

Positive ES cell clones were injected into blastocysts of C57Bl/6J mice and transferred into pseudo-pregnant females. Chimeras were born of most of the injected clo-

nes and germline transmission was initiated by mating the chimeras with C57Bl/6J mice. An overview over the chimeras born for each clone and germline transmission of the shRNA constructs is given in Tab. 4. Only for the construct pbs-U6-Mek1-1-flox-Mek2-2 no colony could be established since the mutated allele was not transmitted to the offspring. Due to time restrictions it was not possible to repeat any earlier step to overcome this problem. For all the other constructs colonies were established, originating from the ES cell clones indicated in Tab. 4.

Construct	Injected clone	Number of chimeras	Germline transmission
pShag-Braf8-flox	89B3	0	-
	89B6	1	yes, founder of colony
	89C2	8	not tested
	89C4	7	not tested
pShag-Mek3	81C5	4	not tested
	81F1	0	-
	81F2	7	yes, founder of colony
pbs-U6-Mek1-1-flox-Mek2-2	972-9	0	-
	972-19	0	-
	972-21	2	no
pbs-U6-Mek1-1	962-5	2	not tested
	962-15	4	yes, founder of colony
	962-19	2	yes, founder of colony

Tab. 4: Chimeras born from the injected clones. Number of chimeras for each injected clone are indicated and germline transmission is noted. From construct pbs-U6-Mek1-1-flox-Mek2-2 no colony was established since germline transmission was not achieved.

3.4 Knockdown of *Braf* in adult forebrain neurons

The technique of shRNA mice is a quite new and unexplored field. To apply this new tool on biological questions, I generated knockdown mice of *Braf*. As shown in section 3.2, p. 21, the conditional knockout of *Braf* has been generated by Chen et al. (2006) and these mice were shown to exert memory deficits, when *Braf* was lost in forebrain neurons.

3.4.1 The shBraf mouse

The generation of shBraf mice is described in section 3.3, p. 24. The shRNA expression cassette in the *Rosa26* locus of these mice was interrupted by a loxP flanked stop cassette, which could be excised by Cre recombinase, which in turn activated shRNA expression. Mice harboring one or two shBraf alleles were normal and showed no obvious difference to their wildtype littermates.

3.4.2 Breeding of conditional shBraf CamKII-cre mice

Germline transmission was obtained with the ES cell clone 89B6 (see section 3.3.6, p. 37). These mice were on a mixed background of 129SvEv/Tac and C57Bl/6J, since the F1 ES cells used for mouse generation were a mixture of two strains. Upon crossing the chimera with wildtype C57Bl/6J females, one generation of backcrossing was performed. Intercrosses of shBraf$^{+/flox}$ mice generated shBraf$^{flox/flox}$ mice, which were mainly used for breeding with CamKII-cre mice to activate shRNA expression in forebrain neurons of adult mice (see section 3.2.2, p. 21). Offspring originating from these matings were to 50% of the genotype shBraf$^{+/flox}$ (control mice) and to 50% shBraf$^{+/flox}$ CamKII-cre (mutant mice). Since the CamKII-cre mice were on pure C57Bl/6J background, this breeding step represented a further backcrossing to C57Bl/6J. So in total shBraf mice were backcrossed to C57Bl/6J mice for two generations to enrich the C57Bl/6J background as much as possible in the given time-frame. The amount of C57Bl/6J genome in the genetic background of the shBraf mice for analysis averaged to 87%.

For test experiments, shBraf$^{flox/flox}$ CamKII-cre mice carrying two shBraf alleles were generated by mating shBraf$^{+/flox}$ CamKII-cre mice with shBraf$^{flox/flox}$ mice. Since it is known that the Cre recombinase driven by the CamKIIα promoter may be expressed already in male germ cells (personal communication by Dr. Ralf Kühn), for these matings it was avoided to combine Cre and the floxed shBraf allele in the male germline, and female shBraf$^{+/flox}$ CamKII-cre mice were used for this breeding strategy.

3.4.3 Deletion of the stop cassette and expression of shBraf

To check the regions in the adult brain, where the shRNA against *Braf* was activated upon Cre mediated recombination, Southern blotting with DNA from different brain regions was performed. The olfactory bulb, hippocampus, striatum, cortex (divided into an anterior and a posterior part), thalamus, midbrain (containing the superior and inferior colliculi amongst others), brainstem (including parts of the spinal chord), and cerebellum were dissected. DNA was isolated from these tissues and digested with

BamHI. Detection of the different alleles with the Rosa5'probe showed the allele with the deleted stop cassette (8.6 kb) in all forebrain regions from shBraf$^{+/flox}$ CamKII-cre mice, only weak in the thalamus and not detectable in brainstem and cerebellum (Fig. 23A). But also in the regions, where shRNA expression was activated, the band from the floxed allele (5.4 kb) was still present, since Cre recombinase was active only in excitatory neurons and not in other cells in the brain, like glia cells for example. As expected, brain tissue (pooled from all the regions dissected) from shBraf$^{+/flox}$ control mice showed, besides the 5.8 kb wildtype band, only the floxed allele, since no Cre recombinase was present to delete the stop cassette.

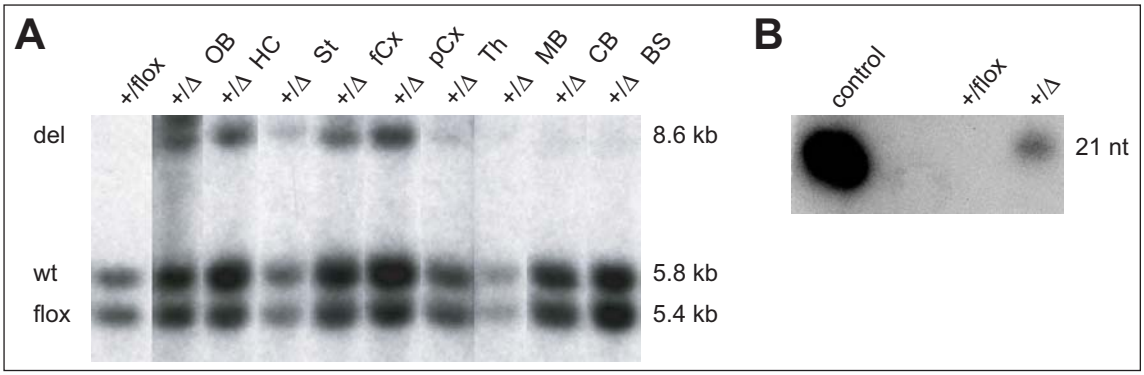

Fig. 23: Activation of shRNA against *Braf* in the adult brain with CamKII-cre. **A**: Southern blot analysis of BamHI digested genomic DNA from different brain regions of adult shBraf$^{+/flox}$ CamKII-cre mice shows Cre mediated deletion of the stop cassette. Lane 1: DNA from whole brains of shBraf$^{+/flox}$ control mice; lane 2-10: DNA from indicated regions of shBraf$^{+/flox}$ CamKII-cre mice (+/Δ). The wildtype *Rosa26* allele (wt) gives a 5.8 kb band and the band from the shRNA allele is shifted from 5.4 kb with the stop cassette (flox) to 8.6 kb after Cre recombination (del). OB: olfactory bulb; HC: hippocampus; St: striatum; fCx: Cortex, frontal part; pCx: Cortex, posterior part; Th: thalamus; MB: midbrain; Cb: cerebellum; BS: brainstem. **B**: On a Northern blot with small RNAs against the sequence of shBraf, the 21 nt band of the processed siRNA against *Braf* is only detectable with the control oligonucleotide and in mutant mice but not in control mice.

To assure that the shRNA is expressed after Cre recombination, the siRNA against *Braf* was detected on a Northern blot with small RNAs. Therefore, small RNAs were isolated from the anterior half of adult brains and the siRNA against *Braf* was detected with a specific oligonucleotide probe. The 21 nt band was detected in mutant shBraf$^{+/flox}$ CamKII-cre mice, but not in control animals (Fig. 23B). This result indicated that the stop cassette indeed blocked transcription of the shRNA *in vivo* successfully. The weak signal in the mutant mice is based on the neuron specific expression of CamKII-cre, so that many non-neuronal cells in the forebrain (not expressing the shRNA) decreased the percentage of cells expressing the shRNA.

3.4.4 Reduction of *Braf* mRNA in adult forebrain

On the mRNA level, quantification of the knockdown efficiency could be assessed with Northern blotting of mRNA from adult brain regions. Since all of the Northern probes against *Braf* tested failed to give reasonable bands, *Braf* mRNA levels could be analyzed only in a qualitative manner by ISH. Paraffin sections from adult mutant and control brains were hybridized with the *Braf* ISH probe (Fig. 24). The signal in posterior brain regions like brainstem and cerebellum showed similar intensities in both brains, mutant and control. In all the other forebrain and midbrain structures in the mutant brain, expression of *Braf* mRNA was highly reduced. For forebrain regions, this knockdown effect was expected due to the expression pattern of Cre recombinase in CamKII-cre mice, but not for the midbrain, where Cre should not be expressed. The reason for this discrepancy between Cre expression and mRNA knockdown could not be clarified.

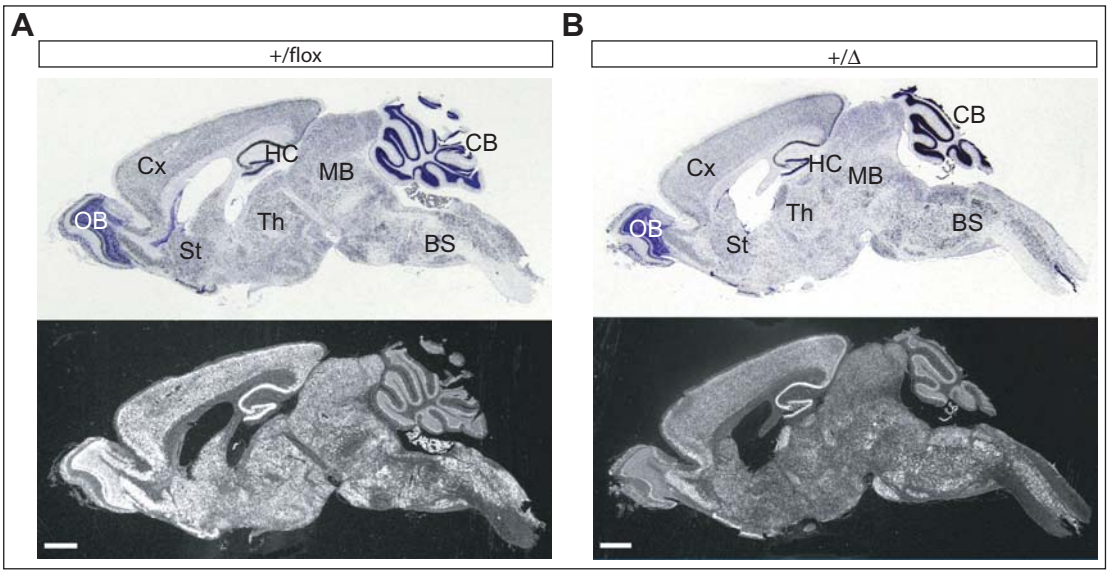

Fig. 24: Reduction of *Braf* mRNA in the adult forebrain of shBraf$^{+/flox}$ CamKII-cre mice. ISH against *Braf* on sagittal sections shows knockdown of *Braf* mRNA in forebrain regions of adult shBraf$^{+/flox}$ CamKII-cre mice (+/Δ, **B**) compared to shBraf$^{+/flox}$ control mice (+/flox, **A**). Brains from male mice at the age of 15 weeks are shown. OB: olfactory bulb, HC: hippocampus, St: Striatum, fCx: frontal cortex, pCx: posterior cortex, Th: Thalamus, MB: midbrain, CB: cerebellum, BS: brainstem; scale bars: 1 mm.

3.4.5 Reduction of BRAF protein in adult forebrain

On the protein level, BRAF expression was analyzed by Western blotting of protein extracted from different brain regions of control and mutant mice. The olfactory bulb, hippocampus, striatum, cortex (divided into an anterior and a posterior part), thalamus, midbrain (containing the superior and inferior colliculi amongst others), brain-

stem (including parts of the spinal chord), and cerebellum were dissected. Protein was isolated from these tissues and BRAF protein was detected by Western blotting (Fig. 25A). BRAF protein was almost completely lost in hippocampus and thalamus of mutant brains, it was highly diminished in olfactory bulb, striatum, and cortex (frontal part). Only slight reduction of protein levels were observed in the posterior part of the cortex and in the midbrain of shBraf$^{+/flox}$ CamKII-cre mice, whereas no change was observed in brainstem and cerebellum of control and mutant mice.

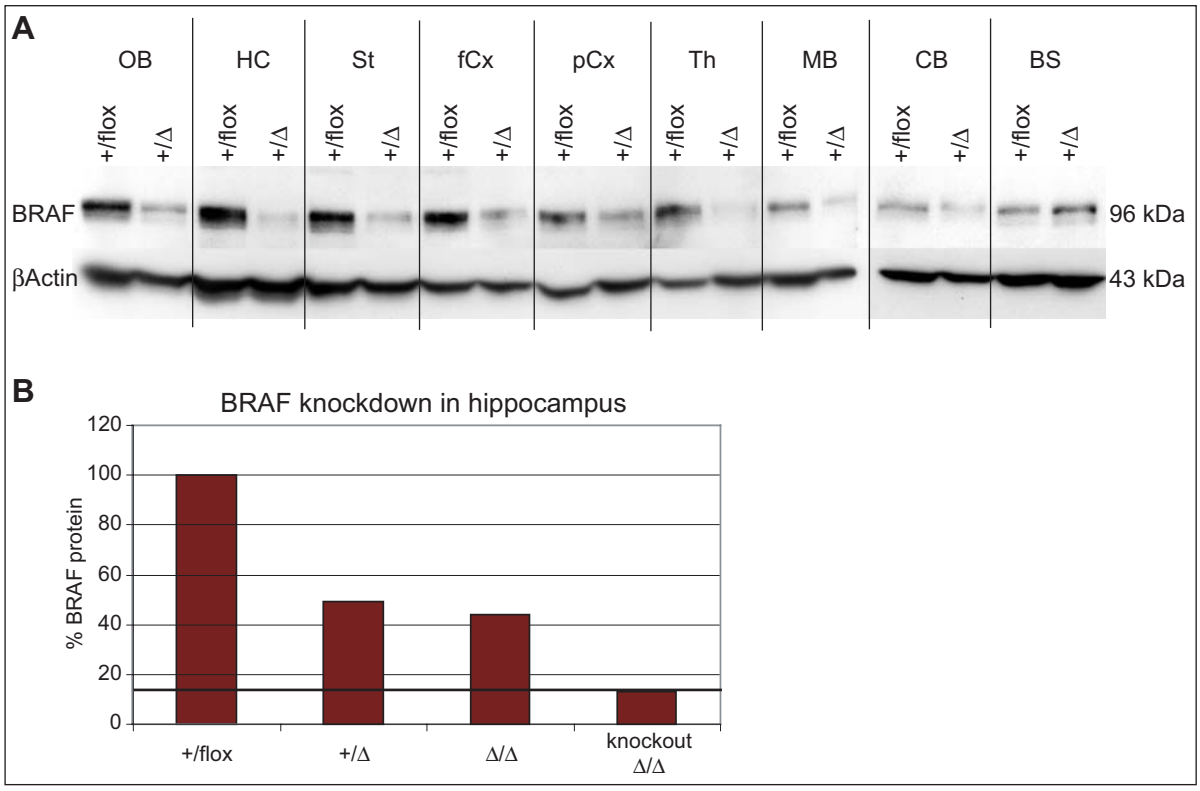

Fig. 25: Reduction of BRAF protein in the adult forebrain of shBraf$^{+/flox}$ CamKII-cre mice. **A**: Western blotting against BRAF shows knockdown of BRAF protein in forebrain regions of adult shBraf$^{+/flox}$ CamKII-cre mice (+/Δ) compared to shBraf$^{+/flox}$ control mice (+/flox). An antibody against β-ACTIN was used as loading control. OB: olfactory bulb; HC: hippocampus; St: striatum; fCx: Cortex, frontal part; pCx: Cortex, posterior part; Th: thalamus; MB: midbrain; Cb: cerebellum; BS: brainstem. **B**: Quantification of BRAF protein level of hippocampus from shBraf$^{+/flox}$ control mice (+/flox) and heterozygous (shBraf$^{+/flox}$ CamKII-cre, +/Δ) and homozygous (shBraf$^{flox/flox}$ CamKII-cre, Δ/Δ) knockdown mice. The protein level of conditional knockout mice (Braf$^{flox/flox}$ CamKII-cre, knockout Δ/Δ) shows the amount of BRAF protein not affected by recombination with CamKII-cre.

Quantification of BRAF protein levels in hippocampus of mutant and control mice showed knockdown of 51% in shBraf$^{+/flox}$ CamKII-cre mice compared to shBraf$^{+/flox}$ control mice. Mice with two copies of shBraf (shBraf$^{flox/flox}$ CamKII-cre mice) showed an only marginally increased knockdown level of 56% compared to control mice (Fig. 25B). The measured values were average protein levels for the entire regions with all cell types existing there. Since Cre recombinase is expressed only in neurons and not

in non-neuronal cells, protein reduction in neurons where Cre recombination took place should be higher than the average values measured here. For comparison, the BRAF protein reduction in Braf conditional knockout (section 3.2.5, p. 24) mice is also shown in Fig. 24B. The remaining 13% protein in these knockout animals reflected BRAF protein expression in non-neuronal cells, which could not be affected by inactivation of *Braf* with CamKII-cre.

3.4.6 Knockdown of *Braf* in the entire body

Since the complete knockout of *Braf* has a dramatic effect on embryonic development (Wojnowski et al., 1997), I tested wether the milder knockdown of *Braf* in the entire body and from early development on showed a similar or different effect than the knockout. For this, shBraf$^{+/flox}$ EIIa-cre mice were generated. Cre recombinase driven by the EIIa promoter is already expressed in oocytes resulting in deletion of the stop cassette in every cell of the animal mimicking an unconditional knockdown (Williams-Simons and Westphal, 1999).

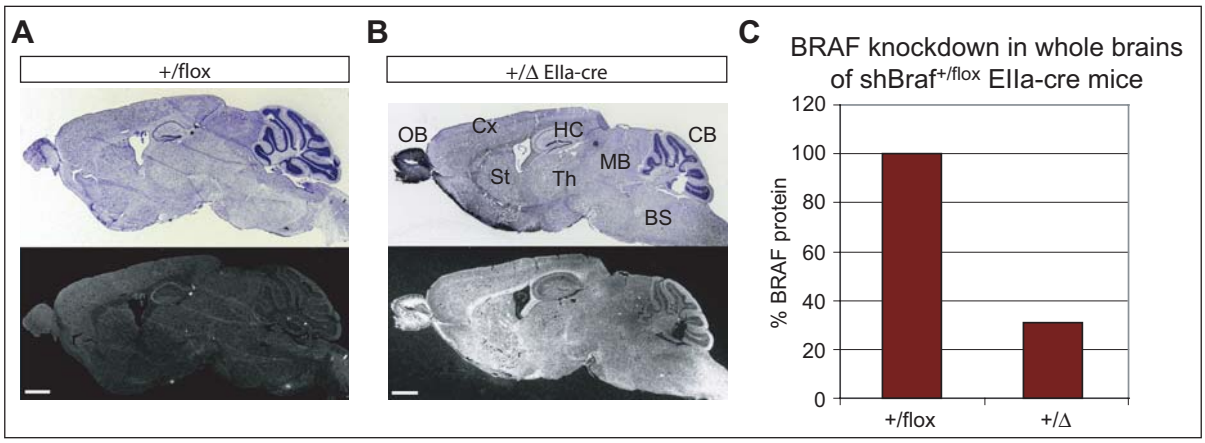

Fig. 26: Unconditional knockdown of *Braf* in shBraf$^{+/flox}$ EIIa-cre mice. ISH shows the expression of shBraf in adult brains of shBraf$^{+/flox}$ EIIa-cre mice (+/Δ EIIa-cre, **B**) but not in shBraf$^{+/flox}$ control mice (+/flox, **A**). OB: olfactory bulb, HC: hippocampus, St: Striatum, Cx: cortex, Th: Thalamus, MB: midbrain, CB: cerebellum, BS: brainstem. **C**: Quantification of BRAF protein level in whole adult brains from shBraf$^{+/flox}$ control mice (+/flox) and heterozygous (shBraf$^{+/flox}$ EIIa-cre, +/Δ) unconditional knockdown mice.

shBraf$^{+/flox}$ EIIa-cre mice survived embryonic development without any obvious defects. They were born and grew up as their littermate controls. Regarding the adult brain, shBraf was expressed in all regions of the brain as shown by an ISH against shBraf (Fig. 26A and B); but the level of shBraf seemed to vary between different brain regions. So in the olfactory bulb, the striatum, and the spinal chord signal for shBraf was very strong, whereas the signal in the cerebellum and the midbrain was quite low

(Fig. 26B). Western blotting of protein from whole brains of shBraf$^{+/flox}$ EIIa-cre mice showed 30% remaining BRAF protein compared to control animals (Fig. 26C).

3.5 Knockdown of *Mek1* and *Mek2* in adult brain

Mek1 and *Mek2* are downstream of *Braf* in the MAPK pathway. To further dissect this signaling cascade, I generated knockdown mice against *Mek1* and *Mek2*. Up to now, no studies have been performed by knocking out these genes in the adult brain and most of the knowledge about the function of *Mek1* and *2* in learning and memory formation has been gained by the use of pharmacological inhibitors. In addition, two genes with such a high homology in their mRNA sequence, like *Mek1* and *2*, are good targets to use the advantage of RNAi to generate double knockdown mice easily and rapidly.

3.5.1 The shMek1/2-flox mouse

The generation of shRNA mice against *Mek1* and *Mek2* is described in section 3.3, p. 24. shMek1/2-flox mice harbored one shRNA expression cassette against both *Mek* genes in the *Rosa26* locus. ShRNA expression in these mice was interrupted by a loxP flanked stop cassette, which could be excised by Cre recombinase, which in turn activated shRNA expression. Mice harboring one or two shMek1/2-flox alleles were all normal and showed no obvious differences to their wildtype littermates.

3.5.2 Expression of Cre recombinase under the Nestin promoter

To express Cre recombinase in the entire nervous system of adult mice, the Cre transgene was controlled by the rat Nestin promoter and enhancer. This Nestin-cre mouse line was generated by Tronche et al. (1999) via injection of an expression vector into mouse oocytes. The construct consisted of the rat Nestin promoter upstream of the Cre recombinase, a human growth hormone polyadenylation signal, and the nervous system specific enhancer from the second intron of the rat Nestin gene. Mice were kept on a C57Bl/6J background for all breeding purposes.

Cre recombinase is expressed in neuronal and glial cell precursors starting at embryonic day 11 (Zimmerman et al., 1994; Tronche et al., 1999). Although expression of Cre recombinase does not last until adulthood, recombined alleles are expected in the whole adult nervous system, including the entire brain, since Cre expression in the precursor cells is sufficient to transmit the recombined allele to the mature neurons and glia cells.

3.5.3 Breeding of conditional shMek1/2-flox Nestin-cre mice

Germline transmission was obtained with the ES cell clone 81F2 (see section 3.3.6, p. 37). These mice were on a mixed background of 129SvEv/Tac and C57Bl/6J, since the F1 ES cells used for mouse generation were a mixture of two strains. Upon crossing the chimeras with wildtype C57Bl/6J mice, one generation of backcrossing was performed. Intercrosses of shMek1/2$^{+/flox}$ mice generated shMek1/2$^{flox/flox}$ mice, which were mainly used for breeding with Nestin-cre mice to activate shRNA expression in the nervous system of adult mice. Offspring originating from these matings were to 50% of the genotype shMek1/2$^{+/flox}$ (control mice) and to 50% shMek1/2$^{+/flox}$ Nestin-cre (mutant mice). Since the Nestin-cre mice were on pure C57Bl/6J background, this breeding step represented a further backcrossing to C57Bl/6J. Alltogether, shMek1/2-flox mice were backcrossed to C57Bl/6J mice for two generations to enrich the C57Bl/6J background as much as possible in the given time-frame. The proportion of C57Bl/6J genome in the genetic background of the shMek1/2-flox mice for analysis averaged to 87%. For test experiments, shMek1/2$^{flox/flox}$ Nestin-cre mice carrying two shMek1/2 alleles were generated by mating shMek1/2$^{+/flox}$ Nestin-cre mice with shMek1/2$^{flox/flox}$ mice.

3.5.4 Deletion of the stop cassette and expression of shMek1/2

To check if the shRNA against *Mek1/2* was activated upon Cre mediated recombination in the entire adult brain, Southern blotting with DNA from different brain regions was performed. The olfactory bulb, hippocampus, striatum, cortex (divided into an anterior and a posterior part), thalamus, midbrain (containing the superior and inferior colliculi amongst others), brainstem (including parts of the spinal chord), and cerebellum were dissected. DNA was isolated from these tissues and digested with BamHI. Detection of the different alleles with the Rosa5'probe showed the allele with the deleted stop cassette (8.6 kb) in all brain regions from shMek1/2$^{+/flox}$ Nestin-cre mice instead of the floxed allele (5.4 kb), but not in tissue (pooled from all the regions dissected) from shMek1/2$^{+/flox}$ control mice (Fig. 27A).

To assure that the shRNA was expressed after Cre recombination, the siRNA against *Mek1* and *2* was detected on a Northern blot with small RNAs. Therefore, small RNAs were isolated from adult brains and the siRNA against *Mek1* and *2* was detected with a specific oligonucleotide probe. The 23 nt band was detected in mutant shMek1/2$^{+/flox}$ Nestin-cre mice, but not in control animals (Fig. 27B). This indicated that the stop cassette indeed blocked transcription of the shRNA *in vivo* sufficiently.

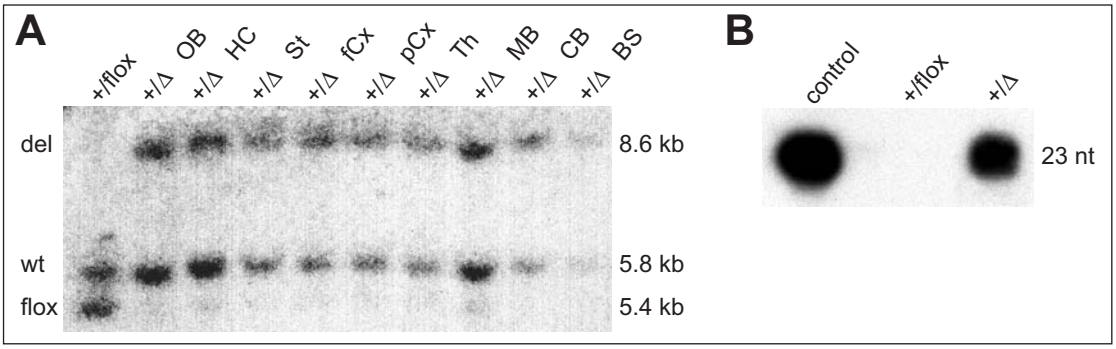

Fig. 27: Activation of shRNA against *Mek1* and *2* in the adult brain with Nestin-cre. **A**: Southern blot analysis of BamHI digested genomic DNA from different brain regions of adult shMek1/2$^{+/flox}$ Nestin-cre mice shows Cre mediated deletion of the stop cassette. Lane 1: DNA from whole brains of shMek1/2$^{+/flox}$ control mice (+/flox); lane 2-10: DNA from indicated regions of shMek1/2$^{+/flox}$ Nestin-cre mice (+/Δ). The wildtype *Rosa26* allele (wt) gives a 5.8 kb band and the band from the shRNA allele is shifted from 5.4 kb with the stop cassette (flox) to 8.6 kb after Cre recombination (del). OB: olfactory bulb, HC: hippocampus, St: Striatum, fCx: frontal cortex, pCx: posterior cortex, Th: Thalamus, MB: midbrain, CB: cerebellum, BS: brainstem. **B**: On a Northern blot with small RNAs against the sequence of shMek1/2, the 23 nt band of the processed siRNA against *Mek1* and *2* is only detectable with the control oligonucleotide and in mutant mice but not in control mice.

3.5.5 Reduction of *Mek1* mRNA in adult brain

Mek1 mRNA level in mutant mice compared to control mice was assessed quantitatively by Northern blotting and qualitatively by ISH. Since the *Mek2* mRNA level was very low in wildtype brains (see section 3.1.4, p. 15), it was not possible to quantify the *Mek2* knockdown effect on this level. But for *Mek1*, Northern blotting of mRNA from whole brains showed a significant decrease in *Mek1* mRNA in shMek1/2$^{+/flox}$ Nestin-cre mice compared to control mice (Fig. 28A). Quantification of the mRNA levels on the Northern blot indicated a remaining amount of *Mek1* mRNA in mutant brains of 35% of the wildtype level (Fig. 28B).

For qualitative analysis of *Mek1* mRNA distribution, paraffin sections from adult mutant and control brains were hybridized with the *Mek1* ISH probe (Fig. 28C and D). The signal was decreased significantly in all brain regions. Only in areas with very high *Mek1* expression in wildtype brains, like the CA3 region of the hippocampus or the piriform cortex, more than only weak signals were still detectable.

3.5.6 Reduction of MEK1 and MEK2 protein in adult brain

On the protein level, MEK protein expression was analyzed by Western blotting of protein extracted from different brain regions of control and mutant mice. The olfactory bulb, hippocampus, striatum, cortex (divided into an anterior and a posterior part), thalamus, midbrain (containing the superior and inferior colliculi amongst others), brain-

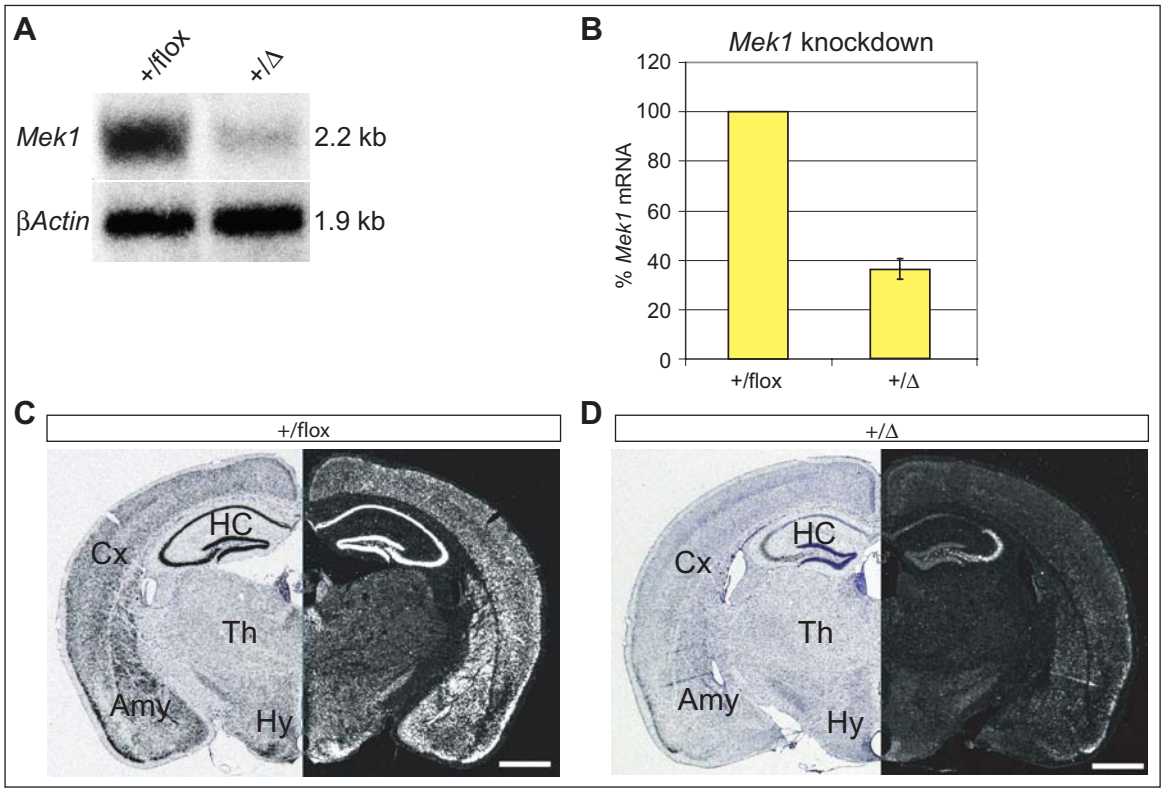

Fig. 28: Reduction of *Mek1* mRNA in the adult brain of shMek1/2$^{+/flox}$ Nestin-cre mice. Northern blotting of mRNA from shMek1/2$^{+/flox}$ Nestin-cre mice (+/Δ) reveals the reduction in *Mek1* mRNA compared to shMek1/2$^{+/flox}$ control mice (+/flox), shown on the Northern blot (**A**) and graphically (**B**). βActin was used as loading control on the Northern blot. ISH against *Mek1* on coronal sections shows knockdown of *Mek1* mRNA in the entire brain of adult shMek1/2$^{+/flox}$Nestin-cre mice (+/Δ, **D**) compared to shMek1/2$^{+/flox}$ control mice (+/flox, **C**). Brains from male mice at the age of 13 weeks are shown. For abbreviations see section 8.1.2, p. 144; scale bars in C and D: 1 mm.

stem (including parts of the spinal chord), and cerebellum were dissected. Protein was isolated from these tissues and MEK1 and 2 were detected by Western blotting (Fig. 29A). The MEK1 protein level was strongly decreased in all brain regions of mutant mice compared to littermate controls. In cerebellum and brainstem, where MEK1 expression in wildtype brains was less intense, MEK1 was only barely detectable in mutant knockdown brains. Also the MEK2 protein level was significantly reduced in all the mutant brain regions, although to a lower extent than for MEK1.

Quantification of MEK protein levels in the entire adult brain of mutant and control mice showed 61% decrease in MEK1 and 44% decrease in MEK2 protein in mutant mice compared to littermate controls. Mice with two copies of shMek1/2 (shMek1/2$^{flox/flox}$ Nestin-cre mice) showed an only marginally increased MEK2 knockdown level of 48% compared to control mice. But the MEK1 reduction was with 71% in homozygous mutants higher than in heterozygous mice (Fig. 29B).

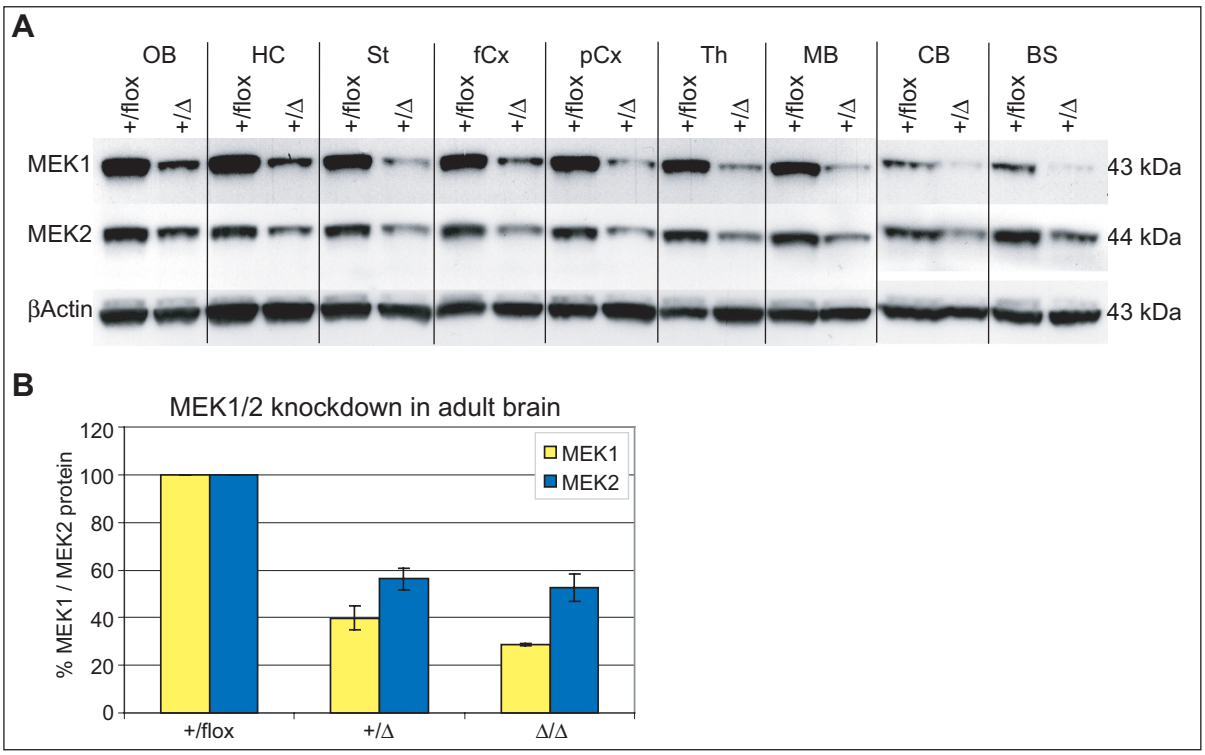

Fig. 29: Reduction of MEK1 and MEK2 protein in the adult brain of shMek1/2$^{+/flox}$ Nestin-cre mice. **A**: Western blotting against MEK1 and MEK2 shows knockdown of MEK proteins in all brain regions of adult shMek1/2$^{+/flox}$ Nestin-cre mice (+/Δ) compared to shMek1/2$^{+/flox}$ control mice (+/flox). An antibody against β-ACTIN was used as loading control. OB: olfactory bulb, HC: hippocampus, St: Striatum, fCx: frontal cortex, pCx: posterior cortex, Th: Thalamus, MB: midbrain, CB: cerebellum, BS: brainstem. **B**: Quantification of MEK protein levels of entire brains from shMek1/2$^{+/flox}$ control mice (+/flox), heterozygous (shMek1/2$^{+/flox}$ Nestin-cre, +/Δ), and homozygous (shMek1/2$^{flox/flox}$ Nestin-cre, Δ/Δ) knockdown mice (Western blot not shown for homozygous mutants).

3.5.7 Knockdown of *Mek1* and *Mek2* in the entire body

Although the complete knockout of *Mek1* has a dramatic effect on embryonic development, *Mek2* is dispensable for mouse development (Giroux et al., 1999; Belanger et al., 2003), I compared the double knockdown of *Mek1* and *Mek2* to the single knockout in the entire body throughout development. For this purpose, shMek1/2$^{+/flox}$ EIIa-cre mice were generated. Cre recombinase driven by the EIIa promoter is expressed in oocytes resulting in deletion of the stop cassette in every cell of the animal mimicking an unconditional knockdown (Williams-Simons and Westphal, 1999).

ShMek1/2$^{+/flox}$ EIIa-cre mice survived embryonic development without any obvious defects. However, after birth their growth was dramatically retarded and they died at the age of six to seven weeks, even when they were not weaned. Apart from this dramatic general growth deficit and early death, no further obvious changes in the brain or in other organs were observed. To assess the underlying causes for this phenotype, further detailed studies are necessary but beyond the scope of this study.

3.5.8 The shMek1 mouse and MEK1 protein reduction in adult brain

The mouse line shMek1 harbored the same construct as shMek1/2 in the *Rosa26* locus, but with an shRNA sequence targeting only *Mek1*. To activate shRNA expression, the stop element in the loop of the shRNA could be removed by Cre recombination. Germline transmission of the mutant allele was obtained with the ES cell clones 962-15 and 962-19 and a colony was expanded as described for shMek1/2 mice (see section 3.5.3, p. 45). Mice harboring one or two shMek1 alleles were all normal and showed no obvious differences to their wildtype littermates.

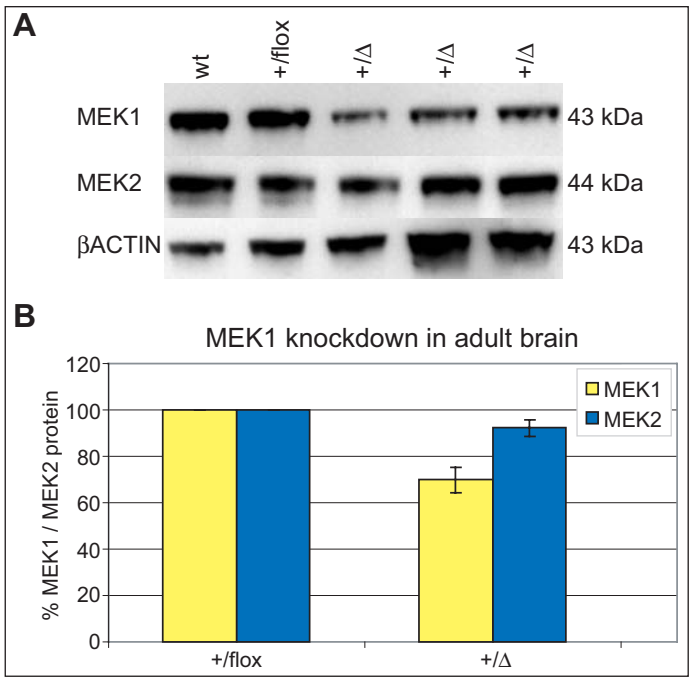

Fig. 30:
MEK1 and MEK2 protein in adult brains of shMek1$^{+/flox}$ Nestin-cre mice. **A**: Western blotting against MEK1 and MEK2 shows marginal knockdown of MEK1 in adult shMek1$^{+/flox}$ Nestin-cre mice (+/Δ) compared to shMek1/2$^{+/flox}$ control (+/flox) and wildtype mice (wt). Specificity of shRNA used is shown by stable protein levels of MEK2 in all genotypes. Protein from three different mutant brains is shown. An antibody against β-ACTIN was used as loading control. **B**: Quantification of MEK protein levels of entire brains from shMek1$^{+/flox}$ control mice (+/flox) and heterozygous knockdown mice (shMek1$^{+/flox}$ Nestin-cre, +/Δ).

Knockdown efficiency for shMek1 *in vivo* was assessed by Western blotting of protein from entire brains of shMek1$^{+/flox}$ Nestin-cre mice and their littermate controls (Fig. 30A). In contrast to the *in vitro* assays, where the level of detectable MEK1 protein was quite low after transfection of the construct expressing shMek1 (see section 3.3.3, p. 31), significantly higher levels of MEK1 were detected in the brains of mutant mice. Quantification of the protein bands by normalization with β-ACTIN revealed only 30% less MEK1 in the knockdown mutants than in control animals (Fig. 30B). On the other hand, MEK2 expression was stable for all genotypes, indicating the specificity of the shRNA for *Mek1* and not for *Mek2*.

3.6 Phenotypic analysis of Braf mutant mice

Mice lacking *Braf* (knockout and knockdown) in the adult forebrain developed normally and showed no obvious abnormalities in gross morphology. But at a closer look,

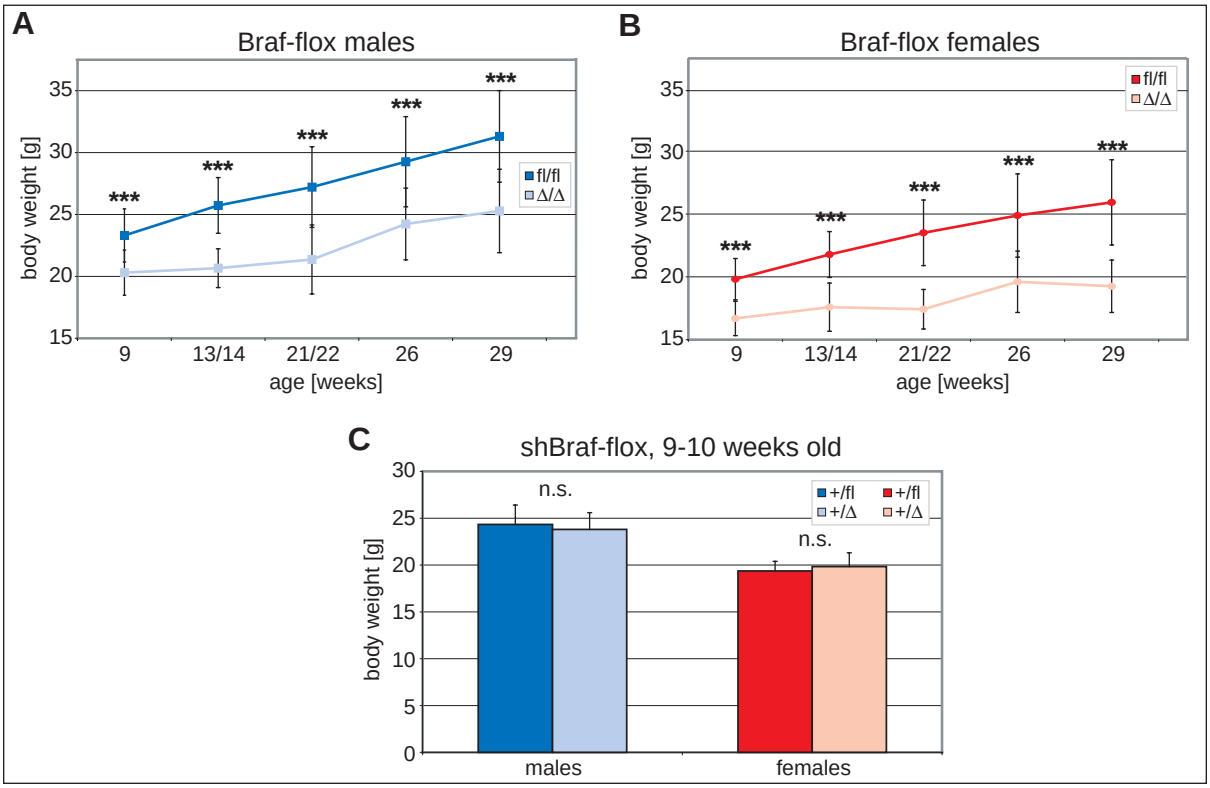

Fig. 31: Body weights of control and mutant mice lacking *Braf* in forebrain neurons. **A**/**B**: Body weight of male (A) and female (B) $Braf^{flox/flox}$ CamKII-cre mice (Δ/Δ) is significantly reduced compared to control animals (fl/fl). **C**: Body weight of male (blue) and female (red) $shBraf^{+/flox}$ CamKII-cre mice (+/Δ) shows no significant difference to control animals (+/fl). n.s.: not significant, ***: $p < 0.001$.

alterations in the body weight of adult mice were visible. In Braf knockout mice, both male and female mutants showed highly significant lower body weight than their littermate controls (t-test: $p < 0.001$; n = 11-29 for each group). Male mutant mice exhibited a weight loss of 15-20% and female mutants of 20-25% (Fig. 31A and B). In contrast to these findings, in shBraf knockdown mice no difference in the body weight between mutant and control mice was found (n = 5-11 for each group at the age of 9-10 weeks; Fig. 31C).

3.6.1 Molecular analysis of loss of *Braf* in adult forebrain neurons

For an initial analysis at the molecular and histological level of Braf mice, the activation or expression, respectively, of molecules downstream to *Braf* was analyzed. Since the MAPK cascade transmits extracellular signals via the activation of several molecules, the signaling was activated to assess any changes in signal transmission on downstream targets. Activation was achieved by a series of mild foot shocks given to the animals. One hour after the treatment, ERK phosphorylation reaches its maximum (Barbara Di Benedetto, unpublished data). First, phosphorylation of ERK1/2 was

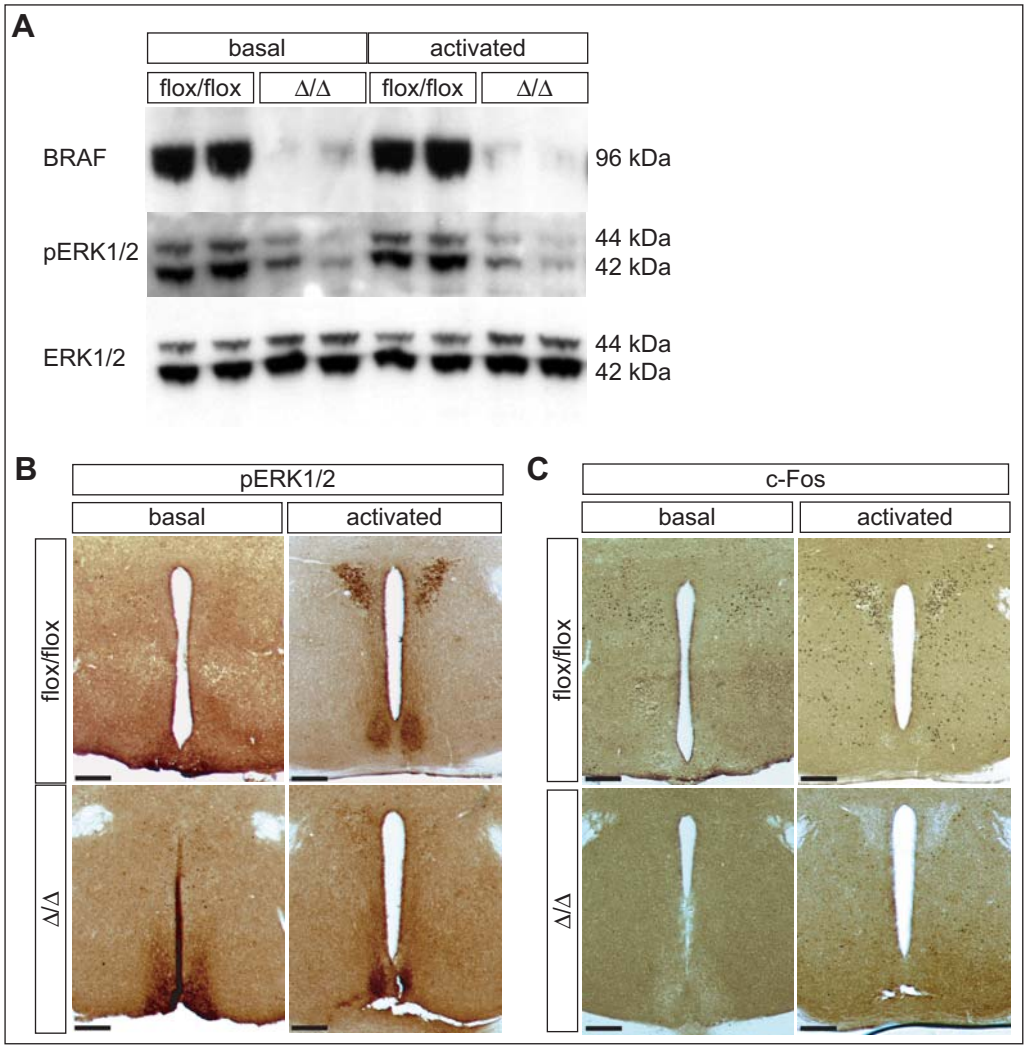

Fig. 32: Effect of loss of *Braf* on downstream molecules. **A**: Western blotting of protein from hippocampus of $Braf^{flox/flox}$ control mice (flox/flox) and $Braf^{flox/flox}$ CamKII-cre mutant mice (Δ/Δ) shows the loss of BRAF in mutants. Reduction of pERK1/2 is shown in the basal as well as in the activated state of mutant mice. An antibody against total ERK1/2 detects an equal amount of protein in both genotypes and activation states. **B**/**C**: IHC for pERK1/2 (B) and c-Fos (C) shows protein expression in the hypothalamus of control (flox/flox) and mutant (Δ/Δ) mice following foot shock (activated) or control treatment (basal). Scale bars in B and C: 2.5 mm.

analyzed by Western blotting of hippocampal protein. Results showed that in mutant mice, lacking BRAF in the hippocampus, a much lower level of phosphorylated ERK1/2 (pERK1/2) was present in the activated state after foot shock, but the differences were also detectable in the basal state. This change in pERK1/2 level was only due to a blocked ERK activation and not due to altered ERK expression, since the total ERK1/2 level was not changed (Fig. 32A).

By immunhistochemistry (IHC) the pERK1/2 activation in the hypothalamus was assessed. Here, pERK1/2 signal increased dramatically after the foot shock compared to the basal state in control animals. Although a signal in single cells was already

visible in the basal state of mutant mice, activation by the foot shock was completely blocked in these animals (Fig. 32B). In the same brain region expression of c-Fos protein, a downstream target of ERK1/2, was strongly increased after foot shock in controls. In mutant $Braf^{flox/flox}$ CamKII-cre mice, however, only very few cells were stained for c-Fos in the activated state. Even the lower c-Fos expression in the basal state was completely abolished in mutant animals (Fig. 32C).

3.6.2 Behavioral analysis of loss of *Braf* in adult forebrain neurons

All behavioral tests were carried out in the GMC. Data acquisition and analysis was performed in cooperation with the subgroup "Behavior", under supervision of Dr. Sabine Hölter-Koch.

- Modified Holeboard

In the modified Holeboard test (mHB) spontaneous behavior of Braf mice in a novel environment was analyzed. Values for all parameters measured are listed in section 8.2.1, p. 146. The most prominent alteration in mutant animals was the locomotor activity. At the beginning of the test, mutants of both sexes started activity significantly later than controls as indicated by the increased latency to the first line crossing (ANOVA: $p < 0.05$; $n = 11\text{-}16$ for each group; Fig. 33A). However, the total number of line crossings and the total distance traveled during the entire test phase was not altered. After the initial delay to the first line crossing, mutants moved faster in the test arena. The mean as well as the maximum velocity was highly increased in mutant mice of both sexes (ANOVA: $p < 0.001$; Fig. 33B). Fig. 33C shows two representative examples of the pathway traveled by control and mutant animals, visualizing the altered forward locomotor behavior of mutant Braf mice. Mutants traveled along long and straight lines, repeating the same passage several times. Additionally, mutant animals stayed averaged closer to the walls of the arena than controls (ANOVA: $p < 0.001$; Fig. 33D).

Regarding the vertical exploratory behavior, indicated by rearing, mutant mice showed a strongly decreased activity than controls. They reared less in the box (ANOVA: $p < 0.001$; Fig. 33E) and not at all on the board (ANOVA: $p < 0.001$; Fig. 33F). At the same time the latency to the first rearing in the box was highly reduced in mutants (ANOVA: $p < 0.05$).

Social affinity tested within the mHB was shown by the contacts of the test animal to its home cage group near the test arena. Mutant animals of both sexes had significantly more group contacts (ANOVA: $p < 0.01$; Fig. 33G), accompanied by a tendenti-

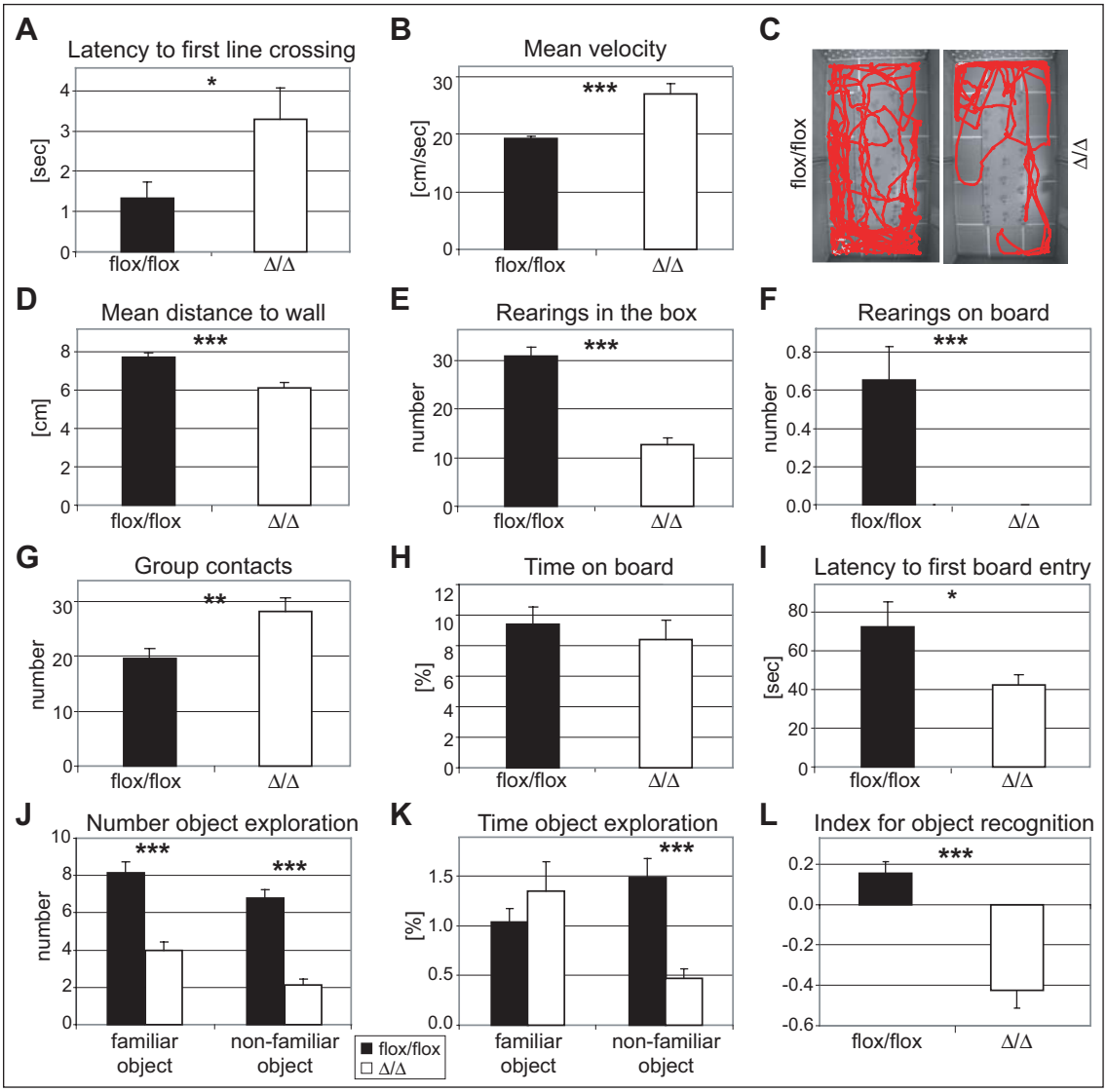

Fig. 33: Behavior analysis of Braf mice in the mHB. Locomotor activity is shown by the latency to the first line crossing (**A**), mean velocity during the entire test phase (**B**), and mean distance to the wall of the box (**D**). Two representative pathways (red) traveled by control and mutant animals are shown in **C**. The number of rearings in the box (**E**) and on the board (**F**) are altered in mutants, as well as the number of contacts to the home cage group (**G**). Anxiety related behavior is shown by the total time spent on the board (**H**) and the latency to the first board entry (**I**). Object exploration and recognition behavior is shown by the total number (**J**) and time (**K**) of each object's exploration and by the object recognition index (**L**). Males and females are shown in a pooled representation, since no sex specific effect was observed. flox/flox: $Braf^{flox/flox}$, Δ/Δ: $Braf^{flox/flox}$ CamKII-cre, *: $p < 0.05$, **: $p < 0.01$, ***: $p < 0.001$.

ally shorter latency to the first contact. But the total time spent in group contact was not altered between mutants and controls.

Concerning anxiety related behavior measured within the mHB, mutant and control mice exhibited a similar number of board entries and equal time spent on the board (Fig. 33H). Only the latency for the first board entry was decreased in mutants (ANOVA: $p < 0.05$; Fig. 33I).

Exploration of a familiar and a non-familiar object placed in the test arena, indicated changes in horizontal exploratory behavior and memory. The number of explorations of both objects was significantly decreased in mutants of both sexes (ANOVA: $p < 0.001$, Fig. 33J), accompanied by an increased latency to the first exploration attempt (ANOVA: $p < 0.001$). In contrary, total time of exploration was only decreased for the non-familiar object (ANOVA: $p < 0.001$), but not for the familiar one (Fig. 33K). Concerning the memory task, the latter preference of the mutants for the familiar object resulted in a negative object recognition index, whereas the positive object recognition index for control animals shows that these mice were able to distinguish between the known and the unknown object (ANOVA: $p < 0.001$, Fig. 33L). The object recognition index is defined as the difference between the exploration time of the non-familiar object and the familiar one, normalized by the total exploration time.

Taken together, the mHB revealed altered locomotor activity, deficiencies in rearing, increased social affinity, decreased object exploration, and impaired memory performance for Braf$^{flox/flox}$ CamKII-cre mice.

- Light-Dark-Box

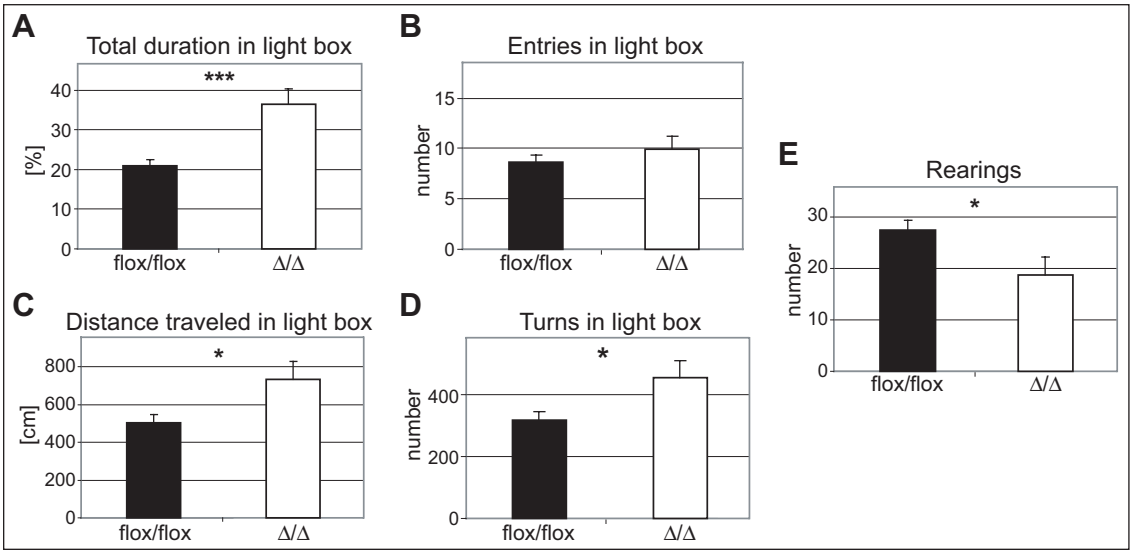

Fig. 34: Behavior of Braf mice in the Light-Dark-Box. Total duration (**A**), number of entries (**B**), distance traveled (**C**), and number of turns in the light compartment (**D**), and total number of rearings in all compartments (**E**) are shown for mutant Braf$^{flox/flox}$ CamKII-cre mice (flox/flox) and control animals (Δ/Δ). Males and females are shown in a pooled representation, since no sex specific effect was observed. *: $p < 0.05$, ***: $p < 0.001$.

Anxiety related behavior was first analyzed with the Light-Dark-Box test. In this task, only genotype specific effects were found for Braf mice. Mutant mice of both sexes spent significantly more time in the light compartment of the box than control animals (ANOVA: $p < 0.001$; $n = 11\text{-}15$; Fig. 34A). However, the number of entries into

the light compartment was not altered (Fig. 34B), indicating an increased duration of each visit of the light box. These observations showed that mutant Braf$^{flox/flox}$ CamKII-cre mice of both sexes had an increased preference for the aversive light compartment than controls. This finding is supported by an increased activity in the light box. Mutant mice traveled a significantly longer distance in the light box (ANOVA: $p < 0.05$; Fig. 34C) and changed the direction more often in this aversive compartment (ANOVA: $p < 0.05$; Fig. 34D). In contrast to this, the total number of rearings in both compartments was reduced in mutants (ANOVA: $p < 0.05$; Fig. 34E).

- Elevated plus maze

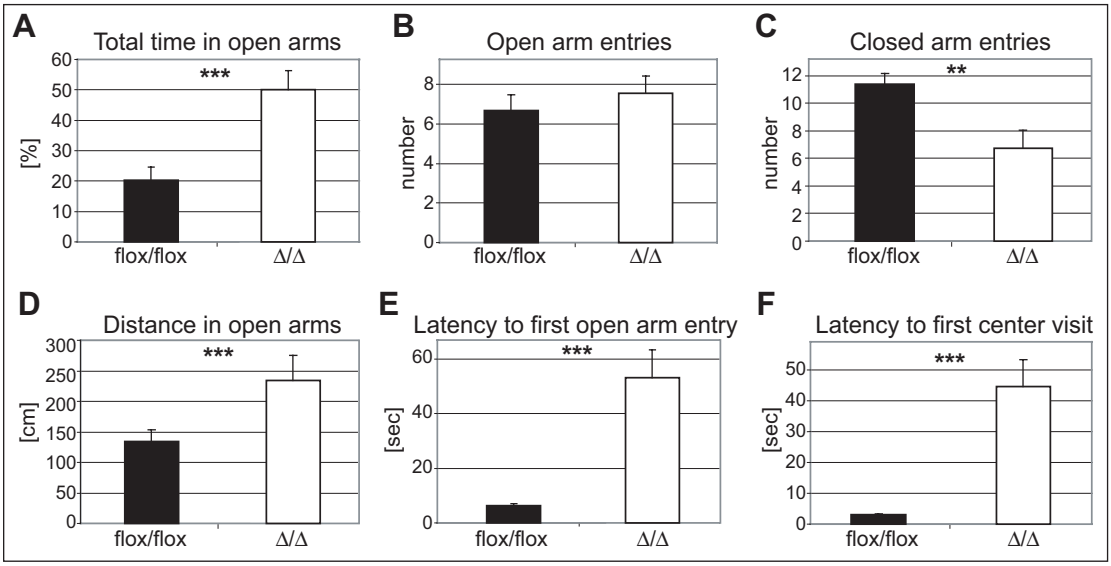

Fig. 35: Behavior of Braf mice in the elevated plus maze. Total duration (**A**) and number of entries in the open arms of the maze (**B**), number of entries in the closed arms (**C**), total distance traveled in the open arms (**D**), and the latencies to the first entry in an open arm (**E**) and to the first center visit (**F**) are shown for mutant Braf$^{flox/flox}$ CamKII-cre mice (flox/flox) and control animals (Δ/Δ). Males and females are shown in a pooled representation, since no sex specific effect was observed. **: $p < 0.01$, ***: $p < 0.001$.

In the second task for the assessment of anxiety related behavior, the elevated plus maze, only genotype specific effects were found for Braf mice. Mutant mice of both sexes spent significantly more time in the open arms of the maze than control animals (ANOVA: $p < 0.001$; $n = 8$-16; Fig. 35A). However, the number of entries to the open arms was not altered (Fig. 35B), indicating an increased duration of each open arm visit. Only the number of entries into the closed arms was decreased in mutants (ANOVA: $p < 0.01$; Fig. 35C). These observations showed that mutant Braf$^{flox/flox}$ CamKII-cre mice of both sexes had an increased preference for the aversive open arms than their control littermates. This fact is supported by an enlarged distance mutants traveled in the open arms (ANOVA: $p < 0.001$; Fig. 35D). But in con-

trast to this, the latency to the first open arm visit was highly increased in mutants (ANOVA: $p < 0.001$; Fig. 35E). Since also the latency to the first center visit was increased in mutants (ANOVA: $p < 0.001$; Fig. 35F), this seems to be due to a delayed start of the exploration of the maze in mutant mice.

- Tail suspension test

In the tail suspension test, indicating motivation and behavioral despair, Braf mice showed no alteration in the time of total activity or immobility, respectively (Fig. 36A). However, the phases of activity and immobility of mutant animals of both sexes were shorter and occurred in a higher frequency than that of controls (ANOVA: $p < 0.001$ for frequency of activity/immobility and mean duration of immobility, $p < 0.05$ for mean duration of activity; n = 9-14 for each group; Fig. 36B and C). According to these observations, the latency to the first immobility phase was significantly decreased in mutant animals (ANOVA: $p < 0.001$; Fig. 36D).

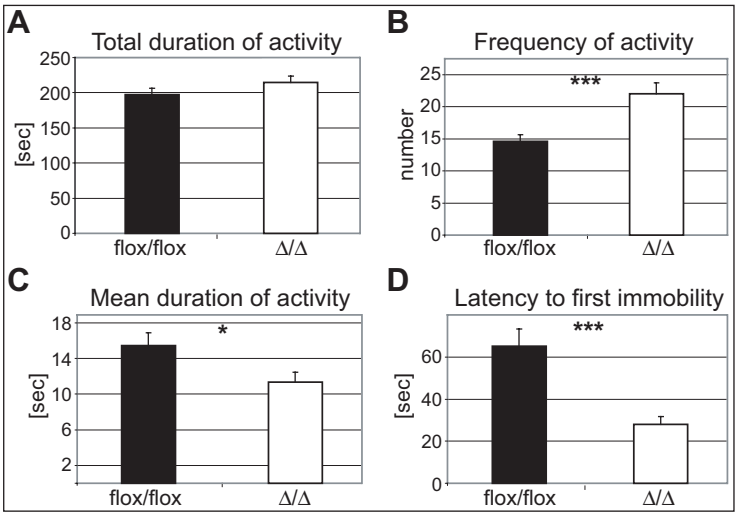

Fig. 36: Activity and immobility behavior of Braf mice in the tail suspension test. Total duration of activity during the 6 min test phase (**A**), frequency (**B**) and mean duration of activity phases (**C**), and latency to the first immobility phase for mutant Braf$^{flox/flox}$ CamKII-cre mice (flox/flox) and control animals (Δ/Δ) are shown. Males and females are shown in a pooled representation, since no sex specific effect was observed. *: $p < 0.05$, ***: $p < 0.001$.

- Forced swim test

The second task for the assessment of motivation and behavioral despair, the forced swim test, revealed genotype and sex specific effects. Mutants of both sexes spent significantly less time actively swimming (ANOVA: $p < 0.001$, n = 15-16 for each group; Fig. 37A). For the total time spent floating (passive behavior) no genotype effect could be detected (Fig. 37B). Looking at different time points during the test phase, also a genotype effect in the second half of the test phase was observed, as

mutants spent less time floating in the last two minutes (ANOVA: $p < 0.01$; Fig. 37E). For the time spent struggling (active escaping behavior), a genotype effect over the entire test phase manifested only in females, since female mutants spent significantly more time struggling than controls (ANOVA: $p < 0.001$; Fig. 37C). This latter observation was even more prominent in the second half of the test phase, where mutants of both sexes struggled significantly more (ANOVA: $p < 0.001$; Fig. 37F).

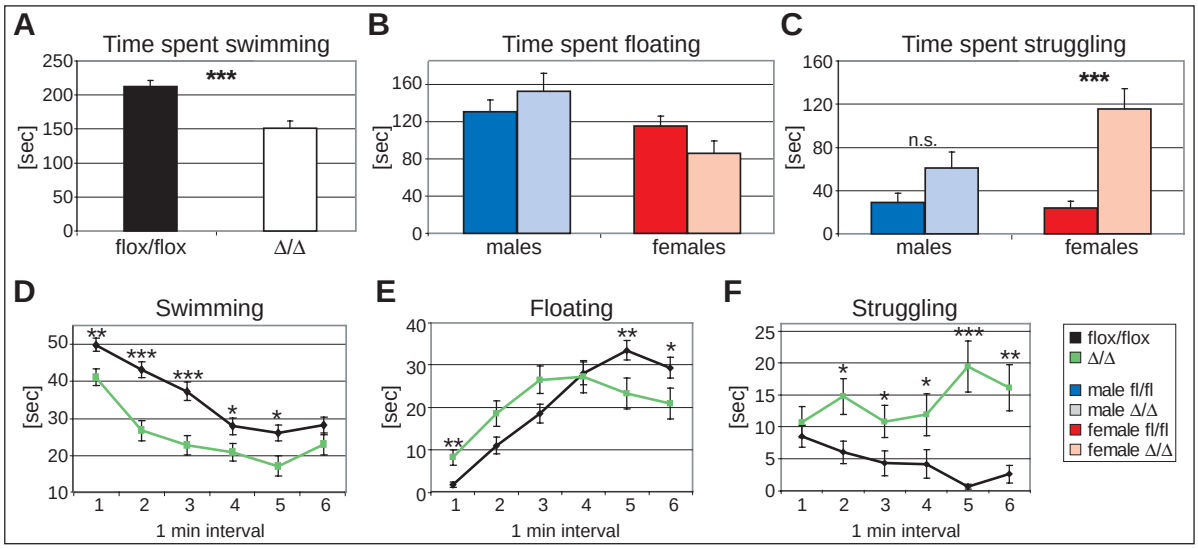

Fig. 37: Behavior of Braf mice in the forced swim test. Time spent swimming (**A**/**D**), floating (**B**/**E**), and struggling (**C**/**F**) during the 6 min test phase are shown for mutant Braf$^{flox/flox}$ CamKII-cre mice (flox/flox, black) and control animals (Δ/Δ, white/green). Total times for the three recorded behavior types are depicted in A-C, and activities in 1 min intervals over the whole test phase are given in D-F. Males and females are shown in a pooled representation in A, D, E, and F, since no sex specific effect was observed. In B and C, data for both sexes are shown separately (males in blue and females in red). n.s.: not significant; *: $p < 0.05$, **: $p < 0.01$, ***: $p < 0.001$.

- Social interaction test

Social behavior as assessed by the social interaction test revealed genotype and sex related differences in Braf mice. Mutant mice of both sexes spent significantly less time with no interaction with the conspecific (ANOVA: $p < 0.05$; $n = 5$-8 for each group; Fig. 38A) and more time with active interaction (ANOVA: $p < 0.001$; Fig. 38B). The latter was indicated by active social behavior like sniffing and grooming, in contrast to passive interaction, which was determined by physical contact without active social behavior. For the time spent in passive interaction a sex difference was revealed. Female control animals spent less time in passive interaction than male controls (ANOVA: $p < 0.05$) and showed no difference to their mutant littermates. However, male mutants spent significantly less time in passive interaction than controls (ANOVA: $p < 0.001$; Fig. 38C).

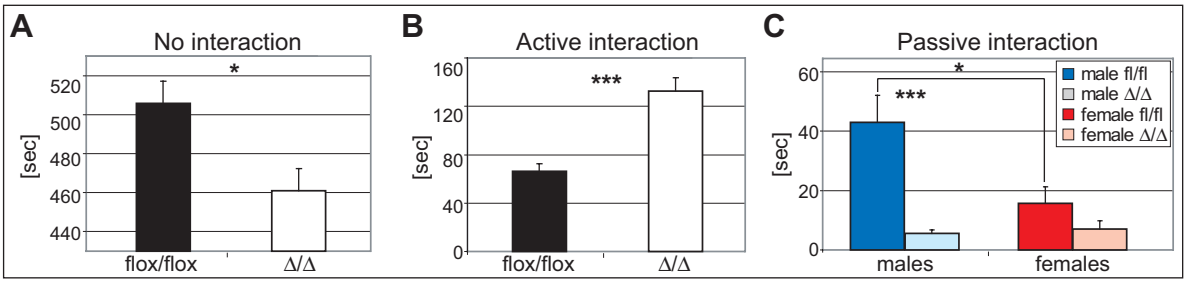

Fig. 38: Investigation time of an unfamiliar subject of the same sex and genotype in the social interaction test of Braf mice. Time spent with no interaction (**A**), active social behavior (**B**), and passive social behavior (**C**) for mutant Braf$^{flox/flox}$ CamKII-cre mice (flox/flox, fl/fl) and control animals (Δ/Δ) is shown. Males and females are shown in a pooled representation in A and B, since no sex specific effect was observed. In C, data for both sexes are shown separately (males in blue and females in red). *: $p < 0.05$, ***: $p < 0.001$.

- Social discrimination test

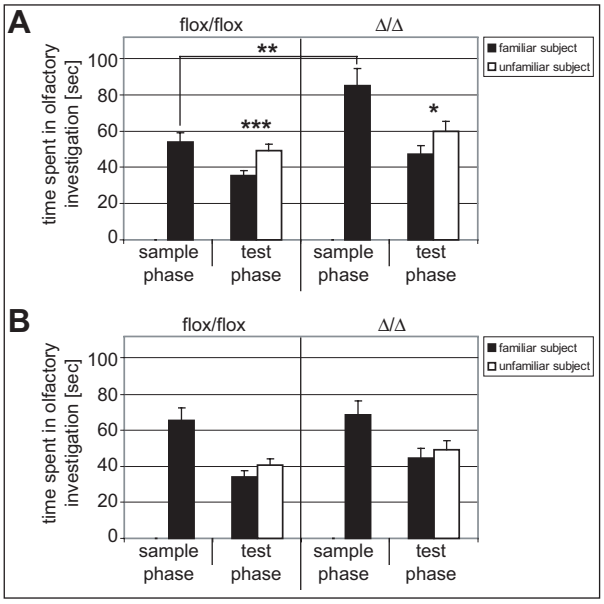

Fig. 39: Social discrimination in Braf mice. Investigation time of a familiar (black) and an unfamiliar subject (white) in males (**A**) and females (**B**) is shown during the sample phase and 2 h after the first exposure to the familiar subject in the test phase. flox/flox: Braf$^{flox/flox}$ control mice, Δ/Δ: Braf$^{flox/flox}$ CamKII-cre mutant mice, *: $p < 0.05$, **: $p < 0.01$, ***: $p < 0.001$. Familiar versus unfamiliar subject and sample phase versus test phase, respectively, were calculated.

The social discrimination test revealed that male Braf mice of both mutant and control genotype did discriminate between familiar and unfamiliar subject since they spent more time investigating the unfamiliar subject during the test phase (t-test: $p < 0.001$ for controls, $p < 0.05$ for mutants; n = 11-15 for each group). Additionally, during the sample phase, where only one subject was presented to the test animal, mutant males spent significantly more time investigating the subject than controls (t-test: $p < 0.01$; Fig. 39A). Nevertheless, female mice, neither controls nor mutants, did not dis-

criminate between the two subjects during the test phase (n = 14 for each group; Fig. 39B). This indicated that the test protocol did not work properly for females, which has been observed previously, since the test paradigm was originally established for male animals (Dr. Sabine Hölter-Koch, personal communication).

- Accelerating rotarod

Motor coordination and balance of Braf mice was assessed by the latency to fall from the accelerating rotarod. Mutant female as well as male Braf$^{flox/flox}$ CamKII-cre mice showed malperformance in this task. The latency to fall from the rotarod was dramatically decreased in mutant animals (ANOVA: genotype effect $p < 0.001$, sex effect n.s.; n = 11-16 for each group; Fig. 40).

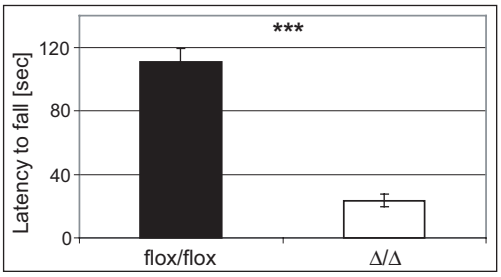

Fig. 40:
Motor coordination and balance of Braf mice. Latency to fall from the accelerating rotarod is significantly reduced in mutant Braf$^{flox/flox}$ CamKII-cre mice (flox/flox) compared to control animals (Δ/Δ). Since no sex specific effect was observed, males and females are shown in a pooled representation. ***: $p < 0.001$.

3.7 Phenotypic analysis of Mek1/2 mutant mice

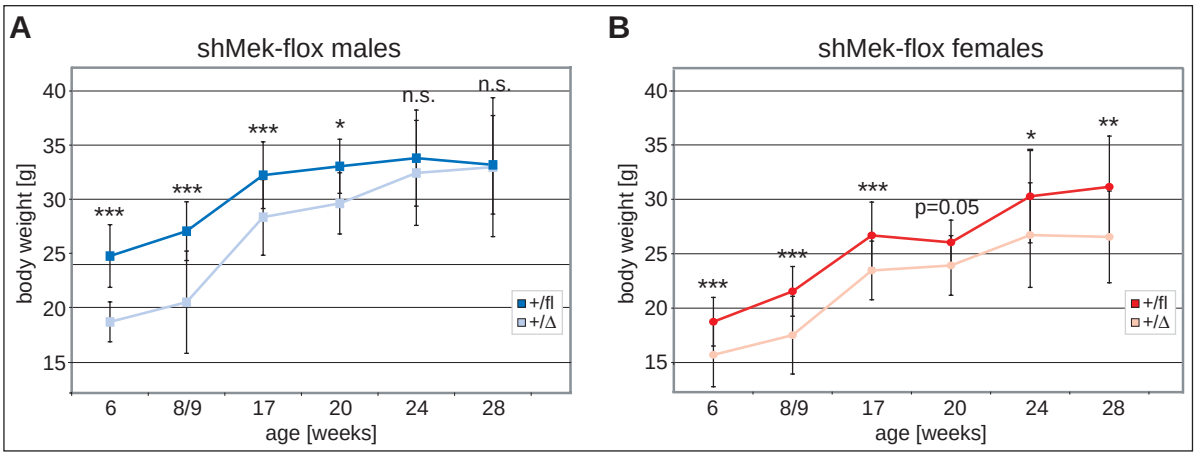

Fig. 41: Body weights of control and mutant mice lacking *Mek1* and *Mek2* in the brain. Body weight from male (**A**) shMek$^{+/flox}$ Nestin-cre mice (+/Δ) is significantly reduced in young mice but reaches the level of controls (+/fl) in older animals. Body weight from female (**B**) shMek+/flox Nestin-cre mice (+/Δ) is significantly reduced compared to control animals (+/fl) throughout life. n.s.: not significant, *: $p < 0.05$, **: $p < 0.01$, ***: $p < 0.001$.

Mice with a reduction of *Mek1* and *Mek2* in the adult nervous system developed normally and showed no obvious abnormalities in gross morphology. At a closer look, alterations in the body weight of adult mice were visible. These body weight diffe-

rences between mutant and control animals changed with age. Until the age of four months shMek$^{+/flox}$ Nestin-cre mutant mice displayed a significantly lower body weight than their littermate controls (25% in males and 15% in females; t-test: $p < 0.001$; n = 12-33 for each group). In the following weeks, male mutants gained so much in weight that they reached an equal level as their control littermates at the age of six months (n = 5-14 for each group; Fig. 41D). In contrast to this, the body weight reduction of 15% in female mutants was quite stable for the observed period (until 28 weeks of age; n = 8-16 for each group; Fig. 41E).

3.7.1 Molecular analysis of reduction of *Mek1/2* in adult brain

For ERK1/2 activation in shMek1/2 mice, animals were subjected to an acute restraint stress procedure. In this test, mice were immobilized for 30 min in small tubes to induce stress and further on to activate pERK1/2. Immediately after the stress procedure pERK1/2 reaches its maximum of activation (Kwon et al., 2006). Levels of pERK1/2, analyzed by IHC, seemed to be slightly reduced in the hypothalamus of naïve mutant brains compared to controls. But after acute restraint stress the ERK1/2 activation reached an equal level in mutant and control hypothalamus (Fig. 42).

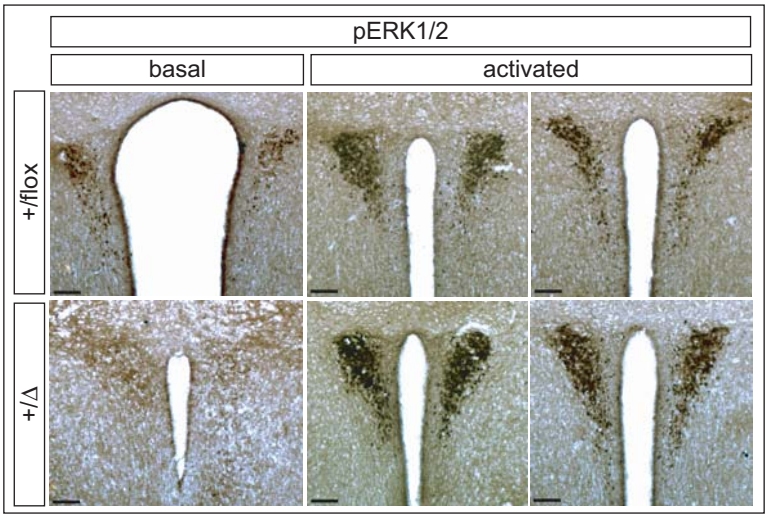

Fig. 42:
Effect of reduction of *Mek1/2* on downstream molecules. IHC for pERK1/2 shows protein expression in the hypothalamus of shMek1$^{+/flox}$ control (+/flox) and shMek1$^{+/flox}$ Nestin-cre mutant (+/Δ) mice following acute restraint stress (activated) or no treatment (basal). Scale bars: 0.1 mm.

3.7.2 Behavioral analysis of reduction of *Mek1/2* in adult brain

All behavioral tests were carried out in the GMC. Data acquisition and analysis was performed in cooperation with the subgroup "Behavior", under supervision of Dr. Sabine Hölter-Koch. For all tests the number of male control animals was lower than supposed, since mutant males revealed strong aggressive behavior against their control cage mates in the IVCs of the GMC, leading to the loss of a number of animals. Due to this aggressive behavior, the surviving control males were separated in single

cages, so that social affinity could not be tested in the mHB, since no home cage group was available.

- Modified Holeboard

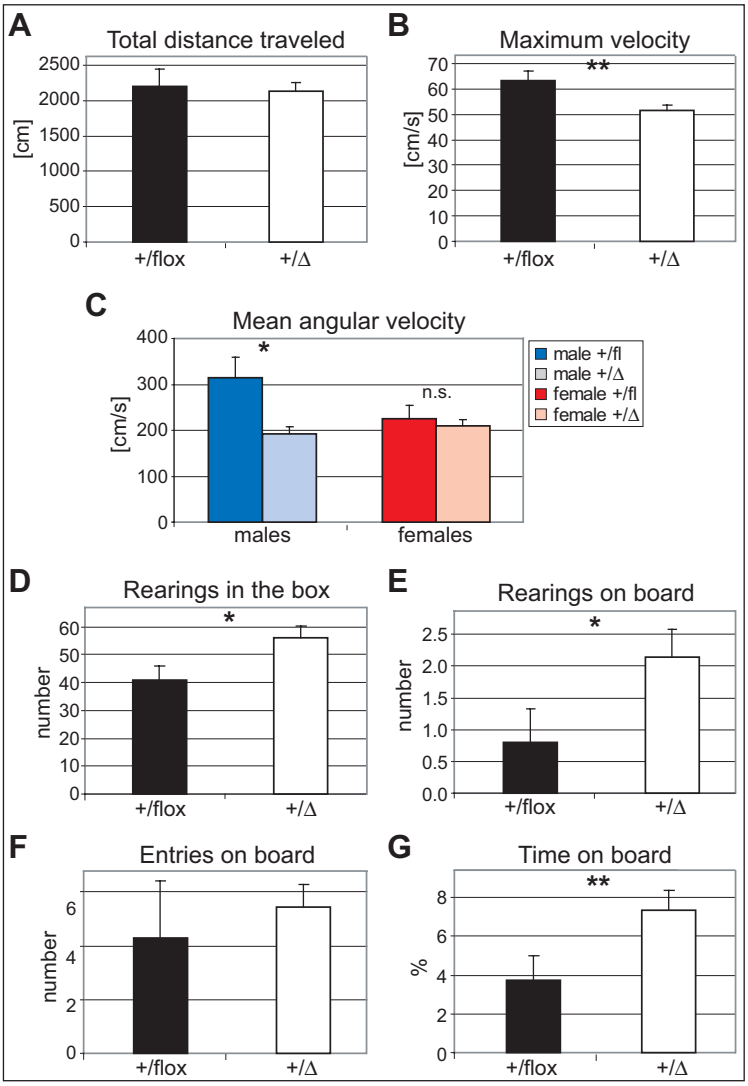

Fig. 43: Behavior analysis of shMek1/2 mice in the mHB. Locomotor activity is shown by the total distance traveled (**A**), maximum velocity reached (**B**), and mean angular velocity (**C**). The number of rearings in the box (**D**) and on the board (**E**) are altered in mutants. Anxiety related behavior is shown by the total number of entries on the board (**F**), and the total time spent on the board during the entire test phase (**G**). Males and females are shown in a pooled representation, since no sex specific effect was observed in the shown parameter. Only in C data for both sexes are shown separately (males in blue and females in red). +/flox: shMek1/2$^{+/flox}$, +/Δ: shMek1/2$^{+/flox}$ Nestin-cre, *: $p < 0.05$, **: $p < 0.01$, n.s.: not significant.

In the mHB spontaneous behavior of shMek1/2 mice in a novel environment was analyzed. Values for all parameters measured are listed in section 8.2.2, p. 149. For locomotor activity, no difference in the total distance traveled by control and mutant mice was measured (Fig. 43A). However, mutants did not reach as high speeds as

controls. The maximum velocity reached by mutants of both sexes was significantly reduced (ANOVA: $p < 0.01$; n = 7-14 for each group; Fig. 43B). The mean angular velocity, displaying how fast the animals turned, was reduced only in male mutants (ANOVA: $p < 0.05$; Fig. 43C).

Regarding the vertical exploratory behavior, indicated by rearing, mutant mice showed an increased activity compared to controls. They reared more often in the box (ANOVA: $p < 0.05$; Fig. 43D) and also on the board (ANOVA: $p = 0.05$; Fig. 43E). The latency to the first rearing was tendentially decreased in mutants on the board (ANOVA: $p = 0.07$) and a decreased latency for males compared to females in the box was revealed (ANOVA: $p < 0.05$).

Concerning anxiety related behavior measured within the mHB, mutant and control mice exhibited a similar number of board entries (Fig. 43F) and no significant difference in the latency to the first board entry. But the total time spent on the board was increased in mutant animals of both sexes (ANOVA: $p < 0.05$; Fig. 43G). So, although mutant shMek1/2 mice did not enter the board more often, each visit on the board was extended.

For all the other parameters measured no genotype or sex specific effects were observed. So, the mHB revealed only a slightly altered locomotor activity, enhanced vertical exploratory behavior, and reduced anxiety related behavior for shMek1/2$^{+/flox}$ Nestin-cre mice.

- Light-Dark-Box

Anxiety related behavior was first analyzed with the Light-Dark-Box test. In this task, male mutant mice spent significantly less time in the light compartment of the box than control males (ANOVA: $p < 0.05$; n = 7-15; Fig. 44A), whereas in female animals no difference was observed. However, the number of entries to the light compartment was not altered, neither in male nor in female mutants, indicating a decreased duration of each visit of the light box for male mutant mice. These observations showed that mutant male shMek1/2$^{+/flox}$ Nestin-cre mice had a decreased preference for the aversive light compartment than control males. This finding is supported by a decreased activity in the light box. Mutant males reared less in the light box (ANOVA: $p < 0.01$; Fig. 44B), traveled tendentially a shorter distance (ANOVA: $p = 0.06$; Fig. 44C), and turned less often in this aversive compartment (ANOVA: $p < 0.05$; Fig. 44D).

In mutant mice of both sexes rearing behavior in the dark compartment was altered. Mutants reared more often in this protected area (ANOVA: $p < 0.001$; Fig. 44E) and showed a reduced latency to the first rearing (ANOVA: $p < 0.05$). However, the

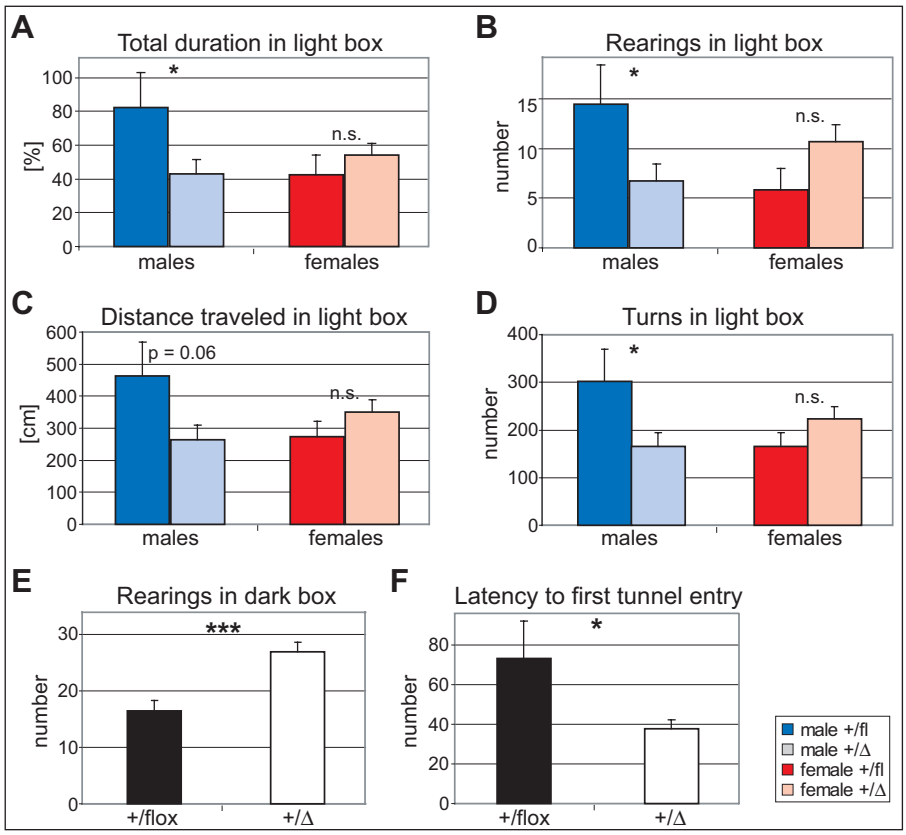

Fig. 44: Behavior of shMek1/2 mice in the Light-Dark-Box. Total duration (**A**), number of rearings (**B**), distance traveled (**C**), and number of turns (**D**) in the light compartment, and number of rearings in the dark compartment (**E**), and latency to the first tunnel entry (**F**) are shown for mutant shMek1/2$^{+/flox}$ Nestin-cre mice (+/flox) and control animals (+/Δ). Data for both sexes are shown separately (males in blue and females in red) in A-D. In E and F, males and females are shown in a pooled representation, since no sex specific effect was observed. *: $p < 0.05$, ***: $p < 0.001$, n.s.: not significant.

increased rearing frequency seemed to be due to the increased time spent in the dark compartment by the male mutants, since the number of rearings normalized by the time spent in the dark compartment revealed no significant alterations. Regarding the tunnel connecting the dark with the light compartment, mutants revealed a decreased latency to the first tunnel entry compared to controls (ANOVA: $p < 0.05$; Fig. 44F). However, they did not enter the tunnel more frequently during the entire test phase.

In total, a strong sex specific effect was observed in the Light-Dark box test of shMek1/2 mice. Male mutants showed increased anxiety related behavior, whereas in female mice no differences were observed in respect to this. In contrary, in the protected area mutants of both sexes revealed an enhanced exploratory behavior.

- Elevated plus maze.

In the second task for the assessment of anxiety related behavior, the elevated plus maze, no significant genotype specific effects were found for shMek1/2 mice (Fig. 45A). Only the trend was observed that mutant mice of both sexes traveled with an

increased mean velocity in the open arms of the maze (ANOVA: p = 0.07; n = 6-14 for each group; Fig. 45B). Additionally, a sex specific effect for the number of entries to the closed arms was observed. Female mice entered the protected arms significantly more often than males (ANOVA: p < 0.05; Fig. 45C).

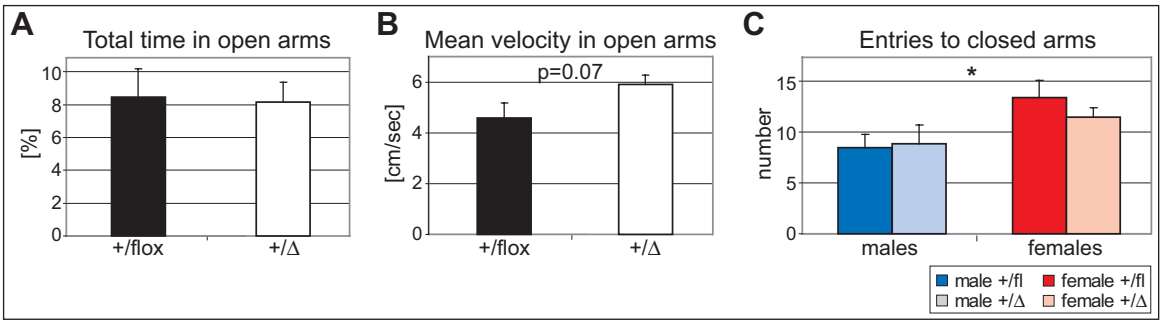

Fig. 45: Behavior of shMek1/2 mice in the elevated plus maze. Total time (**A**) and mean velocity in the open arms of the maze (**B**), and number of entries in the closed arms (**C**) are shown for mutant shMek1/2$^{+/flox}$ Nestin-cre mice (+/flox) and control animals (+/Δ). Males and females are shown in a pooled representation in A and B, since no sex specific effect was observed. In C, data for both sexes are shown separately (males in blue and females in red). *: p < 0.05.

- Tail suspension test

In the tail suspension test, indicating motivation and behavioral despair, for female shMek1/2 mice no genotype specific effects were observed. However, male mutants showed a tendentially decreased activity and therefore increased immobility over the entire test phase (ANOVA: p = 0.07; n = 6-14 for each group; Fig. 46A and B).

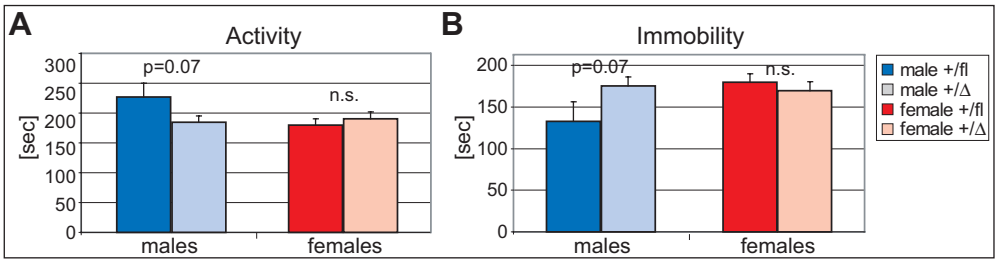

Fig. 46: Activity and immobility behavior of shMek1/2 mice in the tail suspension test. Total duration of activity (**A**) and immobility (**B**) during the 6 min test phase for mutant shMek1/2$^{+/flox}$ Nestin-cre mice (+/flox) and control animals (+/Δ) are shown. Data for both sexes are shown separately (males in blue and females in red). n.s.: not significant.

- Forced swim test

The second task for the assessment of motivation and behavioral despair, the forced swim test, revealed neither genotype nor sex specific effects. All animals tested spent equal time with the three recorded behaviors - active swimming, floating, and struggling - regardless of sex or genotype (Fig. 47).

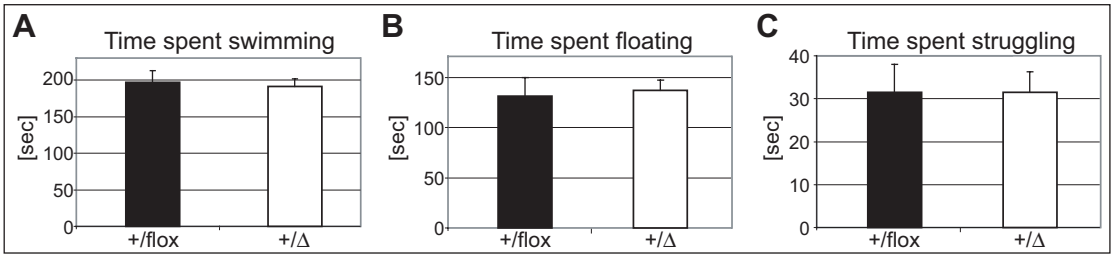

Fig. 47: Behavior of shMek1/2 mice in the forced swim test. Total time spent swimming (**A**), floating (**B**), and struggling (**C**) during the 6 min test phase are shown for mutant shMek1/2$^{+/flox}$ Nestin-cre mice (+/flox) and control animals (+/Δ). Males and females are shown in a pooled representation, since no sex specific effect was observed.

- Social interaction test

Social behavior as assessed by the social interaction test revealed a difference in passive social behavior in shMek1/2 mice. Mutant mice of both sexes spent significantly less time in passive interaction with the conspecific (ANOVA: $p < 0.01$; n = 3-7 for each group; Fig. 48C). For the time spent with no interaction (Fig. 48A) or with active social behavior (Fig. 48B) no genotype or sex specific effects could be observed.

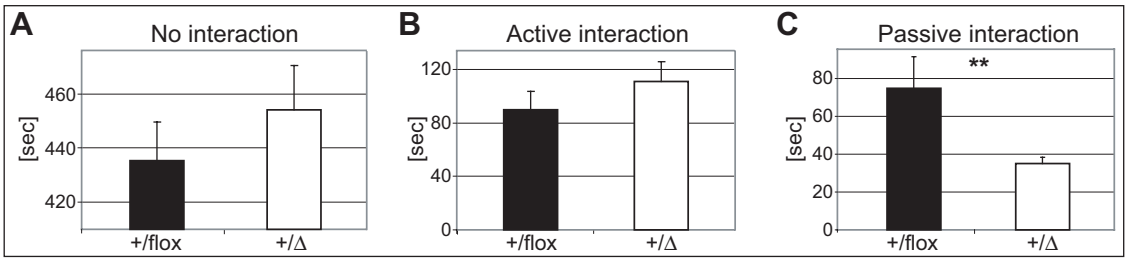

Fig. 48: Investigation time of an unfamiliar subject of the same sex and genotype in the social interaction test of shMek1/2 mice. Time spent with no interaction (**A**), active social behavior (**B**), and passive social behavior (**C**) for mutant shMek1/2$^{+/flox}$ Nestin-cre mice (+/flox) and control animals (+/Δ) is shown. Males and females are shown in a pooled representation, since no sex specific effect was observed. **: $p < 0.01$.

- Social discrimination test

The social discrimination test revealed that shMek1/2 mice of both sexes and genotypes did discriminate between familiar and unfamiliar subject since they spent more time investigating the unfamiliar subject during the test phase (t-test: $p < 0.05$ for male controls, $p < 0.001$ for female controls, $p < 0.01$ for mutants of both sexes; n = 7-16 for each group, Fig. 49). These findings indicate that memory, at least concerning social aspects, is not altered in mutant shMek1/2 mice. Regarding the investigation behavior of both sexes, females spent generally less time investigating one subject

compared to males (note the different scales in Fig. 49A and B). However, this difference did not affect the performance in this test.

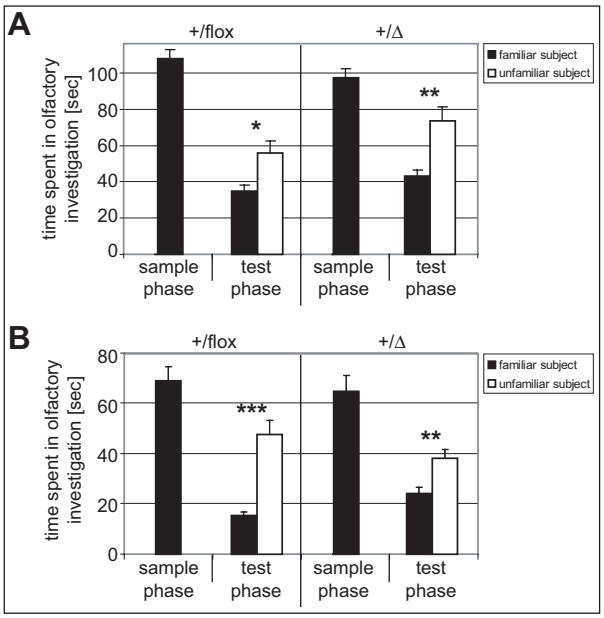

Fig. 49: Social discrimination in shMek1/2 mice. Investigation time of a familiar (black) and an unfamiliar subject (white) in males (**A**) and females (**B**) is shown during the sample phase and 2 h after the first exposure to the familiar subject in the test phase. +/flox: shMek1/2$^{+/flox}$ control mice, +/Δ: shMek1/2$^{+/flox}$ Nestin-cre mutant mice, *: $p < 0.05$, **: $p < 0.01$, ***: $p < 0.001$. Familiar versus unfamiliar subject was calculated.

- Accelerating rotarod

Motor coordination and balance of shMek mice was assessed by the latency to fall from the accelerating rotarod. No significant genotype effect was observed between mutant shMek1/2$^{+/flox}$ Nestin-Cre and control animals (n = 7-14 for each group; Fig. 50).

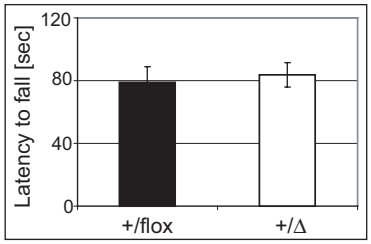

Fig. 50:
Motor coordination and balance of shMek1/2 mice. Latency to fall from the accelerating rotarod is not significantly altered in mutant shMek1/2$^{+/flox}$ Nestin-cre mice (+/flox) compared to control animals (+/Δ). Since no sex specific effect was observed, males and females are shown in a pooled representation.

4 Discussion

4.1 Expression of MAPKs in the adult mouse brain

4.1.1 General considerations for the expression analysis

Among the intracellular signaling pathways, one of the best studied is the canonical MAPK signaling cascade. Activated by various receptor kinases, the MAPK signaling cascade starts with the activation of the RAF kinases which in turn transmit the signal to the MEKs and then downstream to different ERKs. However, despite that the MAPK signaling cascade is hitherto well studied, the biological basis of the differential cellular responses due to its activation is far from being understood. Recently it has been discussed that the duration and strength of the initial signal, that is the activation of the receptors by their ligands, are crucial components of the differential cellular reaction upon its activation. An additional origin of the differential response is maybe the differential expression of components of the MAPK signaling cascade in different cell types. Indeed there are first hints, that not all components of the MAPK signaling cascade are expressed and present in all cell types. Recently, it has been shown that the activation of the canonical MAPK signaling cascade BRAF→MEK1/2→ERK1/2 is restricted to neurons and is not functional in astrocytes in the brain of rats (Dugan et al., 1999). Moreover, it has been described that a direct interaction between BRAF and ERK3 occurs in protein extracts from pyramidal hippocampal neurons, suggesting that this signaling pathway is also restricted to neurons and to the hippocampus (Kim and Yang, 1996).

These examples clearly show that the expression pattern of specific proteins in restricted brain areas is fundamental not only for their biological function in general, but that the differential expression of these proteins has also an important impact on the cell type specific function of molecular networks. Thus, a precise knowledge of the *in situ* expression pattern of genes is necessary to suggest possible functional interactions among activator and effector proteins, i.e. determining cell type and/or brain area specific molecular networks. This is specifically important in the case of signaling pathways in which several but distinct activator and effector proteins are known to exist at different levels of the signaling cascade.

To reveal more details about possible region specific and cell specific activation cascades in the MAPK pathways, I aimed to give a complete description of the differential *in situ* expression of *Braf*, *Mek1*, *Mek2*, and *Mek5* (Fig. 5-9, Tab. 1). In cooperation with Barbara Di Benedetto also the expression patterns of *Erk1*, *Erk2*, *Erk3*, and

Erk5 were described and completed the view on the entire ERK/MAPK cascade (Di Benedetto et al., 2007). The recently shown expression of the members of the MAPK signaling pathway in the CNS by the means of Northern or Western blot analyses does not deliver the spatial information necessary to answer the above posed question about the cellular diversity regarding biological responses to its activation (Brott et al., 1993; Barnier et al., 1995; Ortiz et al., 1995; Morice et al., 1999).

Interestingly, even so in most of the regions examined at least one component of each level of the activation cascade is present, there exist also regions in which only kinases of only one level are present. E.g. in the red nucleus neither *Braf* nor any *Mek* gene could be detected, but it was shown that *Erk*s are well present in this region. This hints towards the hypothesis that the MAPKs present in these regions are activated by alternative pathways (e.g. neurotrophins which also have been shown to activate MAPKs, Simpson et al., 2003) not examined in this study. Another example is the absence of *Braf* from the dentate gyrus (DG) of the hippocampus, indicating that even though BRAF being the most prominent RAF protein in the adult mammalian brain and the most effective kinase in phosphorylating MEK1 and MEK2, it may be possible that in the DG CRAF is responsible for the activation of downstream MEKs (Papin et al., 1996; Wellbrock et al., 2004). So far it is not enough known about the expression pattern of *Craf* in the murine adult brain to prove or to reject this hypothesis (Storm et al., 1990).

Previously published studies always considered *Mek1* and *2* as well as *Erk1* and *2* as two genes with the same function as downstream co-effectors of activators like the NMDA receptors. In contrast to that, I found that in the adult mouse brain the mRNA for *Mek2* is absent from most of the regions, with the exception of very weak signals in subfields of the hippocampus and in few midbrain regions. This indicates that *Mek1* is the main activator of *Erk*s in the adult brain.

For all these results some technical considerations have to be kept in mind. First, one cannot exclude that the expression of low abundant mRNAs was not detected. However, this question was addressed by using the very sensitive technique of radioactive ISH. Furthermore, in cases in which the design of different probes was possible, these distinct probes were tested and the one exhibiting the highest signal intensity was chosen for the study (data not shown). Second, it has to be considered that mRNA expression does not necessarily and completely reflect the expression of the different proteins. Still, the analysis was restricted to the mRNA level because, first, using ISH all different isoforms of one gene could be detected applying one single probe (especially for *Braf* mRNA, which encodes for at least eight different protein

isoforms in the brain, Barnier et al., 1995); and second, for interfering with the MAPK pathway at a genetic level, as used here by specific gene inactivation via RNAi or knockout techniques, the knowledge of the localization of the mRNA and not of the proteins is the crucial factor for the correct design of the experiment.

4.1.2 MAPKs and neurogenesis in the adult brain

Interestingly, the expression study showed that in regions of the adult brain where differentiation of newly generated neurons occurs, like the granular and periglomerular cell layers of the olfactory bulb (OB) or the DG of the hippocampus, specific members of the MAPK signaling pathway are expressed; but their combinations exclude the hypothesis that the canonical MAPK signaling cascade BRAF→MEK1/2→ERK1/2 is activated there. In fact, *Braf* mRNA is absent from all these regions, suggesting that in this process alternative RAF kinases or upstream activator proteins are playing a major role. However, this does not exclude a crucial contribution of more downstream effectors of the canonical MAPK signaling cascade to the neuronal differentiation process. Notably, *Mek1* expression is confined to the granule cell layer of the OB, and also *Erk*s are present in the granule and glomerular cell layer, where new local circuit neurons are undergoing terminal differentiation throughout life. In support of the hypothesis that the MAPK signaling pathway plays a crucial role in neuronal differentiation in the adult central nervous system, it has recently been shown that the activation of receptor kinases via neurotrophins upstream of MAPKs is necessary for the maintenance of the homeostasis between precursor and mature neuronal populations (Simpson et al., 2003). Moreover, recent studies show that neurotrophins are good candidates to contribute to regenerative processes in the OB (Linnarsson et al., 2000; for review see Mackay-Sim and Chuah, 2000).

Interestingly, none of the MAPK signaling components seems to be expressed in the ependymal lining of the olfactory ventricle, nor around the lateral ventricle, regions in which it is known that the neuronal stem cells and the transient amplifying neuronal precursors are located. This exclusion suggests that MAPK signaling is not necessary for the proliferation of adult neuronal stem cells *in vivo*. Indeed recently the WNT signaling pathway has been shown to be crucial for this process (Lie et al., 2005). This promotes a "job-sharing" hypothesis, that these two major signaling pathways cooperate in adult neurogenesis *in vivo*, that means Wnt signaling is responsible for proliferation and MAPK signaling for terminal differentiation.

Similar findings as for the OB neurogenic areas can be described in the second neurogenic region of the adult brain, the DG of the hippocampus. In fact, only *Mek1*

and *Mek5*, among several *Erk*s, are expressed here. The absence of some of the canonical activators of this signaling pathway suggests that also in this neurogenic region alternative upstream factors interact with the expressed MAPK components to regulate their physiological role.

The use of ISH to detect the expression of these genes could be a limiting factor in sensitivity of detection itself, although with the radioactive ISH the most sensitive technique was chosen to perform these analyses. Nevertheless, Western blots performed with protein from different regions of adult mouse brain showed protein expression of BRAF also in the olfactory bulb and MEK2 protein expression in all regions examined (Fig. 25 and 29). These contrary findings between mRNA and protein expression may be due to different sensitivities of detection in ISH and Western blotting. For *Mek2* expression this is quite likely, since almost the entire adult brain is affected by this discrepancy. For *Braf* the additional protein expression in the olfactory bulb may also be due to the detection limit of the ISH, but could equally reflect a real difference between mRNA and protein localization, since only few brain regions are affected. It has also to be considered that the dissection of distinct brain parts can never give such a detailed and accurate impression of the expression pattern due to contamination or inaccuracy upon dissection. Additionally, the expression pattern of *Braf* mRNA itself seems to be affected by strain and/or housing differences. ISH for *Braf* on shRNA control mice, which should reflect a wildtype expression pattern, showed high signals in the OB and in the DG - the neurogenic regions, where the expression study indicated no *Braf* expression (Fig. 24, compare to Fig. 5). Mice for the expression analysis were pure C57Bl/6J males housed in individually ventilated cages in a small room in the GMC. ShRNA mice were on a mixed genetic background of C57Bl/6J (87%) and 129SvEvTac (13%) and were housed in open cages in a huge mouse room. Either *Braf* is differently expressed in C57Bl/6J and 129SvEvTac mice, or - more probably - the housing under higher noise and stress levels in the open cages induced *Braf* expression in neurogenic areas. Therefore, further studies on different mouse strains and under different housing conditions on the mRNA as well as on the protein level would be necessary to elucidate the real role of *Braf* in neurogenesis.

4.1.3 MAPKs and the limbic system: expression in forebrain areas

There is increasing evidence that the RAS-activated RAF→MEK1/2→ERK1/2 pathway can perform critical roles also in terminally differentiated cells, besides the regulation of growth and differentiation in proliferating cells. Moreover, recent findings

suggest that mechanisms that control proliferation and differentiation of neuronal progenitor cells during development, can be responsible for the regulation of synaptic plasticity in the adult nervous system; this could mean that cell cycle activation in neurons and synaptic plasticity are alternative effector pathways (Arendt, 2003; Bichler et al., 2004).

In the limbic system of the rat, the NMDA receptors have been shown to be responsible for activity-dependent synaptic plasticity which leads to acquisition and storage of fear memory in the amygdala and long-term potentiation in the hippocampus through the activation of the ERK/MAPK signaling (Blair et al., 2001; Schafe et al., 2001; Bauer et al., 2002). My findings actually support these models of activation, suggesting that also in the adult brain of the mouse similar modes of activation could occur (English and Sweatt, 1997; Atkins et al., 1998; Schafe et al., 1999; Schafe et al., 2001). Interestingly, I found that in the hippocampus different MAPK members show a restricted regional expression pattern. Namely, among *Mek1* and *Mek2*, only *Mek1* is expressed in the CA1 field, as it is only *Erk2* among *Erk1* and *Erk2*. These findings strongly support the idea that the activation of *Erk2* occurs via *Mek1*, and not via *Mek2* (Xu et al., 1999; Bardwell et al., 2001; Robinson et al., 2002). Regarding another region of the limbic system, the amygdala, it is interesting that most of the components of the canonical MAPK pathway are present in the lateral nucleus, namely *Braf*, *Mek1*, *Erk1* and *Erk2*, but notably, *Mek2* is absent. It has already been shown that ERK/MAPK are phosphorylated in the lateral nucleus of the amygdala in response to fear memory formation in the adult rat brain (English and Sweatt, 1997; Atkins et al., 1998; Impey et al., 1998; Impey et al., 1999; Schafe et al., 2000; Schafe et al., 2001). Our results suggest that this mechanism could also occur in the adult mouse brain, but without activation of MEK2, as far as the findings from the expression study indicate.

Recently it has been reported that the activation of ERK5 in CA3 and DG of the rat hippocampus after cerebral ischemic insult could play a neuroprotective role for the granule cells in these regions (Wang et al., 2005). In addition, Cavanaugh et al. (2001) reported that the MEK5-dependent activation of ERK5 in primary cortical neurons is mediated by neurotrophins, suggesting an alternative role for this part of the MAPK signaling pathway in neuroprotection. Notably, *Mek5* and *Erk5* expression patterns overlap in all the regions of the hippocampus and in the cortical areas.

Mek5 (besides *Erk5* and *Erk3*) is also expressed in the lateral nucleus of the amygdala. This could lead to the hypothesis that the MEK5→ERK5 pathway may be activated also here with neuroprotective functions, as the this is a region of active glut-

amatergic innervation and an excess of glutamate has been shown to exert neurotoxic effects (Nicholls and Attwell, 1990; Rothstein et al., 1996; Gegelashvili and Schousboe, 1997; Kanai, 1997; Tanaka et al., 1997).

Taken together, the results on the expression of these different components of the MAPK pathway give an overview about the regional distribution of these molecules in the adult mouse brain. Based on these data, it is possible to delineate some hypotheses for various brain regions suggesting activation cascades within the MAPKs, alternative upstream activators and functions. So MAPKs may play a role in cell survival and differentiation in the neurogenesis of the OB and DG, but with another upstream activator than BRAF or only upon induction of BRAF expression by mild long term stressors. Signaling via MEK1 and ERK2 might be involved in long term potentiation in the hippocampus and memory formation in the amygdala. The MEK5-ERK5 cascade may contribute to neuroprotective functions in the cortex, in the hippocampus and in the amygdala.

4.2 Conditional gene knockdown in the adult mouse brain

For the analysis of the roles of *Braf* and *Mek1/2* in anxiety and depression related diseases, a new technique to generate mouse models in a fast and easy manner was established. This novel technique uses RNA interference to inactivate one or two related genes in the adult mouse brain. To circumvent possible embryonic lethality due to inactivation of an essential gene in the entire body already during development, a conditional RNAi approach was developed, in which gene knockdown was initiated in a tissue and time dependent manner.

4.2.1 Efficiency of simple and conditional shRNA expression vectors

The human U6 promoter is an RNA polymerase III promoter driving the expression of the endogenous small nuclear RNA *U6* (Kunkel et al., 1986) and is often used to drive the expression of shRNA constructs *in vitro* and *in vivo* (Dykxhoorn et al., 2003). RNA polymerase III promoters do not require far-reaching regulatory elements and transcribe naturally short RNAs. In addition, the transcripts from these promoters also do not harbor long poly-adenylation sequences at their end, since a short polythymidine sequence (a cluster of 4-5 Ts) serves as stop signal (Das et al., 1988). Therefore, RNA polymerase III promoters, especially the human U6 promoter, are ideal promoters to drive shRNA expression.

I designed first several expression vectors with the U6 promoter driving the expression of shRNAs with different target sequences. Upon testing these non-conditional shRNA vectors for their knockdown efficiency *in vitro*, I selected the one or two best vectors for each gene (Fig. 16 and 17). Already at this step it was obvious that the target sequences predicted by different programs, differed a lot in their knockdown efficiencies. This makes it essential to test several sequences *in vitro* before continuing with the experiment.

ShRNA expression from the most efficient constructs was then blocked by the insertion of a transcriptional stop cassette. Previously, various configurations for the positional effect of the transcriptional stop cassette within shRNA vectors have been tested by Dr. Ralf Kühn and the loop region was elucidated as best position for insertion of the stop cassette (Hitz et al., 2007). The stop element is flanked by loxP sites, so that Cre recombinase is able to delete the stop cassette and thereby activate shRNA transcription. It was shown that the insertion of the loxP flanked stop segment into the loop region of shRNA vectors disrupts RNAi induction efficiently and that such vectors can be activated through Cre mediated recombination. After activation, these vectors showed similar knockdown efficiencies as the non-conditional parental constructs. Due to the position of the stop cassette, the loop region of the shRNA transcribed from these expression constructs is elongated by 34 nt. In contrast to former studies asserting a 9 nt loop sequence being the most efficient configuration (Brummelkamp et al., 2002), the elongated loop sequence did not interfere with shRNA efficiency in this case.

In the shRNA vectors tested for *Braf* and *Mek1/2*, the stop cassette resulted in different effects for different target sequences. Before Cre mediated recombination, it blocked the transcription of all shRNA sequences efficiently. But after activation, not all shRNA constructs gave rise to similar knockdown efficiencies as their parental non-conditional constructs (Fig. 18 and 19). So, for some target sequences the elongated loop region seems to disturb RNAi whereas for others it has no effect. Here, I chose the most efficient constructs for mouse production.

4.2.2 Recombinase mediated cassette exchange into *Rosa26* locus

For the genomic integration of shRNA expression vectors, various approaches are available (Gordon, 1993). Transgenic RNAi mice have been generated by pronuclear injection (Hasuwa et al., 2002; Carmell et al., 2003; Coumoul et al., 2005), by lentiviral infection (Ventura et al., 2004) or electroporation of ES cells (Kunath et al., 2003). All these approaches result in random, multicopy integrations of the shRNA

vector and therefore require a laborious analysis of multiple lines due to the influence of the genomic environment and the vector copy number on transgene expression (Kunath et al., 2003; Coumoul et al., 2005). Apart from the time and resources needed for this initial screening of mouse lines, it is not applicable to conditional shRNA vectors since multicopy integrations could undergo unpredictable and non-functional rearrangements through Cre mediated recombination. Hence, a single copy approach using a defined and well-characterized genomic locus is preferable.

The hypoxanthine phosphoribosyltransferase (*Hprt*) and the *Rosa26* locus are frequently used for the genomic integration of expression vectors and have also been used for shRNA vectors (Oberdoerffer et al., 2005; Seibler et al., 2005; Yu and McMahon, 2006). Since the *Hprt* locus is affected by X-inactivation in female mice, I chose the *Rosa26* locus for integration of shRNA vectors. It has been previously shown that conditional shRNA expressed from one vector copy in the *Rosa26* locus gives rise to highly efficient gene knockdown after Cre mediated recombination, comparable to transient transfections of multiple vector copies (Hitz et al., 2007). Thus, the *Rosa26* locus allows effective and reproducible U6 promoter driven transcription of shRNA and the amount of shRNA transcribed from one single vector integrant is sufficient for efficient gene knockdown. The functionality of the U6 promoter within a defined chromosomal locus, like *Rosa26*, provides the basis for conditional RNAi in mice using a single vector copy that is recombined by Cre recombinase into a single, predictable product.

To circumvent the laborious and inefficient homologous recombination step for mouse generation, the recombinase mediated cassette exchange (RMCE) system was used to produce ES cells harboring one copy of the shRNA expression vector in the *Rosa26* locus. With this approach the frequency of properly recombined ES cell clones among selection of positive clones is much higher than with homologous recombination. In this work, for each of the four shRNA constructs selected by the above screenings a stable ES cell line with the conditional shRNA construct in the *Rosa26* locus was established, i.e. one cell line with an shRNA for *Braf*, one for Mek1 and *Mek2* in one shRNA, one for *Mek1* alone, and one for *Mek1* and *Mek2* with two independent shRNAs in tandem.

4.2.3 shRNA mice against *Braf* and Mek

Upon blastocyst injection, all the established ES cell lines gave rise to chimeric mice. Unfortunately, only for three of the four shRNA constructs germline transmission was obtained. For the double knockdown of *Mek1* and *Mek2* with two independent

shRNAs a mouse line could not be established. Mice harboring one of the three other shRNA constructs are viable, fertile, show no overt phenotype, and do not express the specific shRNA before Cre mediated recombination.

I used two different Cre expressing mouse lines - both expressing Cre recombinase in a brain specific manner - to activate shRNA transcription. In shBraf$^{+/flox}$ CamKII-cre mice Cre mediated recombination occurred only in neurons of forebrain regions of the adult brain and in shMek1/2$^{+/flox}$ Nestin-cre mice in all cells of the adult brain, as described previously (Fig. 23 and 27; Minichiello et al., 1999; Tronche et al., 1999). Consequently, in these tissues shRNA expression and reduction of mRNA and protein was detectable. The extent of specific mRNA and protein knockdown reaches ~70% in case of *Braf* and *Mek1* and ~50% for *Mek2* (Fig. 24/25 and 28/29). Important to mention here is, that shMek1/2$^{+/flox}$ Nestin-cre mice produce one shRNA targeting *Mek1* and *Mek2* at once. Although the efficiency of RNAi is not identical for both genes, it shows that it is feasible to knockdown several related genes simultaneously.

For shMek1 mice, harboring an shRNA against *Mek1* only, the protein knockdown efficiency reached only 30%, although the same construct showed a much higher knockdown in transient transfection assays *in vitro* (Fig. 18 and 30). Either the single copy approach is not sufficient for this special shRNA sequence, or different regulatory mechanisms in ES cells and adult neurons affect this shRNA more than others. Due to the low knockdown efficiency, this mouse line was not further investigated.

As the low knockdown efficiency of shMek1 mice suggests, the single copy approach, although working for most of the shRNAs, may not be sufficient for less potent shRNA sequences. In these cases the number of active siRNAs in the cell may limit gene silencing. To test whether increased shRNA levels result in improved knockdown, the residual target gene expression in single copy heterozygous and double copy homozygous shRNA mice was compared for shMek1/2 mice. Only a moderate (~5-10%) but no dramatic increase in knockdown efficiency was observed in homozygous shRNA mice (Fig. 29B).

4.2.4 shRNA mice as fast and easy alternative to knockout mice

The shMek1/2 mice, harboring one shRNA construct for two genes, and the approach for two shRNAs on one construct in tandem show a high potential of this technique in comparison to classical knockout strategies. ShRNA mice will facilitate functional studies of gene families, in which the loss of one gene may be compensated by other family members (Grady et al., 1997; Cammalleri et al., 2006). Addressing such questions with conventional knockout strategies implies an enormous effort of

breeding and genotyping to obtain double or even triple knockout animals. With RNAi, generating multiple knockdown mice is not more effort as compared to single knockdown mice. Furthermore, the production of shRNA expressing mice is much faster and easier than that of knockout mice, especially with the use of RMCE. Thus, in 3-4 months even conditional knockdown mice can be generated whereas at least 12 months are required for the production of a classical unconditional knockout strain. Moreover, the effort of breeding shRNA mice is significantly decreased since only one shRNA allele is required to exert the knockdown of the targeted gene and breeding for homozygosity (as for knockout mice) is not required. In addition, the doubling of the shRNA copy number and the use of different shRNA target sequences offer the option to exploit differences in efficiency of shRNA sequences to produce allelic series as refined models of genetic diseases beyond the "all or nothing" principle of knockout mice (Hemann et al., 2003).

4.2.5 Non-conditional knockdown of *Braf* and *Mek1/2*

In addition to the brain specific activation of RNAi, an initial experiment was performed to compare the effects of the mild knockdown level to the complete knockout in the entire body. By activation of shRNA expression with EIIa-cre mice, which express Cre recombinase already in oocytes, a non-conditional knockdown was mimicked (Williams-Simons and Westphal, 1999). Complete knockout of *Braf* as well as *Mek1* causes embryonic lethality due to placental defects (Wojnowski et al., 1997; Giroux et al., 1999). In contrast to this, shBraf$^{+/flox}$ EIIa-cre mice as well as shMek1/2$^{+/flox}$ EIIa-cre mice were born. This indicates that 30% of the wildtype protein level is sufficient to rescue the developmental defect observed in the knockout animals of both genes. ShBraf$^{+/flox}$ EIIa-cre mice were completely viable and showed no overt phenotype compared to their littermate controls. However, shMek1/2$^{+/flox}$ EIIa-cre mice were dramatically reduced in body size and died at the age of 6-7 weeks, even when they were not weaned and allowed to be nursed by the mother for longer than the usual three weeks. Besides the very small body size, no obvious malformation or phenotype, which may cause the early death of these mutant mice, was observed, so that this phenotype was not further investigated. However, these mutant mice show that 30% of the normal BRAF level is sufficient to overcome all obvious phenotypes, whereas 30% of the normal MEK1 level is only sufficient to overcome the placental phenotype of the complete *Mek1* knockout but causes further dramatic defects in young mice.

4.3 Loss of *Braf* in the adult mouse forebrain

4.3.1 Knockout of *Braf* blocks downstream MAPK signaling

In Braf$^{flox/flox}$ CamKII-cre mutant mice, *Braf* was completely lost in neurons of the adult forebrain. According to the canonical MAPK pathway, in which BRAF activates ERK1 and ERK2 via MEK1 and MEK2 by phosphorylation, ERK phosphorylation was also lost in these mutants, as shown in the hippocampus and hypothalamus (Fig. 32) and already in a previous study by Chen et al. (2006). Upon activation in wildtype cells, ERK translocates into the nucleus and activates numerous substrates, including transcription factors, e.g. ELK1 or CREB. One of the downstream targets of the MAPKs, whose transcription is initiated in this way, is c-Fos, a so called immediate early gene (Cammarota et al., 2000). I could show that in mutant mice lacking BRAF in forebrain neurons c-Fos expression is abolished in the hypothalamus (Fig. 32). These findings show that at least in the brain regions analyzed here the activation of ERK1/2 and thereby the downstream signaling to c-Fos upon foot shock is mediated exclusively by BRAF. So CRAF, the second protein of the RAF family expressed in adult brain (Storm et al., 1990), is not involved in ERK1/2 activation in these regions, or at least, it can not compensate for the loss of BRAF regarding the downstream signaling. Accordingly, no region in the adult brain was found, in which the level of CRAF protein was elevated due to the loss of BRAF (Chen et al., 2006; and data not shown). All this highlights the essential and unique function of BRAF in neurons for MAPK signaling and activation of downstream effectors like c-Fos.

4.3.2 Disturbed behavior in *Braf* deficient mice

Since the loss of BRAF abolished ERK1/2 and c-Fos downstream signaling in adult forebrain, the behavior of Braf mutant mice was dramatically altered. Previously, Chen et al. (2006) described deficits in hippocampus dependent learning and memory and an impaired long term potentiation in Braf$^{flox/flox}$ CamKII-cre mice. It has to be considered that they used a different CamKII-cre mouse line, which has not been extensively described and may have a more restricted expression pattern than the CamKII-cre mouse used in my study. This may explain some discrepancies in the phenotype.

The behavioral test battery applied here for these mice included tests for the assessment of general behavior in a novel environment, anxiety and depression related behavior, social aspects, and motor coordination.

- Locomotion and activity

Most strikingly was a strongly increased stereotypic behavior observed in the home cages as well as in the modified Holeboard (mHB). In the home cages stereotypic behavior was manifested by unrested jumping along the walls of the cage. In the novel environment of the mHB, mutants showed a strikingly altered traveling pathway in the test arena, as they used straight lines more than a zigzag-like exploratory path and they repeated the same passages several times in a stereotypic way (Fig. 33C). This stereotypic behavior may lead to the loss of maternal care, which female mutants showed to their pups, culminating in infanticide. Additionally, the forward locomotion of Braf mutant mice was increased, as indicated by an increased mean velocity in the mHB and an increased distance traveled in the Light-Dark-Box (Fig. 33 and 34).

In contrast to the obvious hyperactivity is the initial immobility Braf mutant mice exhibit in the first seconds in a novel environment. Especially in the elevated plus maze, where the mice were placed at the end of the narrow closed arm at the beginning of the test, the latency to reach the center for the first time was dramatically enhanced (Fig. 35F). Not so prominent but still remarkable was this effect in the mHB, where the latency for the first line crossing was increased (Fig. 33A). In the Light-Dark-Box, an enhanced latency was not observed. The first locomotor parameter measured in this test is the first tunnel entry, which showed no significantly increased latency. Unfortunately, no adequate recording for the initial locomotor behavior in the dark compartment was performed. Concluding from the mHB and the elevated plus maze, Braf mutant mice seem to be initially inhibited in a novel environment, despite their hyperactivity. This immobility is not likely based on neophobia, since animals with increased anxiety in a novel environment show longer phases of immobility or hypoactivity.

- Impaired motor coordination and other affected parameters

Although Braf mutant mice exhibited obvious hyperactivity, they showed strongly impaired motor coordination as assessed by the accelerating rotarod (Fig. 40). Previous studies did not reveal any impairment on the rotarod for *Braf* deficient mice, but as mentioned above, a different expression pattern of Cre recombinase has to be considered for these studies (Chen et al., 2006). With the CamKII-cre strain used here, the impairment in motor coordination seemed not to affect horizontal locomotion. Vertical activity, however, may be affected, as the strongly decreased rearing activity observed in all the tests suggests. Especially in the mHB it was striking that mutant animals reared only one third as often as controls in the box and not at all on the

board. In addition to this, mutants stayed closer to the wall than controls (Fig. 33D-F). These findings may be caused by the impaired motor coordination of the mutants, leading to inability to rear without any assistant wall nearby. Also for any other parameter depending on motor coordination, as the activity phases in the tail suspension test for example, this impairment has to be considered.

- Anxiety related behavior

Anxiety related behavior was assessed in three independent tests and at least in two of them Braf mutant mice showed decreased anxiety. In the Light-Dark-Box, mutants spent more time in the aversive light compartment than controls and in the elevated plus maze, time spent in the open arms was more than doubled in mutants compared to controls. In both cases, the observed effect was not due to the hyperactivity of mutant mice, since the number of entries into the aversive compartments was never increased, indicating not more visits due to enhanced locomotion but increased duration of each visit (Fig. 34 and 35). Also an altered behavior due to impaired vision in mutant animals could be excluded, since Braf mice have been examined for intact vision and differences between mutants and controls have not been found (Dr. Claudia Dalke, data not shown).

Only in the mHB, anxiety related parameters were not so clearly altered. In this test, the board indicates the aversive, unprotected area. However, mutant and control animals spent equal time on the board. The only parameter giving a hint for an anxiolytic behavior in mutants was the latency to the first board entry, which was reduced in mutant animals (Fig. 33). This effect indicated that the aversion for the board was lowered in mutants, so that they entered this compartment earlier during the test phase. However, the question if this effect is based on the general hyperactivity of mutants can not be clearly answered. On the other hand, also the total time spent on the board may be biased by the hyperactive behavior. So, the interpretation of the findings of the mHB is quite difficult and controversial. But together with the highly significant findings of the Light-Dark-Box and the elevated plus maze, it should be undisputed that mutant Braf mice exhibit a robust anxiolytic phenotype.

- Social behavior

The social behavior of Braf mice was mainly assessed by the social interaction test. Also here side effects caused by hyperactivity of the mutants must be considered to influence the results. In the social interaction test mutants spent less time with no interaction with the conspecific than controls. It has to be considered that the enhanced locomotion of mutant animals in the small test arena inevitably leads to an

increased number of contacts with the conspecific. These accidental contacts due to enhanced locomotion should be mainly passive contacts, since no active sniffing or grooming behavior is expected in this case. Remarkably, it was observed that especially mutant males spent less time in passive interaction than control males. This indicates that at least for male mutants the increased time spent in social contact is not accidental. In mutant females, no significant reduction of passive interaction was observed, but also no increase. Additionally, the time spent in active contact to the conspecific was increased in both sexes (Fig. 38). Taken together, the findings indicate enhanced active social interaction of mutants despite their hyperactivity.

Consistent with these findings is the increased number of group contacts measured in the mHB (Fig. 33G). On the other hand, the latency to the first group contact showed a tendency to the opposite direction, so that mutants started later in the test phase to contact their cage mates, and the total duration of group contacts was not altered at all. Together with the stereotypic traveling path of the mutants, described above, the increased number of group contacts in the mHB may be an artifact generated by the repeated usage of the same passages, e.g. along the partition to the home cage group (Fig. 33C). So the findings by the mHB can not be interpreted unequivocally regarding the social behavior of Braf mice, but together with the convincing results from the social interaction test, I suggest an increased social affinity to conspecifics for the mutants.

- Depression like behavior

The forced swim test revealed reduced behavioral despair in Braf mutant mice. Although no alterations in the time spent with floating - as indicator for despair - were observed, struggling - an escaping behavior - was highly increased, especially in the second half of the test phase (Fig. 37). One could argue that the enhanced struggling behavior was due to better condition of the mutants so that they did not exhaust as fast as control animals. Regarding the impairment in motor coordination of the mutants and the fact that they spent less time swimming during the entire test phase, increased physical stamina is very unlikely. So, these findings suggest an antidepressant behavior of mutant animals.

However, the tail suspension test was not consistent with these results. The duration of activity and immobility behavior during the entire test phase was not altered, so no conclusions regarding the antidepressant phenotype can be drawn from this test. At a closer look, the single activity and immobility phases alternated more often at a higher frequency in mutants, revealing some kind of restlessness (Fig. 36). This may be due to reduced physical ability for the active behavior, which may be caused by the

motor impairment. According to this, mutant mice exhausted earlier so that they were physically forced to react with more immobility phases. However, this is speculative. Fact is, that an antidepressant phenotype of Braf mutants could not be observed in the tail suspension test. Either this phenotype is not robust enough to be revealed by different test paradigms, or a potential antidepressant effect in mutants was obscured by the restless behavior in the tail suspension test. All in all, the findings of the forced swim test should not be omitted and so it can be supposed that Braf mutant mice exhibit antidepressant like behavior. Moreover, the specificity of the phenotype for one depression test is not unusual and may give a hint towards the molecular systems affected in the mutants, since there are also some antidepressant drugs known, which show their effect in the forced swim test but not in the tail suspension test (Cryan et al., 2005).

- Memory function

It has already been described that $Braf^{flox/flox}$ CamKII-cre mutants displayed deficits in hippocampus dependent learning and memory functions (Chen et al., 2006). These mice exhibited impaired spatial learning in the Morris water maze, where a hidden platform below the water surface has to be found (D'Hooge and De Deyn, 2001). In my studies, an explicit memory task was not performed. Within the mHB the discrimination between a familiar and a non-familiar object was assessed. In accordance with the learning deficit observed by Chen et al. (2006), mutants did not recognize the familiar object in this task, as indicated by exploration time (Fig. 33K and L). However, in the social discrimination task, where the animals had to discriminate between a familiar and a non-familiar conspecific, at least male mutants were able to perform (Fig. 39A). For females, a statement cannot be given, since neither control nor mutant females were able to discriminate, which was mainly due to a failure of the test protocol often observed for females in this test paradigm. The discrepancy of learning ability between objects and conspecifics may be artificial due to the hyperactivity and enhanced social affinity of mutants described above, but it can also reflect different learning mechanisms dependent and independent of *Braf*.

4.3.3 Molecular basis of the behavioral phenotype of Braf mutants

The behavioral analysis revealed a hyperactive, anxiolytic, and antidepressant phenotype with impaired motor coordination, enhanced social affinity to conspecifics, and partly impaired learning and memory functions in $Braf^{flox/flox}$ CamKII-cre mutant mice. All these findings are far beyond the previously described hippocampus dependent learning and memory deficit in *Braf* deficient mice (Chen et al., 2006). The Cam-

KII-cre mice used in this previous study are not extensively described, but it is shown for the thalamus and hypothalamus, for example, that *Braf* is still intact, whereas in the mice used in my study, *Braf* is lost in the neurons of these regions (Fig. 11). This extended knockout of *Braf* in the brain may be the reason for the broader phenotypic alterations found in my study.

Looking at the molecular level of Braf mutant animals, first the direct downstream signaling of BRAF via ERK1/2 was abolished. ERK1 deficient mice and mice expressing a dominant-negative MEK1 in neurons have been shown to display alterations in learning and memory, but no impairment in the accelerating rotarod for example has been reported (Mazzucchelli et al., 2002; Shalin et al., 2004). Most of the studies on MAPK function were performed with inhibitors of MEK1/2. Although contradictory results in regard of depression related behavior have been published, these studies clearly show an involvement of MEK1/2 in depression (Huang and Lin, 2006; Duman et al., 2007). Regarding the anxiolytic phenotype observed in Braf mutants, no direct influence by members of the MAPK cascade has been reported. However, many molecules and receptors known to be involved in the modulation of anxiety and depression related behavior signal via MAPKs: e.g. serotonin (5-HT) receptors, corticotropin releasing hormone receptors (CRHR), dopamine receptors, NMDA receptors, estrogen, and neurotrophins (Einat et al., 2003; Beom et al., 2004; Refojo et al., 2005; Setalo et al., 2005; Werry et al., 2005; Ivanov et al., 2006). Recently it has been shown *in vitro* that $GABA_A$ receptors, which are also known to be involved in anxiety and mood disorders, are regulated by ERK1/2 (Bell-Horner et al., 2006). Regarding all these different regulatory systems as possible molecular effectors for the complex phenotype of Braf mutant mice, it is difficult to elucidate the right candidate pathways. In the following I will discuss two possible signaling systems and the putative role of BRAF therein.

- BRAF as modulator of GABA signaling

Diazepam is a benzodiazepine (BDZ) and is used as a therapeutic drug with mainly anxiolytic effects. Like all BDZ, it is an agonist of $GABA_A$ receptors and enhances $GABA_A$ signaling and thereby inhibits the behavioral output. Wildtype mice treated with diazepam exhibit a similar phenotype as observed in Braf mutants here. Beside the anxiolytic effect, diazepam mediates myorelaxation leading to strong impairment in the accelerating rotarod task, altered locomotor activity, enhanced social interaction, and impaired memory function (Rudolph et al., 1999; File et al., 2001). Additionally, mice treated with diazepam displayed a latency to the first movement in a Light-Dark-Box test similar to the effect observed for Braf mutants in the mHB and elevated

plus maze (Lepicard et al., 2000). Only the sedative effect mediated by diazepam was not displayed by BRAF deficient mice.

BDZ bind to the α and γ subunit of $GABA_A$ receptors and it has been shown that different types of these subunits are responsible for different aspects of the pleiotropy of diazepam mediated effects (Rudolph and Mohler, 2004). So the sedative effect of diazepam is mediated exclusively by the α1 subunit as revealed by studies with mice expressing a mutated, diazepam insensitive α1 subunit (Rudolph et al., 1999). Considering this, the loss of BRAF seems to have a similar effect as diazepam exerts via the α2 and/or α3 subunit of $GABA_A$ receptors. In fact, it has recently been shown that intact MAPK signaling via ERK1/2 can negatively modulate the α subunits of $GABA_A$ receptors (Bell-Horner et al., 2006). This finding would be consistent with an enhanced activation of $GABA_A$ receptors due to the loss of BRAF/MAPK signaling (Fig. 51). The remaining discrepancy that diazepam does not mediate any antidepressant effect whereas the Braf mutants show this phenotype, may be caused by the sedative effect, which may obscure any potentially decreased immobility in the forced swim test for example. Unfortunately, it is not analyzed how mice with the mutant α1 subunit perform in depression related test paradigms upon diazepam treatment. The antidepressant aspect of the phenotype may also be mediated by impaired $GABA_B$ receptors. They are G-protein coupled receptors, which signal via MAPKs, so that the loss of BRAF can block $GABA_B$ signaling (Fig. 51; Vanhoose et al., 2002). It has been shown that knockout or inhibition of these receptors leads to an antidepressant phenotype that is detectable in the forced swim test but not in the tail suspension test, as observed in Braf mutants as well (Mombereau et al., 2004).

To test the hypothesis of an involvement of GABA receptors in the phenotype of Braf mutant mice, further experiments are necessary. The activity of $GABA_A$ receptors could be analyzed by the measurement of GABA-induced peak current amplitudes in brain slices, and a rescue of the phenotype could be aimed by selective GABA antagonists, e.g. bicuculline or picrotoxin (Dalvi and Rodgers, 1996). More basically, it has still to be clarified if wildtype BRAF as well as the Cre used here are co-expressed with $GABA_A$ and $GABA_B$ receptors in the same cells, e.g. in the pyramidal cells of the hippocampus (MacLennan et al., 1991). So, the regulation of $GABA_A$ receptor activity by BRAF as molecular basis for the complex phenotype of Braf mutants is only a suggestion until further experiments prove this theory.

- BRAF in the downstream signaling of CRHR1

A second system involved in the regulation of anxiety and linked to MAPKs in the brain is the signaling by corticotropin releasing hormone (CRH). CRH is a neuropep-

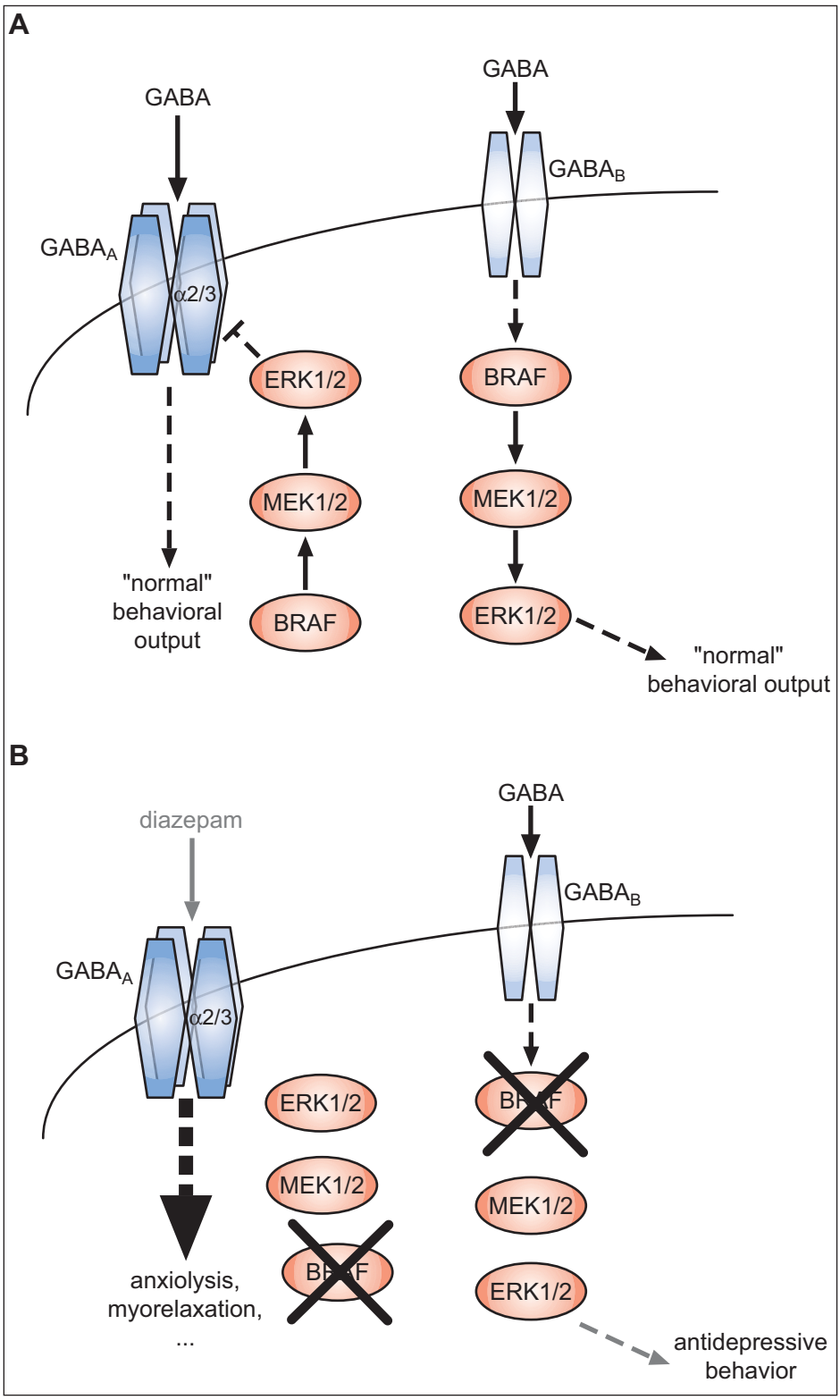

Fig. 51: Schematic representation of a putative cooperation of $GABA_A$ and $GABA_B$ receptors with BRAF. In the wildtype state BRAF regulates the α2 and/or α3 subunit of $GABA_A$ receptors negatively and acts as downstream effector of $GABA_B$ receptors (**A**). Upon loss of BRAF $GABA_A$ receptors are hyperactive similar to diazepam treatment and signaling of $GABA_B$ receptors is blocked (**B**). Dashed lines indicate activation via several molecules in between.

tide, which signals via two different receptors, CRHR1 and CRHR2. Via CRHR1 it modulates the secretion of adrenocortocotropic hormone (ACTH) and corticosterone (CORT) from the pituitary in response to stressors and other stimuli. Additionally, CRH mediates emotional behavior independently of ACTH by its action in the amygdala as well as ACTH dependent via the pituitary (for review see Millan, 2003). Thus, knockout of CRHR1, in the entire brain or in forebrain neurons only, leads to reduced anxiety and increased locomotor activity caused by alterations in the regulation of ACTH and CORT (Timpl et al., 1998; Muller et al., 2003). Also known is an involvement of increased CRH expression in depressive and stress related disorders, and antidepressant drugs targeting CRH or its receptor are in development (Muller and Wurst, 2004). Additionally, it has been shown that CRHR1 signals via ERK1/2 in several brain regions as hippocampus and basolateral complex of amygdala, but not in the hypothalamus (Refojo et al., 2005). So, the anxiolytic and antidepressant phenotype of Braf mutants may be caused by an impairment in CRHR1 signaling. By analyzing the levels of ACTH and CORT under basal conditions and after stress in Braf mutants, alterations in this system might become visible. However, the motor phenotype and all impairments caused by the loss of ERK1/2 activation in the hypothalamus can not be explained by an inhibited CRHR1 signaling so far. Thus, further analyses are necessary to prove or reject the hypothesis of CRH signaling involved in the *Braf* phenotype. Moreover, this complex phenotype may also be influenced by different regulatory systems, since MAPK signaling is involved in a variety of molecular systems.

4.3.4 Body weight is affected by loss of *Braf* in neurons

Morphological Braf mutants appeared normal without any overt phenotypes. But in comparison with their control littermates, mutants were significantly smaller and showed a clear reduction in body weight from adolescence throughout adulthood (Fig. 41A and B). Regarding the hyperactive locomotion of the mutants, it can not be excluded that the enhanced physical activity caused the body weight reduction. However, hyperactivity may cause reduced weight but not a smaller size as observed in Braf mutants (data not shown). Since *Braf* was lost in forebrain neurons including the hypothalamus, the knockout may affect the body weight and size via hormonal regulation. Ghrelin, for example, a hormone mediating the opposite effects of Leptin in the hypothalamus, has been reported to activate ERK1/2 signaling and c-Fos expression and its inactivation leads to reduced body weight and size and an anxiolytic and antidepressant phenotype similar to the one observed here for the Braf knockouts (Ruter et

al., 2003; Ariyasu et al., 2005; Kanehisa et al., 2006; Mousseaux et al., 2006). Additionally, activation of Ghrelin is linked to CRH, which fits to the hypothesis of an impaired CRH signaling in Braf mutants discussed above (Mozid et al., 2003).

Knockdown of *Braf* in the same brain regions did not affect the body weight of mutant mice. This may indicate that a lowered BRAF activity of approx. 30% of the wildtype level is sufficient to keep the regulatory system for energy homeostasis in balance. On the other hand, (although not yet tested explicitly) mutant shBraf mice seemed not to display a similar hyperactivity as knockouts. These findings suggest either a very close related regulation of body weight and hyperactivity or the reduced body weight in knockout mice being a secondary effect to the hyperactivity. In any case, this finding shows a benefit of comparing knockout to knockdown mouse models, as it reveals deeper insights into the underlying regulatory mechanisms and the minimal protein amounts necessary to maintain specific functions. In regard to this, analysis of the behavioral phenotype of Braf knockdown mice would be of great interest.

4.4 Reduction of *Mek1* and *Mek2* in the adult mouse brain

4.4.1 Knockdown of *Mek1* and *Mek2* does not block downstream signaling

In the MAPK cascade MEK1 and MEK2 are activated by RAF proteins. Beside BRAF, also CRAF is expressed in the adult brain and signals via MEK1/2 (Kyriakis et al., 1992; Morice et al., 1999). Thus, it is suggested that BRAF acts more restricted than MEK1/2, which transmit the signals of both BRAF and CRAF. Accordingly, loss of MEK1/2 in adult mouse brain is supposed to display a more dramatic effect than the loss of BRAF alone. Unfortunately no brain specific MEK1 knockout mouse model has been generated so far and the MEK2 knockout mice have not been analyzed regarding behavior to test this hypothesis. The brain specific MEK1/2 knockdown mice analyzed here show only a reduction and no complete loss of MEK1/2 in the adult mouse brain, so that a milder effect as suggested for MEK1/2 knockout mice was expected.

I could show that the reduction of MEK1/2 in shMek1/2 mutants was not sufficient to block ERK1/2 activation in the brain (Fig. 42). Nevertheless, the reduced MAPK signaling was expected to cause some alterations in the brain of these mice and in fact resulted in a behavioral phenotype.

4.4.2 Slightly disturbed behavior in Mek1/2 knockdown mice

As it was intended to compare *Braf* deficient mice with *Mek1/2* deficient mice, the same behavioral test battery was used for both analyses. So, also Mek1/2 knockdown mice were subjected to tests for the assessment of general behavior in a novel environment, anxiety and depression related behavior, social aspects, and motor coordination. In general, only few altered parameters were found in all the tests and often only males showed differences whereas females behaved more like the control animals.

- Motor coordination, exploration, and activity

One of the most prominent and severe alterations in Braf mutants was the motor impairment indicated by malperformance on the accelerating rotarod. shMek1/2$^{+/flox}$ Nestin-cre mice did not show any deficit in the performance on the rotarod (Fig. 50). In accordance to this, they also did not have any difficulties in vertical exploration behavior as rearing. On the contrary, rearing was enhanced in the mHB and the dark compartment of the Light-Dark-Box for both sexes (Fig. 43 and 44). Together with a reduced latency to the first tunnel entry in the Light-Dark-Box, this indicated an enhanced exploratory behavior in a non-aversive environment. For general locomotor activity no big differences were observed, as the total distance traveled in the mHB was not altered at all and the maximum velocity in this test was only slightly reduced for both sexes (but not the mean velocity; Fig. 43). The decrease of the mean angular velocity in male mutants may indicate a slightly reduced locomotor activity in males only.

Taken together, shMek1/2 mutants displayed increased exploratory behavior and no motor impairment. Male mutants additionally exhibited moderately decreased locomotor activity.

- Anxiety related behavior

Results from the tests for anxiety related behavior were contradictory in some way. In the Light-Dark-Box only male mutants spent less time in the aversive light compartment and exhibited a reduced activity in this partition, whereas females showed no significant differences to their control littermates (Fig. 44). Moreover, mutants of both sexes spent more time on the unprotected board in the mHB (Fig. 43). In the elevated plus maze, the third test paradigm assessing anxiety related behavior, all mice spent a similar time in the unprotected open arms. Only the mean velocity in the open arms was tendentially enhanced in mutants, indicating a slightly enhanced activity in these compartments (Fig. 45). So, the data from the mHB suggest reduced

anxiety for mutants of both sexes, whereas the Light-Dark-Box revealed increased anxiety for male mutants, and the elevated plus maze showed no significantly altered anxiety behavior at all.

One possible explanation for these controversial findings may be that shMek1/2 mutants did not exhibit alterations in general anxiety, but react distinct to different environments. Thus, light could be a highly aversive component for male mutants, whereas the unprotected board in the mHB may induce less anxiety response in mutants of both sexes. Regarding the different anxiety inducing parameters used here, an important aspect to be considered is intact vision. So, the effect observed in the Light-Dark-Box may not be due to enhanced anxiety of the aversive compartment but rather due to an increased sensitivity of the mutants' eyes for the bright light. To exclude a visual impairment, examination of the eyes of these animals will be necessary.

- Social behavior

Social behavior of shMek1/2 mice as assessed with the social interaction test was not dramatically altered. Only the time spent in passive interaction with the conspecific was significantly reduced in mutants of both sexes, but not the time spent in active or in no interaction (Fig. 48). Since passive interactions can occur by chance, this effect may also be caused by altered locomotor or exploratory activity and not by real social behavior. Unfortunately, the social component in the mHB was not tested, so that results of a second test paradigm are not available to give hints for this question. It has also to be considered that most of the male animals, especially mutant males, were singly housed and it is known that housing conditions can influence behavioral parameters (personal communication by Magdalena Kallnik). Additionally, it was observed that male mutants behaved very aggressive against their control cage mates in the individually ventilated cages used in the GMC. Although not satisfyingly tested, this suggests a disturbed social behavior at least for male mutants.

- Depression like behavior

No outstanding alterations regarding depressive behavior was observed in shMek1/2 mice. Only in the tail suspension test, male mutants displayed tendentially less activity and more immobility, indicating enhanced behavioral despair (Fig. 46). In contrast to this, no differences were measured in the forced swim test, the second test paradigm assessing depression like behavior (Fig. 47). These findings lead to two possible conclusions: either male mutants in fact suffer from a depressive phenotype,

which is so weak that it shows up in only one of the two tests, or the effect observed in the tail suspension test is an artifact of altered locomotion as described above.

4.4.3 (Dis-)Similarities between Mek1/2 knockdown and Braf knockout mice

As discussed above, a more restricted function was expected for *Braf* than for *Mek1* and *Mek2*. On the other hand, downstream signaling to ERK1/2 was only blokked in Braf but not in shMek1/2 mutants, thus suggesting more severe effects in the knockouts. According to the findings of the behavior analyses, Braf knockout mice revealed much more alterations, from impaired motor coordination, hyperactivity, memory deficits, and enhanced social affinity to an antidepressant and anxiolytic phenotype. In contrast to this, Mek1/2 knockdown mice showed contradictory results for anxiety related behavior, including increased anxiety in the light box, a tendency towards depressive behavior, and aggressive social behavior. The only consistent results for *Braf* and *Mek1/2* deficient mice were enhanced exploratory behavior (for shMek1/2 mutants at least in non-aversive compartments) and a remarkable reduction in body weight and size. There are several putative reasons for this discrepancy. Technically, it has to be considered that in shMek1/2 mice knockdown is mediated by an shRNA, the efficiency of which was only assessed by Western blotting and off-target effects can not be excluded. Since the knockdown is certainly less efficient than the knockout, the MEK1/2 protein amount that is still present in the brains of shMek1/2 mutants may compensate for many possible effects, which might be observed in a complete knockout. But may it also revert some phenotypes to the opposite? This question can not be clarified so far. In addition it has to be considered that two different Cre mouse strains have been used to induce the knockout or knockdown, respectively. Surprisingly, the more restricted expression pattern of CamKII-cre mediated the more severe and broader phenotype of Braf mutants.

Regarding the signaling cascade, BRAF and MEK1/2 are indeed supposed to act in line, but they are still two different proteins. So, they may also exert different functions. It has been reported that BRAF can directly associate with ERK3, suggesting a signaling cascade without MEK1/2 (Kim and Yang, 1996). Although the function of this non-canonical MAPK signaling is not yet known, it may also be affected in Braf mutants and contribute to the phenotype. Additionally, other MEK1/2 independent downstream actions of BRAF, which are not yet known, could be responsible for the discrepancies between the phenotypes of the two mouse models described in this study.

4.5 Conclusions and outlook

Already the expression study of different members of the MAPK signaling cascade showed that not in all regions of the adult brain a canonical activation of the classical MAPK pathway is possible, but that alternative activation mechanisms must exist. The contradictory behavioral phenotypes of Braf knockout and Mek1/2 knockdown mice support this idea. To understand the molecular systems that are influenced by the loss of BRAF or MEK1/2 in these mouse mutants further experiments are necessary. As proposed above, first an involvement of hyperactive $GABA_A$ receptors and blocked $GABA_B$ receptor signaling or inhibition of CRHR1 signaling should be investigated. This knowledge will be of great benefit, first to understand the mechanisms of action of BRAF and MEK1/2 in the adult brain, and second to suggest new targeting molecules for putative anxiolytic and antidepressant drugs. For both purposes, analysis of the Braf knockdown mutants could give further insights. As shown with the shBraf EIIa-cre mice, the knockdown overcomes the developmental phenotype of the knockout. For the adult brain the knowledge of the threshold for each single endophenotype can first help to understand the molecular mechanisms and second give hints of the intensity, with which a putative novel drug has to affect its target molecule to induce the desired effect.

This study gave a first insight into the roles of BRAF and MEK1 and MEK2 in anxiety and depression disorders and it provided the tools for further investigations. Furthermore, a new tool for stable and conditional gene knockdown in the mouse was established, which will not only facilitate the dissection of MAPK signaling but of many other genes, too.

5 Material

5.1 Instruments

autoclave	Aigner, type 667-1ST
balances	Sartorius, LC6201S, LC220-S
bottles for hybridization	ThermoHybaid
cassettes for autoradiography	Amersham, Hypercassette
centrifuges	Sorvall, Evolution RC; Eppendorf, 5415D, 5417R; Heraeus, Varifuge 3.0R, Multifuge 3L-R
chambers for electrophoresis (DNA)	MWG Biotech; Peqlab
cryostat	Mikrom, HM560
developing machine	Agfa, Curix 60
digital camera	Zeiss, AxioCam MRc
DNA sequencer	Applied Biotech, DNA Analyzer 3730
electric homogenizer	IKA, Ultra-Turrax T25 basic
fear potentiated startle apparatus	Med Associates Inc., Startle Stimulus Package PHM-255A, ANL-925C Amplifier
freezer (-20°C)	Liebherr
freezer (-80°C)	Heraeus HFU 686 Basic
fridges (4°C)	Liebherr
gel documentation system	Herolab, E.A.S.Y.
gel-/blottingsystem “Criterion” (protein)	BioRad
gel-/blottingsystem “Xcell SureLockTM Mini-Cell” (protein/RNA)	Invitrogen
glass pipettes	Hirschmann
glassware	Schott
ice machine	Scotsman, AF 30
imaging analyzer	Fuji, FLA-3000
incubators (for bacteria)	New Brunswick Scientific, innova 4230
incubators (for cells)	Heraeus
laminar flow	Nunc Microflow 2
light source for microscopy	Leica KL 1500
liquid szintillation counter	Hidex, Triathler
luminometer	Berthold, Orion I
magnetic stirrer / heater	Heidolph, MR3001
microscope	Zeiss Axioplan 2
microwave oven	Sharp R-937 IN
motor pestle	Sigma
Neubauer counting chamber	Brand
oven for hybridization	Memmert, UM 400; MWG-Biotech, Mini 10; ThermoElectron, Shake’n’Stack

paraffin embedding machine	Leica, EG1160
PCR machine	Eppendorf, MasterCycler Gradient
pH-meter	InoLab, pH Level 1
photometer	Eppendorf, Biophotometer 6131
pipetteboy	Eppendorf, Easypet; Hirschmann, Pipettus akku
pipettes	Gilson; Eppendorf
power supplies for electrophoresis	Consort, E443; Pharmacia Biotech, EPS200; Thermo, EC250-90, EC3000-90
radiation monitor	Berthold, LB122
rotating rod apparatus	Bioseb, Letica LE 8200
shaker	Heidolph, Promax 2020
slide warmer	Adamas instrument, BV SW 85
sonifier	Branson sonifier, cell disrupter B15
stereomicroscope	Zeiss, Stemi SV6
thermomixer	Eppendorf, comfort
ultramicrotom	Microm, HM 355S
UV-DNA/RNA-crosslinker	Scotlab, Crosslinker SL-8042; Stratagene, UV-Stratalinker 1800
UV-lamp	Benda, N-36
vortex	Scientific Industries, Vortex Genie 2
water bath	Lauda, ecoline RE 112; Leica, HI1210; Memmert, WB7
water conditioning system	Millipore, Milli-Q biocel

5.2 Chemicals

[α-thio-35S]-ATP	Amersham
[α-thio35S]-UTP	Amersham
1kb+ DNA Ladder	Invitrogen
3,3'-diaminobenzidine (DAB)	Sigma
α-32P-dCTP	Amersham
acetic acid	Merck
acetic anhydride	Sigma
agarose (for gel electrophoresis)	Gibco Life Technologies, Biozym
ammonium acetate	Merck
ampicillin	Sigma
Ampuwa	Fresenius
bacto agar	Difco
bacto peptone	BD Biosciences
bicine	Fluka
bis-tris	Sigma

β-Mercaptoethanol	Sigma, Gibco
boric acid	Merck
bovine serum albumin (BSA)	NEB (20 mg/ml), Sigma
bromphenol blue	Sigma
calcium chloride ($CaCl_2$)	Sigma
carrier DNA	Sigma
chlorobutanol	Sigma
Complete® Mini (protease inhibitors)	Roche
cresyl violet acetate	Sigma
CriterionTM XT Bis-Tris-gels, 10% (protein)	BioRad
dextran sulphate	Sigma
dithiotreitol (DTT)	Roche
DMEM	Gibco
DMSO	Sigma
dNTP (100 mM dATP, dTTP, dCTP, dGTP)	MBI
DPX	Fluka
EDTA	Sigma
EGTA	Sigma
ethanol absolute	Merck
ethidiumbromide	Fluka
ethylene glycol	Sigma
fetal calf serum (FCS)	PAN
Ficoll 400	Sigma
formamide	Sigma
freezing medium	Tissue Tek, OCT compound
FuGENE 6 transfection reagent	Roche
γ-32P-dATP	Amersham
gelatin	Sigma
glucose	Sigma
glycerol	Sigma
Hepes	Gibco
human chorion gonadotropin (hCG/Ovogest)	Intervet
hydrochloric acid (HCl)	Merck
hydrogen peroxide, 30%	Sigma
isopropanol	Merck
kanamycin	Sigma
M2 medium	Sigma
magnesium chloride ($MgCl_2 \cdot 4H_2O$)	Merck
MEM nonessential aminoacids	Gibco
MES hydrate	Sigma
methanol	Merck
mineral oil	Sigma
MOPS	Sigma

Nonidet P40 (NP-40)	Fluka
NuPAGE® Novex Bis-Tris gels, 10% (protein)	Invitrogen
orange G	Sigma
PBS (for cell culture)	Gibco
PIPES	Sigma
polyvinylpyrrolidone 40 (PVP 40)	Sigma
potassium chloride (KCl)	Merck
potassium ferricyanid ($K_3Fe(CN)_6$)	Sigma
potassium ferrocyanid ($K_4Fe(CN)_6 \bullet 3H_2O$)	Sigma
potassium hydroxid (KOH)	Sigma
potassium phosphate ($KH_2PO_4 \bullet H_2O$, K_2HPO_4)	Roth
pregnant mare's serum gonadotropin (PMSG)	Intervet
RapidHyb buffer	Amersham
RNaseZAP®	Sigma
RotiHistoKit® I	Roth
RotiHistol®	Roth
salmon sperm DNA	Fluka
SeeBlue® Plus2 Prestained protein ladder	Invitrogen
skim milk powder	BD Biosciences
SmartLadder DNA marker	Eurogentec
sodium acetate (NaOAc)	Merck, Sigma
sodium chloride (NaCl)	Merck
sodium citrate	Sigma
sodium desoxycholate	Sigma
sodium dodecylsulfate (SDS)	Merck
sodium hydroxide (NaOH)	Roth
sodium phosphate ($NaH_2PO_4 \bullet H_2O$, Na_2HPO_4)	Sigma
spermidin	Sigma
sucrose	Sigma
TBE urea gels, 15% (RNA)	Invitrogen
TBE urea sample buffer (2x)	Invitrogen
triethanolamine	Merck
TriReagent	Sigma
Tris (Trizma-Base)	Sigma
Triton-X 100	Biorad
Trizol	Invitrogen
tRNA	Roche
trypsin	Gibco
tryptone	BD Biosciences
Tween 20	Sigma
xylol	Merck
yeast extract	Difco

5.3 Kits

β-Gal reporter gene assay	Roche
DNA Maxi Prep Kit	Qiagen
DNA Highspeed Maxi Prep Kit	Qiagen
DNA Mini Prep Kit	Qiagen
ECL Detection Kit	Amersham
ECL plus Detection Kit	Amersham
QIAquick Gel Extraction Kit	Qiagen
mirVana™ miRNA Isolation Kit	Ambion
NorthernMax®-Gly Kit	Ambion
PCR Purification Kit	Qiagen
RediPrime DNA Labeling Kit	Amersham
RNeasy Mini Kit	Qiagen
SuperScript First-Strand Synthesis System for RT-PCR	Invitrogen
TOPO TA Cloning Kit	Invitrogen
Vectastain Elite ABC Kit	Vector Labs
Wizard Genomic DNA Purification Kit	Promega

5.4 Commonly used stock solutions

loading buffer for agarose gels	15% 200 mM 1 - 2%	Ficoll 400 EDTA orange G
paraformaldehyde solution (PFA, 4%)	4%	PFA w/v in PBS
PBS (1x)	171 mM 3.4 mM 10 mM 1.8 mM	NaCl KCl Na_2HPO_4 KH_2PO_4 pH 7.4
SSC (saline sodium citrate, 20x)	3 M 0.3 M	NaCl sodium citrate pH 7.0
sucrose solution (20% or 25%)	20% / 25%	sucrose w/v in PBS
TAE (10x)	0.4 M 0.1 M 0.01 M	Tris base acetate EDTA
TBE (10x)	0.89 M 0.89 M 0.02 M	Tris base boric acid EDTA
TBS (10x)	0.25 M 1.37 M	Tris-HCl pH 7.6 NaCl
TBS-T (1x)	1 x 0.05%	TBS Tween 20
TE (Tris-EDTA)	10 mM 1 mM	Tris-HCl pH 7.4 EDTA

Tris-HCl	1 M	Tris base pH 7.5

5.5 Solutions for the work with bacteria

LB medium (Luria-Bertani)	10 g 5 g 5 g ad 1 l	Bacto peptone yeast extract NaCl H2O
LB agar	98.5% 1.5%	LB medium Bacto agar pH 7.4
LB^{amp} medium	LB medium with 50 µg/ml ampicillin	
LB^{amp} agar	LB agar with 100 µg/ml ampicillin	
LB^{kan} medium	LB medium with 25 µg/ml kanamycin	
LB^{kan} agar	LB agar with 50 µg/ml kanamycin	
$CaCl_2$ solution	60 mM 15% 10 mM autoclave or filter sterile	$CaCl_2$ glycerol PIPES pH 7.0

5.6 Solutions for cell culture

F1 medium	15% 20 mM 1x 0.1 mM 1500 u/ml in	FCS (PAN) Hepes MEM nonessential aminoacids β-mercaptoethanol LIF DMEM
feeder medium	10% in	FCS DMEM
freezing medium (1x)	15% 10% in	FCS (PAN) DMSO DMEM
Luciferase assay buffer	25 mM 15 mM 4 mM 2 mM 1 mM 100 µM 75 µM	glycylglycine potassium-phosphate pH 8.0 EGTA ATP DTT coenzyme A luciferin pH 8.0
gelatin solution	1% in	gelatin H_2O

5.7 Solutions for Southern blot analysis

Church buffer	0.5 M	Na_2HPO_4
	0.5 M	NaH_2PO_4
	1%	BSA
	7%	SDS
	1 mM	EDTA pH 8.0
	0.1 mg/ml	salmon sperm DNA
Denaturation solution	0.5 M	NaOH
	1.5 M	NaCl
Neutralizing solution	0.1 M	Tris-HCl pH 7.5
	0.5 M	NaCl
Stripping solution	0.4 M	NaOH
Wash solution I	2 x	SSC
	0.1%	SDS
Wash solution II	0.2 x	SSC
	0.1%	SDS

5.8 Solutions for Northern blot analysis

Wash solution I	2 x	SSC
	0.1%	SDS
Wash solution II	0.2 x	SSC
	0.1%	SDS

5.9 Solutions for Western blot analysis

Blocking solution milk	4%	skim milk powder in TBS-T
Blocking solution BSA	5%	BSA in TBS-T
Tris glycine blotting buffer (10x)	0.25 M	Tris
	1.92 M	glycine
Tris glycine blotting buffer (1x)	10%	10 x blotting buffer
	10%	methanol
Laemmli buffer (5x)	313 mM	Tris-HCl pH 6.8
	50%	glycerol
	10%	SDS
	0.05%	bromphenolblue
	25%	ß-mercaptoethanol
RIPA buffer	50 mM	Tris-HCl pH 7.4
	1%	NP-40
	0.25%	sodium desoxycholate
	150 mM	NaCl
	1 mM	EDTA
	1 tablet	Complete protease inhibitor
	ad 50 ml	H_2O

NuPAGE transfer buffer (10x, for NuPAGE gels)	250 mM 250 mM 10 mM 0.05 mM	bicine bis-tris EDTA chlorobutanol
NuPAGE transfer buffer (1x, for NuPAGE gels)	10% 10%	10 x transfer buffer methanol
MOPS running buffer (10x, for Criterion gels)	500 mM 500 mM 1% 10 mM	MOPS Tris SDS EDTA pH 7.7
MES running buffer (10x, for NuPAGE gels)	500 mM 500 mM 1% 10 mM	MES Tris SDS EDTA pH 7.2

5.10 Solutions for RNA *in situ* hybridization

ammonium acetate stock solution (10x)	3 M	NH_4OAc
NTE buffer (5x)	0.5 M 10 mM 5 mM	NaCl Tris-HCl pH 8.0 EDTA pH 8.0 autoclave
triethanolamine solution	0.1 M	triethanolamine pH 8.0 (with HCl)
proteinase K buffer (PK buffer)	50 mM 5 mM	Tris-HCl pH 7.6 EDTA pH 8.0 autoclave
hybridization mix	50% 20 mM 300 mM 5 mM 10% 0.02% 0.02% 0.02% 0.5 mg/ml 0.2 mg/ml 20 mM	formamide Tris-HCl pH 8.0 NaCl EDTA pH 8.0 dextrane sulphate Ficoll 400 PVP40 BSA tRNA carrier DNA, acid cleaved DTT
chamber fluid	50% 2 x	formamide SSC

5.11 Solutions for immunhistochemistry

cryo protection solution	30% 30% 0.1M	ethylene glycol glycerol PBS
TBS	0.05 M 0.15 M 0.05 mM	Tris-HCl pH 7.5 NaCl NaF
TB	0.05 M	Tris-HCl pH 7.5

5.12 Solution for Nissl staining

cresylviolet staining solution	0.5% 2.5 mM 0.31% ad 500 ml	cresylviolet sodium acetate acetic acid H_2O filter before use

5.13 Enzymes

alkaline phosphatase	Shrimp alkaline phosphatase (SAP), Roche
DNase I (RNase-free)	Roche
Klenow fragment of DNA Polymerase I	NEB
PCR-Mastermix 5x	Eppendorf
polynucleotide kinase (PNK)	NEB
proteinase K	Roche
restriction enzymes	Roche, MBI, NEB
RNA polymerases (T7, SP6)	Roche
RNase A	Serva
RNasin RNAse inhibitor	Roche
T4 DNA ligase	NEB
terminal transferase	Roche

5.14 Antibodies

Antibody	Organism	Dilution	Company
α-βActin, polyclonal	mouse	1:100.000 (W)	Abcam
α-BRAF, polyclonal	rabbit	1:600 (W)	Santa Cruz Biotechnology
α-c-FOS, polyclonal	rabbit	1:1.000 (W) 1:1.000 (I)	abcam
α-CRAF, monoclonal	mouse	1:1.000 (W)	BD Transduction Labs.
α-HPRT, polyclonal	rabbit	1:400 (W)	Santa Cruz Biotechnology
α-MEK1, polyclonal	rabbit	1:1.000 (W)	Santa Cruz Biotechnology
α-MEK2, monoclonal	mouse	1:2.500 (W)	BD Transduction Labs.
α-mouse, polyclonal, peroxi-dase-conjugated	goat	1:1.000 - 1:5.000 (W)	Dianova

Antibody	Organism	Dilution	Company
α-phospho-ERK1/2, polyclonal	rabbit	1:1.000 (W) 1:400 (I)	Cell Signalling Technology
α-rabbit, polyclonal, biotinylated	goat	1:300 (I)	Dianova
α-rabbit, polyclonal, peroxidase-conjugated	goat	1:5.000 (W)	Dianova
α-total ERK1/2, polyclonal	rabbit	1:1.000 (W)	Cell Signalling Technology

5.15 *E.coli* bacteria strain

DH5α	Gibco Life Technologies

5.16 Murine ES cell lines

IDG3.2	R. Kühn (F1 cells, wt)
IDG3.2-26.10-3	R. Kühn (F1 cells, for RMCE)

5.17 Mouse strains

C57Bl/6J	
C57Bl/6J-Tg(pPGKneobpA)3Ems/J	(for feeder cells)
CamKII-Cre	
EIIa-Cre	
Nestin-Cre	

5.18 Vectors and plasmids

Name of plasmid	Construct from	Description
pBluescript II KS+	Stratagene	
pbs-lox2272-neo-lox2272	P. Steuber-Buchberger	Contains a stop cassette for conditional shRNA vectors
pCAG-C31Int(NLS)-bpA	R. Kühn	Expression of C31Int driven by the CAG promoter
pCRII-Rosa5'probe	R. Kühn	Contains the Southern probe 5'Rosa locus
pCRII-TOPO	Invitrogen	TOPO TA cloning vector
pNEB-lox-RLuc-lox	R. Kühn	Contains a stop cassette for conditional shRNA vectors
pRMCE	R. Kühn	Donor vector for RMCE
pScreenIt	Invitrogen	Screening system for shRNA efficiency

5.19 Oligonucleotides

5.19.1 Oligonucleotides for PCR amplification

Name	Sequence	Conditions	Size of product
Braf_9 Braf_11 Braf_17	5'-GCATAGCGCATATGCTCACA-3' 5'-CCATGCTCTAACTAGTGCTG-3' 5'-GTTGACCTTGAACTTTCTCC-3'	94°C 45 sec 60°C 60 sec 72°C 60 sec 30 x	357 bp (wt) 413 bp (flox) 282 bp (del) (genotyping Braf mice)
Braf_ISH1_fwd2 Braf_ISH1_rev	5'-AGCTAGATGCCCTTCAGCAA-3' 5'-ATGAACATTGGGAGCTGAGG-3'	95°C 60 sec 48°C 60 sec 72°C 60 sec 35 x	845 bp (mouse *Braf*-gene, for *in situ* probe)
Cre1 Cre2	5'-ATGCCCAAGAAGAAGAGGAAGGT-3' 5'-GAAATCAGTGCGTTCGAACGCTAGA-3'	94°C 30 sec 55°C 40 sec 72°C 90 sec 30 x	447 bp (genotyping Cre-mice, mutant allele)
Cre4	5'-TGCATTACCGGTCGATGCAAC-3'	94°C 30 sec 52°C 30 sec 72°C 35 sec 35 x	391 bp, with Cre2 (genotyping Ella-Cre-mice, mutant allele)
expgk3 exneo2	5'-CACGCTTCAAAAGCGCACGTCTG-3' 5'-GTTGTGCCCAGTCATAGCCGAATAG-3'	94°C 60 sec 65°C 60 sec 72°C 60 sec 30 x	280 bp (alternative genoty-ping sh-mice/RMCE cells, mutant allele)
hygro1 hygro2	5'-GAAGAATCTCGTGCTTTCAGCTTC-GATG-3' 5'-AATGACCGCTGTTATGCGGCCATTG-3'	94°C 60 sec 65°C 60 sec 72°C 60 sec 30 x	552 bp (genotyping RMCE cells, acceptor allele)
Mek1_ISH_fwd2 Mek1_ISH_rev	5'-GCCAGCATCTGAGCCTTTAG-3' 5'-AAAGTGGTTAAAAGGGGTTTCA-3'	95°C 60 sec 48°C 60 sec 72°C 60 sec 35 x	849 bp (mouse *Mek1*-gene, for *in situ* and Northern probe)
Mek2_ISH_fwd Mek2_ISH_rev	5'-CCATGCATTTGAAAACCAAA-3' 5'-ATTCAGATTGTGGGCAGGAG-3'	95°C 60 sec 50°C 60 sec 72°C 60 sec 35 x	444 bp (mouse *Mek2*-gene, for *in situ* probe)
Mek5_ISH_fwd Mek5_ISH_rev	5'-TTATCGCCTGCCTTCTGTCT-3' 5'-AAAAATGCCCCGTAAAATCC-3'	95°C 60 sec 45°C 60 sec 72°C 60 sec 35 x	805 bp (mouse *Mek5*-gene, for *in situ* probe)
Rosa5'HA_for2 Rosa3'HA_rev2	5'-CGTGTTCGTGCAAGTTGAGT-3' 5'-ACTCCCGCCCATCTTCTAG-3'	95°C 60 sec 57°C 40 sec 72°C 60 sec 30 x	536 bp (genotyping sh-mice, wt allele)
U6_for Rosa3'HA_rev2	5'-GAGGGCCTATTTCCCATGAT-3' 5'-ACTCCCGCCCATCTTCTAG -3'	95°C 60 sec 57°C 40 sec 72°C 60 sec 35 x	941 bp (genotyping sh-mice, mutant allele)

5.19.2 Oligonucleotides for sequencing

Name	Sequence	Annealing temperature
M13for	5'-GTAAAACGACGGCCAGT-3′	48°C

Name	Sequence	Annealing temperature
M13rev	5'-CAGGAAACAGCTATGAC-3′	46°C
SP6	5'-ATTTAGGTGACACTATAG-3′	46°C
T3	5'-AATTAACCCTCACTAAAGGG-3′	52°C
T7	5'-GTAATACGACTCACTATAGGGC-3′	59°C

5.19.3 Oligonucleotides for cloning

Name	Sequence
shBraf1-A	5'-caatcagtttgggcaacgagagaagcttgtctcgttgcccaaactgattgctttttg-gaaa-3'
shBraf1-B	5'-gatctttccaaaaaagcaatcagtttgggcaacgagacaagcttctctcgttgcc-caaactgattgcg-3'
shBraf4-A	5'-cctcattacctggctcactcactagaagcttgtagtgagtgagccaggtaat-gaggctttttggaaa-3'
shBraf4-B	5'-gatctttccaaaaaagcctcattacctggctcactcactacaagcttctagtgagt-gagccaggtaatgaggcg-3'
shBraf5-A	5'-gtcctcagcgggaaaggaagtcatgaagcttgatgacttcctttcccgctgaggac-ctttttggaaa-3'
shBraf5-B	5'-gatctttccaaaaaaggtcctcagcgggaaaggaagtcatcaagcttcatgacttc-ctttcccgctgaggaccg-3'
shBraf6-A	5'-ctctgcatcaatggacaccgttagaagcttgtaacggtgtccattgatgca-gagctttttggaaa-3'
shBraf6-B	5'-gatctttccaaaaaagctctgcatcaatggacaccgttacaagcttctaacggtgtc-cattgatgcagagcg-3'
shBraf7-A	5'-gagattcctgatggacagatgaagcttgatctgtccatcaggaatctccttttttg-gaaa-3'
shBraf7-B	5'-gatctttccaaaaaaggagattcctgatggacagatcaagcttcatctgtccat-caggaatctccg-3'
shBraf8-A	5'-gagaggagttacatgttgaagaagcttgttcaacatgtaactcctctccttttttg-gaaa-3'
shBraf8-B	5'-gatctttccaaaaaaggagaggagttacatgttgaacaagcttcttcaacatgtaact-cctctccg-3'
shBraf9-A	5'-cttactggagaggagttacagaagcttgtgtaactcctctccagtaagcttttttg-gaaa-3'
shBraf9-B	5'-gatctttccaaaaaagcttactggagaggagttacacaagcttctgtaactcctctc-cagtaagcg-3'
ShMek1-A	5'-ccttctacagcgacggcgagatcagaagcttgtgatctcgccgtcgctgtag-aaggctttttggaaa-3'
ShMek1-B	5'-gatctttccaaaaaagccttctacagcgacggcgagatcacaagcttctgatctcgc-cgtcgctgtagaaggcg-3'
ShMek2-A	5'-cgacggcgagatcagcatctgcagaagcttgtgcagatgctgatctcgccgt-cgctttttggaaa-3'
ShMek2-B	5'-gatctttccaaaaaagccgacggcgagatcagcatctgcacaagcttctgcagatgct-gatctcgccgtcgcg-3'
ShMek3-A	5'-acggcgagatcagcatctgcatgaagcttgatgcagatgctgatctcgccgtcttttt-tggaaa-3'

Name	Sequence
ShMek3-B	5'-gatctttccaaaaaagacggcgagatcagcatctgcatcaagcttcatgcagatgct-gatctcgccgtcg-3'
ShMek1-1-A	5'-cagctaattgactctatggccaacgaagcttggttggccatagagtcaattagc-tgctttttggaaa-3'
ShMek1-1-B	5'-gatctttccaaaaaagcagctaattgactctatggccaaccaagcttcgttggccata-gagtcaattagctgcg-3'
ShMek1-2-A	5'-ccaaattgtacttgtgtcatgaagcttgatgacacaagtacaatttgggctttttg-gaaa-3'
ShMek1-2-B	5'-gatctttccaaaaaagcccaaattgtacttgtgtcatcaagcttcatgacacaagta-caatttggcg-3'
ShMek2-1-A	5'-ttaccggcactcactatcaaccctgaagcttgagggttgatagtgagtgccgg-taacttttttggaaa-3'
ShMek2-1-B	5'-gatctttccaaaaaagttaccggcactcactatcaaccctcaagcttcagggttgata-gtgagtgccggtaacg-3'
ShMek2-2-A	5'-gctaaggtcggtgagctcaagaagcttgttgagctcaccgaccttagccttttttg-gaaa-3'
ShMek2-2-B	5'-gatctttccaaaaaaggctaaggtcggtgagctcaacaagcttcttgagctcaccgac-cttagccg-3'

5.19.4 Oligonucleotides for Northern blotting

Name	Sequence	remark
shBraf8 sense probe	5'-ggagaggagttacatgttgaa-3′	siNorthern probe for shBraf
shBraf8 as pos control	5'-ttcaacatgtaactcctctcc-3′	positive control for siNorthern probe shBraf
shMek3 sense probe	5'-gacggcgagatcagcatctgcat-3′	siNorthern probe for shMek1/2
shMek3 as pos control	5'-atgcagatgctgatctcgccgtc-3′	positive control for siNorthern probe shMek1/2

5.19.5 LNA oligonucleotide for *in situ* hybridization

Name	Sequence
shBraf8	5'-ggagaggagttacatgttgaa-3'

5.20 Plastic ware and other material

cell culture dishes	Nunc
centrifuge tubes 15 ml, 50 ml	Falcon
cleaning columns	Amersham, MicroSpin S-300; Roche, mini Quick Spin Oligo Columns
coverslips	Menzel Gläser, 24 mm x 50 mm; 24 mm x 60 mm
cuvettes for electroporation	Biorad, 0.4 cm cuvettes
developer (in situ hybridization)	Kodak D19
embedding pots	Polysciences, Peel-A-Way
films for autoradiography	Kodak, Biomax MS, Biomax XAR, Biomax MR

films for chemiluminescence detection	Amersham, Hyperfilm
filter paper	Whatman 3MM (Kat.-Nr.:3030 917)
filter tips 20 µl, 200 µl, 1 ml	Art, Starlab
fixer (in situ hybridization)	Kodak fixer (Kat.-Nr.: 197 1720)
gloves	Kimberley-Clark, Safeskin PFE, Safeskin, Nitrile
nylon membrane for DNA transfers	Amersham, Hybond N Plus
one-way needles	Terumo, Neolus 20G, 27G
one-way syringes	Terumo, 1ml, 10ml, 20ml
Pasteur pipettes	Brand
PCR reaction tubes 0,2 ml	Biozym
pipette tips	Gilson
plastic pipettes (1 ml, 5 ml, 10 ml, 25 ml)	Greiner
PVDF membrane for Western blotting	Pall Biosciences
reaction tubes (0.5 ml, 1.5 ml, 2 ml)	Eppendorf
slides	Menzel Gläser, Superfrost Plus
tissue cassettes	Merck
tissue embedding molds	Polysciences, Inc.

6 Methods

6.1 Molecularbiology

6.1.1 General methods for the work with DNA

- Determination of the concentration of nucleic acids

Concentrations of nucleic acids were determined by measuring the optical density (OD) in a photometer at the wavelength of 260 nm. OD_{260} of 1 corresponds to 50 µg double stranded DNA per ml, 33 µg single stranded DNA per ml, and 40 µg RNA per ml, respectively. Purity of DNA was assessed by the relation of OD_{260}/OD_{280}, which should not exceed a value of 1.8.

- Preparation of plasmid DNA

DNA mini- or maxi-preps were carried out with the corresponding Qiagen kits following manufacturer's instructions. For mini-preps 2 ml of an overnight culture of bacteria were used, for maxi-preps 200 ml cultured bacteria were applied.

- Isolation of genomic DNA

For isolation of genomic DNA from all kinds of tissues and ES cells (mouse tails, mouse brain tissue) the Wizard genomic DNA purification kit was used following manufacturer's instructions. To isolate genomic DNA from ES cells, cells from a 24-well or a 6-well were used. For mouse brain tissue, the brain (or parts of it) was first homogenized with a small motor pestle in PBS and then only a small portion of the homogenate was used for further proteinase K digestion and DNA extraction.

- Precipitation of DNA

0.1 Vol. 3M sodium acetate (NaOAc), pH 5.2, and 3 Vol. 100% Ethanol (EtOH) were added to the solution containing the DNA to be precipitated. The mixture was shortly vortexed and incubated for 1 hour to overnight at -20°C. Then the DNA was pelleted at 14.000 x g for 10 min and washed with 70% EtOH. The pellet was air dried and solved in an appropriate buffer (e.g. TE).

- Restriction digest of plasmid-DNA

Reaction conditions, amount of enzyme and type of buffer were applied following manufacturer's instructions. Samples were digested for 2 hours or overnight at 37°C (unless an other temperature was recommended for the enzyme). For each µg of DNA and for each restriction site in the plasmid 2 u of enzyme were used. For the

digestion of genomic DNA a separate protocol was used (see 5.1.4). If necessary, sticky vector ends were blunted with Klenow fragment of DNA polymerase I. Therefore, 5 u of Klenow and 25 nMol dNTPs were added after the restriction digest and incubated for 20 min at RT.

- Gel electrophoresis of DNA fragments

For electrophoretical separation of DNA fragments according to their size, DNA samples were run on agarose gels and stained with ethidium bromide either in the gel itself or in the running buffer. Standard gels were of 1% agarose in 1x TAE buffer, for a better resolution of bands of similar size agarose concentrations of 2% were used. DNA samples were loaded on the gel with 5x loading buffer, the 1kb+ ladder or the Smartladder (for Southern blotting) were used as length standard and a voltage of 80-120 V was applied for 30 min to several hours depending on the sizes of the DNA fragments to be separated. Pictures of the gels were taken on a UV desk with short wave UV radiation (254 nm).

- Isolation of DNA fragments from agarose gels

To isolate DNA fragments of a specific size from agarose gels, the bands were visualized on long wave UV radiation (366 nm) to prevent damage of the DNA. The band of interest was cut out with a clean scalpel and elution of DNA was performed using the Qiagen Gel Extraction Kit following manufacturer's instructions.

- Dephosphorylation of DNA fragments

During cloning of DNA fragments religation of an open vector should be minimized. With alkaline phosphatase (SAP, shrimp alkaline phosphatase) the terminal phosphates of the DNA can be removed, so that DNA ligase cannot join these ends with each other. For this purpose 0.1 u SAP were added to the vector DNA after digestion and incubated for 60 min at 37°C. For inactivation of the enzyme 5 mM EDTA pH 8.0 were added and the sample was heated to 75°C for 20 min.

- Ligation of DNA fragments

To ligate a DNA fragment into a vector, linearized vector and insert DNA were used in a molar ratio of approximately 1:3. The reaction was performed by T4 DNA ligase at RT for 15 min for sticky ends and 30 min for blunt ends using 400 u and 100 to 200 ng of DNA in total.

For the cloning of PCR fragments, the TOPO TA Cloning Kit was used. The linearized vector conjugated with Topoisomerase I allows subcloning without ligase. The reaction was performed following manufacturer's instructions.

- Polymerase chain reaction (PCR)

For amplification of DNA fragments from either genomic DNA or vector DNA, polymerase chain reaction (PCR) was performed. About 20-400 ng of DNA template were used with the Eppendorf 5x PCR Mastermix in 25 µl total reaction volume.

The following cycles were passed:

	3 min	94°C	(initial melting of the template DNA)
30 x	1 min	94°C	(cyclic melting of the template DNA)
	40 sec	xx°C	(annealing, dependent on primer sequence)
	1 min	72°C	(template dependent elongation)
	10 min	72°C	(terminal elongation / completion)
	∞	4°C	(cooling until processing)

The specific conditions for each pair of primers are listed in materials.

- Sequencing of DNA fragments

To determine the DNA sequence of a cloned or amplified DNA fragment, sequencing analysis was performed on a DNA sequencer. For amplification of the DNA fragment and incorporation of labeled stop nucleotides, a PCR reaction with 5 pmol of one specific primer and a reaction mix (Big Dye and sequencing buffer) was performed with the following cycles:

	5 min	95°C	(initial melting of the template DNA)
25 x	30 sec	95°C	(cyclic melting of the template DNA)
	15 sec	xx°C	(annealing, dependent on primer sequence)
	4 min	60°C	(template dependent elongation)
	10 min	72°C	(terminal elongation / completion)
	∞	4°C	(cooling until processing)

The specific condition for each primer is listed in materials.

After the PCR reaction, the sample was purified by ethanol precipitation, the DNA was resuspended in pure H_2O (Ampuwa), and at least half of the sample was loaded on the sequencer.

For difficult sequences or structures (e.g. hairpin structures, GC rich fragments), sequencing analysis with approved methods was provided by SequiServe, Vaterstetten, Germany.

6.1.2 General methods for the work with RNA

For all RNA work RNase free solutions, tubes and pipette tips were used. Glass and plastic equipment was cleaned with RNaseZAP® and fresh MilliQ water before use.

- Tissue preparation for RNA extraction

Mice were asphyxiated with CO_2, decapitated, and the brain was dissected removing bones and meninges. The whole brain or dissected parts of it were immediately frozen on dry ice or liquid nitrogen to prevent degradation of RNA. Tissue was processed directly or stored at -80°C.

- Isolation of total RNA

Total RNA from cells or mouse tissue was extracted with TriReagent or Trizol following manufacturer's instructions. RNA concentration was determined using a photometer, where an OD_{260} of 1 corresponds to 40 µg RNA per ml. Isolated RNA was stored at -80°C if not processed immediately.

- Preparation of short RNAs from brain tissue

Half mouse brains were used for the extraction of small RNAs with the mirVana miRNA isolation kit following manufacturer's instructions. Due to specific columns and binding conditions RNA molecules between 10 and 200 nt can be highly enriched during this procedure. RNA concentration was determined using a photometer, where an OD_{260} of 1 corresponds to 33 µg RNA per ml. Isolated small RNAs were stored at -80°C.

- Reverse transcription of mRNA into cDNA

cDNA was generated by reverse transcription of mRNA by SuperScriptII, a reverse transcriptase. Approximately 15 µg of total RNA were incubated with random hexamer primers, dNTPs, SuperScriptII, and the corresponding buffers at 42°C following manufacturer's instructions. The RNA template was digested by RNase H incubation, and the quality of the cDNA was checked on an agarose gel before using it for further PCR reactions.

6.1.3 Methods for the work with bacteria

- Production of competent bacteria

E.coli bacteria (DH5α) were cultivated on a LB agar plate without antibiotics overnight at 37°C. One single colony was inoculated to 5 ml LB medium and again incuba-

ted overnight on a shaker. 4 ml of this culture were added to 400 ml of fresh LB medium and incubated on a shaker for several hours. When the cell suspension reached absorption of 0.375 at 590 nm, but not higher than 0.4, bacteria were transferred to precooled 50 ml tubes, chilled on ice for 5-10 min and centrifuged (1,600x g, 7 min, 4°C). Each pellet was carefully resuspended in 10 ml ice-cold $CaCl_2$ solution. Cells were centrifuged again (1,100x g, 5 min, 4°C) and each pellet was resuspended in 2 ml ice-cold $CaCl_2$ solution. Bacteria were then ready for direct transformation or were aliquoted and frozen at -80°C.

- Transformation of competent bacteria

50 µl suspension of competent bacteria were carefully thawed on ice and approximately 25 ng of plasmid DNA were added. The sample was mixed carefully and incubated on ice for 10 min. After a heat shock (90 sec at 42°C) and chilling on ice 1 ml LB medium were added. Bacteria were incubated at 37°C for 45 min gently shaking. Then the transformed bacteria were plated on LB plates containing an appropriate antibiotic and incubated overnight at 37°C.

6.1.4 Analysis of genomic DNA by Southern blotting

- Restriction digest and blotting of genomic DNA

8-20 µg of genomic DNA were digested with an appropriate restriction enzyme in 30 µl total volume. For better restriction accuracy 3.3 mM spermidine was added to the sample and DNA was digested for 3 hours to overnight at 37°C. Cleaved DNA was run on a 0.8% agarose/TBE gel for 14 to 20 hours at 30 to 50 V, depending on the length of the expected bands. For a higher blotting efficiency of large DNA fragments, the gel was agitated in 0.25 M HCl for 30 min to depurinate the DNA. After a brief rinse in H_2O, DNA on the gel was denatured for 1 hour in denaturing solution and neutralized again for 1 hour in neutralization solution. Single stranded DNA was then blotted overnight via capillary transfer using 20x SSC and a nylon membrane. After DNA transfer the membrane was briefly rinsed with 2x SSC and UV cross-linked, before proceeding with the hybridization.

- Production of radioactive DNA probes

50-100 ng of DNA probe was radioactively labeled with α-^{32}P-dCTP using the Rediprime II labeling kit following manufacturer's instructions. Unincorporated radioactive nucleotides were removed by centrifugation with a Microspin S-300 column. 1 µl of the probe was measured in a liquid scintillation counter to determine the labeling

efficiency. 200,000-800,000 cpm/ml Church buffer were used for hybridization. Probe that was not used immediately was stored at -20°C for up to 2 weeks.

- Hybridization

The membrane was prehybridized with Church buffer in a hybridization bottle for at least 1 hour at 65°C. After denaturing the labeled DNA probe at 95°C and chilling it on ice, the probe was added to the Church buffer and the membrane was hybridized at 65°C for 5 hours to overnight.

To eliminate unspecifically hybridized probe, the membrane was washed with wash solution I 2x for 30 min at 65°C. If necessary a third washing with wash solution II was added.

If the membrane should be used again for hybridization with another probe after the first hybridization step, the old signal could be washed away with stripping solution. After 20 min at RT in the stripping solution the membrane was briefly rinsed with 2x SSC and hybridization was performed as described above, starting with prehybridizing.

- Autoradiography

The hybridized membrane was wrapped in transparent films and exposed to an autoradiography film for 1-3 days at -80°C. For weak signals the Biomax MS film was used together with a Biomax screen to intensify the signal 6x compared to a conventional film without enhancer screen. After exposition the film was developed in a developing machine.

6.1.5 Analysis of RNA by Northern blotting

- Northern blotting of total RNA

Northern blotting of total RNA was performed using the NorthernMax-Gly Kit following manufacturer's instructions. Briefly, 15 µg of total RNA extracted from mouse brain were mixed with loading buffer and run on a 1% agarose gel. RNA on the gel was blotted on a nitrocellulose membrane, and the membrane was prehybridized with ULTRAhyb buffer in a hybridization bottle for at least 30 min at 65°C.

To generate a radioactively labeled DNA probe for hybridization with the RNA on the membrane, 50-100 ng of DNA template were labeled with α-^{32}P-dCTP using the Rediprime II labeling kit following manufacturer's instructions. Unincorporated radioactive nucleotides were removed by centrifugation with a Microspin S-300 column. After denaturing the labeled probe at 95°C and chilling it on ice, the probe was added to the ULTRAhyb buffer and the membrane was hybridized overnight at 65°C. The next day,

to eliminate unspecifically hybridized probe, the membrane was washed with the wash solutions provided with the NorthernMax-Gly Kit according to the manual. For the β-Actin probe, prehybridization and hybridization was carried out at 42°C.

After washing, the membrane was exposed to a Kodak BioMax MS film for several hours or overnight at -80°C, depending on the signal intensity. The film was developed using a developing machine. For quantification of band intensities the membrane was exposed to an Imaging Plate, from which signals were detected and scanned with the FLA-3000 imaging analyzer.

- Northern blotting of small RNAs

2 or 3 µg of small RNAs were mixed 1:1 with 2x TBE urea sample buffer, denatured at 70°C for 3 min, chilled on ice, loaded on a precasted 15% TBE urea gel and run at 180 V for 75 min. The electrophoretically separated RNA was blotted on a nylon membrane for 1 hour at 30 V using the Xcell IITM Blot Module and RNA was fixed to the membrane by cross-linking. The membrane could be stored at -20°C or used subsequently for hybridization. Therefore the membrane was prehybridized in a 50 ml plastic tube for at least 1 hour at 40°C in RapidHyb buffer.

To generate a radioactively labeled oligonucleotide probe for hybridization with the shRNA on the membrane, 10 pmol of the probe oligonucleotide were labeled with 70 µCi γ-^{32}P-dATP by incubation with 20 u polynucleotide kinase (PNK) at 37°C for 30 min. The reaction was stopped by heating to 65°C for 20 min. The labeled probe was chilled on ice, added to the RapidHyb buffer and the membrane was hybridized overnight at 40°C. To eliminate unspecifically hybridized probe, the membrane was washed the next day 2x for 30 min with wash solution I and 1x for 15 min with wash solution II. Subsequently, the membrane was exposed to a Kodak BioMax MR film for several hours or one day, depending on the intensity of the signal, and the film was finally developed in a developing machine.

6.1.6 Analysis of protein by Western blotting

- Preparation of protein and determination of protein concentration

Tissue and protein samples were kept on ice during all steps of preparation. ES cells were homogenized in RIPA buffer by pipetting and cell debris in the homogenate was pelleted by centrifugation for 15 min at 4°C (13,000 rpm). For mouse brains (whole brains or brain parts), tissue was homogenized in RIPA buffer with a small motor pestle or an electrical homogenizer depending on the volume of buffer. For 1 g of tissue approximately 10 µl of buffer were used. DNA in the homogenate was shea-

red by sonification and cell debris was pelleted by centrifugation. The supernatant containing the proteins was removed and stored at -20°C.

For determination of protein concentration with the BCA protein assay kit 1 µl of protein was mixed with 49 µl of RIPA buffer as diluent and 1 ml of BCA working reagent was added. Samples were incubated at 37°C in a water bath for 30 min, cooled down to RT and absorption was measured at 562 nm in a photometer. A BSA standard curve, included in each measurement, was used to correlate the absorption to the protein concentration.

- SDS polyacrylamide gel electrophoresis (SDS-PAGE) and blotting

Proteins were separated according to their size with SDS-PAGE (Laemmli, 1970). The precasted gel systems from Invitrogen (NuPAGE® Novex) and Biorad (Criterion™ XT) were used. 50 µg of total protein were mixed with 1/5 of 5x Laemmli buffer, denatured at 95°C for 3-5 min, chilled on ice and loaded onto the gel. As molecular weight marker 5 µl of the SeeBlue® Plus2 standard were loaded. After running the gel at 200 V for 1-1.5 hours, the gel was blotted on a PVDF membrane, which has been activated by soaking in 100% methanol. Blotting was performed at 30 V for 1 hour with the module from Invitrogen or at 50 V for 2 hours to overnight with the Biorad apparatus. When the blotting time exceeded 2 hours, it was performed at 4°C, otherwise at RT.

- Immunochemical reaction

After blocking the membrane with 4% skim milk (5% BSA for phospho-proteins) in TBS-T for ½ hour (RT) to overnight (4°C) to prevent unspecific signals, the membrane was incubated for 1 hour (3 hours to overnight for αBRAF) with the first antibody in TBS-T, washed with TBS-T, incubated with the second horseradish-peroxidase-conjugated antibody for 45 to 60 min in TBS-T and washed again with TBS-T. The detection reaction was initiated with ECL detection reagent following manufacturer's instructions and the membrane was exposed to a chemiluminescent film for 5 sec to several minutes, depending on the signal intensity. Films were then developed with a developing machine.

For quantification of band intensities ECL plus was used instead of ECL detection reagent. In addition to the chemiluminescent signal generated from the ECL reagent, the ECL plus reagent emits a chemifluorescent signal, which can be detected with a fluorescent image analyzer and quantified. After scanning of the fluorescent signal, a film was exposed to the membrane to additionally visualize the luminescent signal.

6.2 ES cell culture

Pluripotent embryonic stem (ES) cells represent the inner cell mass of blastocysts and are able to differentiate into divergent cell types *in vivo* as well as *in vitro*. Nevertheless it is possible to cultivate ES cells and keep them undifferentiated (Smith et al., 1988; Williams et al., 1988). Therefore they are cultivated under special conditions. Here, the cultivating medium was supplemented with Leukemia inhibiting factor (LIF), specially tested fetal calf serum (FCS) was used, and ES cells were grown on feeder cells (mouse fibroblasts, see 5.2.1) at 37°C and 5% CO_2. During expansion, ES cells were splitted every two days to avoid confluent growing, which would give rise to differentiation of the cells.

By injecting genetically modified ES cells into blastocysts, the ES cells can contribute to all cell lineages, including germ cells. After implanting of these early embryos into the uterus of pseudo-pregnant foster mothers, chimeras are born, which consist partly of cells derived from the blastocyst used for injection and partly of cells derived from the ES cells. Germline chimeras transmit an ES cell derived mutant chromosome to their progeny, which then consist to 100% of the mutant cells.

The mouse ES cell line IDG3.2, used here, originates from the F1 generation of the mouse strains C57Bl/6J and 129SvEv/Tac. ES cells were not only used for the generation of genetically modified mice, but also for test experiments to determine the efficiency of different hairpin constructs. Whereas ES cells for mouse generation were always grown on a monolayer of feeder cells, ES cells for transient experiments were grown on gelatin coated cell culture dishes without feeder cells. Therefore the dish was overlayed with 1% gelatin solution before the solution was sucked off again and the ES cells were plated.

6.2.1 Preparation of feeder cells

Feeder cells are mouse fibroblast cells, which have been mitotically inactivated by mitomycin c treatment. Primary neomycin resistant fibroblasts were obtained from embryos of the transgenic mouse strain C57Bl/6J-Tg(pPGKneobpA)3Ems/J at the age of E14.5 to E16.5 under sterile conditions. Cultivated primary fibroblasts were expanded for two passages and grown on 10 cm cell culture dishes until confluence. Cells were incubated with medium containing 10 µg/ml mitomycin c for 2 hours at 37°C. After intensive washing with PBS, feeder cells were trypsinized and plated on a fresh culture dish or frozen at -80°C (in 1x freezing medium) for later use. Feeder cells were plated at a density of 2-2.5 x 10^4 cells/cm^2 at least several hours (better one day) prior to plating of ES cells.

6.2.2 Splitting of ES cells

For expansion, cells were splitted every two days when colonies have grown nicely but not yet to confluence. The medium was suck off, cells were washed with PBS and trypsinized for 5 min at 37°C until cells detached from the surface. The reaction was stopped by adding an equal amount of medium to the cells and the suspension was resuspended carefully by pipetting and splitted on several fresh culture dishes depending on the desired amount of cells per dish. For determination of cell number, 10 µl of cell suspension were pipetted in a Neubauer counting chamber and ES cells were counted. The cell number of one quadrant multiplied by 10,000 corresponded to the number of cells in one ml cell suspension.

6.2.3 Freezing and thawing of ES cells

ES cells were stored -80°C for short term storage (up to 2-3 months) or in liquid nitrogen for long term storage. Cells were trypsinized as described in 5.2.2, centrifuged, resuspended in ice cold 1x freezing medium, and pipetted into a 2 ml cryovial. Vials were frozen in a freezing container at -80°C. Due to the isopropanol in the freezing container the temperature is lowered very slowly inside until it reaches the final temperature of the freezer after several hours. For long term storage, the vials were then transferred into liquid nitrogen. For freezing of cells on multi well plates, cells were trypsinized, resuspended with a small amount of medium, and ice cold 2x freezing medium was added in a ratio of 1:1, so that the final concentration of freezing medium in each well was 1x. Plates were wrapped in cellulose and frozen at -80°C. The cellulose prevents the fast freezing of the cells.

Cells were thawed in the water bath at 37°C, diluted with medium, centrifuged, resuspended in fresh medium, and plated on dishes with or without feeder cells. For small volumes of frozen cells, cells were diluted in a larger volume of medium and plated directly. For this procedure, medium was changed the next day as soon as possible to get rid of the DMSO from the freezing medium.

6.2.4 Transfection of ES cells using a transfection reagent

To introduce foreign DNA into cells, several vehicles can be used. The transfection reagent used here was FuGENE 6, a multi-component lipid-based reagent that can complex with DNA and transport it into cells. DNA was used as circular plasmid and also a mixture of several plasmids could be cotransfected.

First, DNA had to be sterilized by precipitation. Therefore an appropriate amount of the DNA plasmid was precipitated and washed with ethanol as described in 5.1.1.

Decanting of the ethanol and drying and dissolving of the DNA pellet in sterile H_2O was performed under a laminar flow. For transfection, a DNA concentration of 100 ng/µl was used.

One day prior to transfection, cells were plated on a gelatin coated 24-well plate (approx. 40,000 cells/well). For transfection, for each well 2 µl FuGENE 6 was mixed with 66 µl DMEM and incubated for 5 min at RT. The DNA was added to the FuGENE/DMEM mixture and incubated for at least 15 min at RT. The old medium of the cells was exchanged by 600 µl fresh F1 medium and the FuGENE/DMEM/DNA mixture was added. Cells were grown overnight at 37°C, then the medium was changed to remove the FuGENE/DNA mixture. Two days after transfection, cells were harvested for analysis.

6.2.5 Chemiluminescence reporter gene assays

To assess the activity of β-Galactosidase (β-Gal) and firefly-luciferase (Luc) after transfection of the corresponding expression plasmids, reporter gene assay for both genes were performed. The preparation of cell lysates and measurement of β-Gal activity were performed with the b-Gal reporter gene assay kit following the manufacturer's protocol. Thereby a substrate for β-Gal was added to 50 µl of the cell lysate, which resulted in light emission at 475 nm initiated by the cleaved substrate after a shift of the pH value. The intensity of the emitted light was measured for 5 sec in a plate luminometer.

For the detection of Luc activity, 20 µl of each lysate were mixed with 100 µl Luciferase assay buffer and measured for 5 sec in the luminometer. The Luc oxidized the luciferin contained in the assay buffer, which then emitted light at 490 nm.

6.2.6 Electroporation of ES cells

A physical method to bring foreign DNA into ES cells is electroporation, in which the cell membranes are permeabilized transiently with short electrical impulses, so that DNA can pass through the emerging pores into the cell. Circular plasmid DNA stays transiently in the cells and linearized plasmids can be integrated into the genome. Also here cotransfection of several plasmids is possible. Cotransfection of a specially designed circular plasmid together with an expression vector for an integrase results in integration of a defined fragment of the circular plasmid into the genome of the cell, according to the recombination event catalyzed by the integrase.

For each sample to be electroporated 10^6 - 10^7 ES cells have been used. Cells were harvested from their culture dish(es) by trypsination, centrifuged at 1,200 rpm for

5 min, washed with PBS, centrifuged again and resuspended in 800 µl PBS containing the DNA to be electroporated. A maximum of 50 µg of total DNA was used for 10^7 cells; for lower cell numbers accordingly less DNA was used. The cell/DNA suspension was pipetted into an electroporation cuvette and electroporated with 300 V and 500 µF for 2 ms. For transient experiments, where a transfection efficiency as high as possible was needed, a voltage of 320 V was used for 3 ms. After transfection, cells were allowed to recover for 5 min at RT, diluted in medium and plated on 4-5 fresh culture dishes (when 10^7 cells have been used, otherwise on accordingly less dishes). For stable transfections dishes with feeder cells and for transient experiments gelatin coated plates were used. Cells were grown for two days at 37°C. For transient experiments, cells were harvested for analysis or were further grown in selection medium for stable experiments.

6.2.7 Selection and picking of stably transfected clones

For the selection of clones with stably integrated vector, two days after the transfection the specific antibiotic was added to the medium. Selection with the neomycin analog Geneticin (G418) is based on the expression of a neomycin resistance gene from the vector after integration into the genome. With G418 at a concentration of 140 µg/ml in the medium, only resistant cells survive and can form colonies, whereas cells with no vector integrated die during selection. Selection medium was applied for 5-7 days until round, light breaking, and prominent colonies had formed and most of the single cells had died.

Colonies were picked with a 20 µl pipette from the culture dish containing PBS into a 96-well plate containing 50 µl trypsin in each well to dissociate the colony. After a maximum time of 20 min in the trypsin, 50 µl medium was added, picked cells were resuspended and plated on a fresh 96-well plate with feeder cells in a total volume of 300 µl medium. Medium was changed the next day to remove dead cells and cells were expanded on larger wells as soon as the former wells have grown dense. Cells on 24-well plates were splitted onto several plates with feeder cells and plates coated with gelatin. Cells on a feeder layer were frozen at -80°C in 1x freezing medium or further expanded, and cells on gelatin coated plates were grown to confluence and used for DNA extraction and genotyping.

6.2.8 Screening for recombined clones

DNA was extracted from cells growing on gelatin coated plates to avoid extraction of DNA from feeder cells. ES cells were grown to confluence, washed twice with PBS,

and either directly used for DNA extraction or frozen dry at -20°C. DNA extraction is described in 5.1.1. DNA was used for PCR analysis for an initial screening and for Southern blotting for confirmation.

6.3 Animal husbandry

6.3.1 Animal facilities

All mice were kept and bred in the GSF animal facility in accordance with national and institutional guidelines. Mice were group housed (if not mentioned else) with five mice per cage at maximum in open cages and maintained on a 12 hours light/dark cycle with food and water ad libitum. The temperature was 22 ± 2°C and relative humidity 55 ± 5%. For behavior analyses in the German Mouse Clinic (GMC), mice were housed in individually ventilated cages (IVC) due to hygienical reasons. Animals were not transferred before the age of eight weeks to the GMC.

For breeding single or double matings were set up and pups were weaned at an age of three weeks. At weaning mice got earmarks for identification.

6.3.2 Blastocyst injection and embryo transfer

For the production of mouse blastocysts (E3.5), female C57BL/6J mice were superovulated to increase the number of ovulated oocytes. Superovulation was performed with analoga of the gonadotropins follicle-stimulating hormone and luteinizing hormone. The hormones were injected intraperitoneally (i. p.) at noon, starting with 7.5 u of pregnant mare's serum gonadotropin (PMSG) to induce maturation of the follicles. 48 hours later 7.5 u of human chorion gonadotropin (hCG/Ovogest), which initiates the ovulation of the oocytes, were injected. After the injection of hCG, female mice were mated with one male of the same strain for one night. The uteri of pregnant females were dissected 3 days post coitum and blastocysts were flushed with M2 medium. One isolated blastocyst was fixed with one capillary of the micromanipulator and with a second capillary 10-20 mutant ES cells were injected into the blastocoel, where they will contribute to the inner cell mass.

As foster mothers for these early embryos pseudo-pregnant CD1 females were used. Pseudo-pregnancy was achieved by mating the females to sterile, vasectomized males. For the embryo transfer under anesthetic (dosage dependent on body weight, normally 0.25 ml of 1% ketamine and 0.1% rompun in isotonic saline solution), the retroperitoneal cavity of the foster mother was opened and ovaries and uterus were dissected. The proximal sides of the uterus were perforated with a thin cannula

and up to 10 manipulated blastocysts per side were transferred to the uterus via this opening. The surgery field was closed again with clips and the foster mothers were kept on warming plates until awakening. To avoid dehydration of the cornea and therefore prevent blindness of the mice, the eyes were kept wet with 0.9% NaCl during surgery.

6.3.3 Establishment of new mouse lines

16 days after embryo transfer chimeric mice were born. Since the wildtype cells from the blastocyst coded for black fur color and the modified ES cells gave agouti fur color, chimeric mice showed a mixture of black and agouti fur. The higher the contribution of the ES cells were, the higher was the ratio of agouti to black fur.

Chimeras were mated to wildtype C57Bl/6J mice to obtain offspring with germline transmission of the modified allele. Mice, which have received the modified allele from their chimeric parent, were identified by genotyping.

6.3.4 Activation of the MAPK pathway *in vivo*

- Acute restraint stress procedure

Male mice were single housed for at least three days before testing. Acute restraint stress was applied by placing each mouse in a 50 ml conical tube for 30 min. To ensure sufficient ventilation, the tip of the tube was cut so that the mouse was able to breath normally. Control mice were not subjected to the stress procedure. Immediately after the stress, mice were killed, perfused with 4% PFA, and brains were dissected.

- Foot shock

Foot shock was applied with the test apparatus and according to the protocol for fear-potentiated startle in the GMC. Male mice were placed in the startle boxes and the program was started. After a 5 min accommodation interval, ten foot shocks (0.5 sec, 0.4 mA) were applied to the animals, interrupted by variable inter-trial intervals of 180-330 sec. Control mice were subjected to the same context and procedure, but without receiving the foot shocks. Animals were put back in their home cages and they were killed 60 min after the end of the program.

6.4 Histological methods

6.4.1 Perfusion

Mice were asphyxiated with CO_2 and the thoracic cavity was opened to dissect the heart. A blunt needle was inserted through the left ventricle into the ascending aorta and the right atrium was snipped. Using a pump vessels were rinsed with PBS until the liver became pale and then perfusion was carried out with 4% paraformaldehyde/PBS for approximately 5 min. After perfusion was complete the mouse was decapitated and the brain was dissected removing bones and meninges. For postfixation the brain was kept in 4% paraformaldehyde/PBS for 1 hour at RT to overnight at 4°C, depending on the subsequent procedure.

6.4.2 Paraffin sections

- Paraffin embedding

After perfusion brains were postfixed for 1-2 hours at RT, dehydrated in an ascending ethanol scale, and equilibrated and embedded in paraffin. Using an automated embedding machine, the program is as follows:

step	reagent	temp. [°C]	time [min]	remarks
dehydration	30% EtOH	RT	90	
dehydration	50% EtOH	RT	90	
dehydration	75% EtOH	RT	90	
dehydration	85% EtOH	RT	90	
dehydration	95% EtOH	RT	90	
dehydration	100% EtOH	RT	90	
dehydration	100% EtOH	RT	60	under vacuum
clarification	RotiHistol	RT	60	under vacuum
clarification	RotiHistol	RT	60	under vacuum
paraffination	50% RotiHistol / 50% paraffin	65	60	under vacuum
paraffination	paraffin	65	60	under vacuum
paraffination	paraffin	65	480	under vacuum
embedding	paraffin	65 to RT		

- Cutting paraffin embedded tissue with the microtome

Paraffin embedded brain tissue was first mounted on a tissue cassette with paraffin and fixed on the microtome. 8 µm thick sections were cut and put into a water bath (37-42°C) for flattening. Sections were mounted on slides and dried on a heating plate and/or in an incubator at 37°C. Slides with slices were stored at 4°C or directly used.

6.4.3 Frozen sections

After perfusion brains were postfixed for 1 hour at RT and equilibrated in 20% sucrose solution o/n at 4°C. For immunhistochemistry of phosphorylated proteins, solutions for perfusion were used ice-cold, brains were postfixed overnight at 4°C and 25% sucrose solution was used.

- Free-floating sections

Brains were frozen on dry ice or at 20°C and fixed on an object holder with freezing medium. On a cryostat slices of 30 or 40 µm were cut and collected in PBS. For storage longer than overnight the slices were kept in cryoprotection solution at -20°C.

- Mounted sections

For ISH the slices were mounted on slides during cutting. For this purpose 20 µm thin slices were cut, mounted directly on slides and slides were kept at -20°C or -80°C (for longer storage).

6.4.4 *in situ* hybridization on paraffin sections

For the detection of mRNA expression on brain sections, radioactive ISH on paraffin section was performed. During the whole procedure RNase free solutions and materials were used to avoid degradation of the mRNA and the RNA probe.

- Synthesis of ^{35}S labeled RNA probes

Radioactively labeled RNA probes for in situ hybridization were generated by *in vitro* transcription with an appropriate RNA polymerase in the presence of [α-thio^{35}S]-UTP. As templates, plasmids containing part of the cDNA of the gene to analyze and promoters for the RNA polymerases T7 and SP6 were linearized shortly behind the end of the cDNA sequence with an appropriate restriction enzyme.

A 1x transcription reaction was composed as follows (up to 2x the sample was processed in one reaction tube, if needed):

3 µl	10x transcription buffer
3 µl	dNTP mix (rATP/rCTP/rGTP 10mM each)

1 µl	0.5 M DTT
1 µl	RNasin (RNase inhibitor; 40 u/µl)
1.5 µg	linearized plasmid DNA template
3 µl	[α-thio-^{35}S]-UTP (12.5 mCi/mM)
ad 29 µl	H_2O
1 µl	RNA polymerase (T7 or SP6; 20 u/µl)

The reaction was incubated at 37°C for 3 hours in total. After the first hour another 0.5 µl of RNA polymerase was added to facilitate the transcriptional process. After transcription the DNA template was destroyed by adding 2 µl of RNase-free DNase I and incubation at 37°C for 15 min. Probes were purified with the RNeasy Mini Kit following manufacturer's instructions and activity was measured with a liquid scintillation counter.

- Hybridization

Before hybridization paraffin sections were dewaxed and pretreated as follows:

step	**time**	**solution**	**remarks**
dewaxing	2 x 15 min	RotiHistol	
rehydration	2 x 5 min	100% Ethanol	
rehydration	5 min	70% Ethanol	
rehydration	3 min	H_2O	
fixation	20 min	4% PFA in PBS	on ice
wash	2 x 5 min	1x PBS	
permeabilization	7 min	20 µg/ml proteinase K in proteinase K buffer	
wash	5 min	1x PBS	
fixation	20 min	4% PFA in PBS	on ice
wash	5 min	1x PBS	
acetylation / denaturation of ribosomes	10 min	0.1 M triethanolamine-HCl	add 600µl acetic anhydride; rapidly stirring
wash	2 x 5 min	2x SSC	
dehydration	1 min	60% Ethanol	
dehydration	1 min	70% Ethanol	
dehydration	1 min	95% Ethanol	
dehydration	1 min	100% Ethanol	

Slides were air dried and prehybridized for at least 1 hour at 57°C with hybridization mix. For hybridization, the labeled probe was used at a concentration of 70,000 cpm/µl in hybridization mix, whereas 100 µl of solution were used per slide. The probe in the hybridization mix was denatured at 90°C for 2 min, chilled on ice and pipetted on the prehybridized slides. Slides were covered with coverslips and kept in a humid chamber with chamber fluid during hybridization at 57°C o/n.

After hybridization, cover slips were removed and slides were washed according to the following protocol:

step	**time**	**solution**	**temp.**
wash, low stringency	4 x 5 min	4x SSC	RT
RNA digestion	20 min	20 µg/ml RNase A in 1x NTE buffer	37°C
wash	2 x 5 min	2x SSC / 1mM DTT	RT
wash	10 min	1x SSC / 1mM DTT	RT
wash	10 min	0.5x SSC / 1mM DTT	RT
wash	2 x 30 min	0.1x SSC / 1mM DTT	64°C
wash	2 x 10 min	0.1x SSC / 1mM DTT	RT
dehydration	1 min	30% Ethanol in NH_4OAc solution (1x)	RT
dehydration	1 min	50% Ethanol in NH_4OAc solution (1x)	RT
dehydration	1 min	70% Ethanol in NH_4OAc solution (1x)	RT
dehydration	1 min	95% Ethanol in NH_4OAc solution (1x)	RT
dehydration	2 x 1 min	100% Ethanol in NH_4OAc solution (1x)	RT

Slides were air dried and exposed to an autoradiography film (BioMax MR) for 2 days. For a detailed analysis slides were dipped with a photo emulsion (diluted 1:1 with H_2O) and stored at 4°C in the dark for an appropriate time depending on the signal intensity (estimated by the results from the film; in general 2-6 weeks). For developing, slides were equilibrated to RT, developed for 5 min, rinsed in H_20 and fixed for 7 min. After rinsing the slides for 25 min in floating tap water, remaining emulsion on the backside was scratch with a razor blade and slides were counterstained with cresyl violet.

6.4.5 *in situ* hybridization with LNA probes on frozen sections

For the detection of shRNAs on brain sections, radioactive ISH on frozen sections was performed. During the whole procedure RNase free solutions and materials were used to avoid degradation of the shRNAs.

- ^{35}S labeling of LNA probes

As probe for the ISH of shRNAs oligonucleotides complementary to the antisense strand of the shRNA were used. By the use of LNA (locked nucleic acid) nucleotides instead of DNA nucleotides in several positions of the oligonucleotide, high sensitivity and signal intensity was provided also with such small probes. LNA oligonucleotides were provided by Exiqon, Inc., Denmark.

A 3'-end labeling reaction was performed with terminal transferase and composed as follows:

0.5 µM	LNA oligonucleotide
4 µl	5x TdT reaction buffer
2 µl	15 mM $CoCl_2$
6 µl	[α-thio-^{35}S]-ATP (10 mCi/ml)
2 µl	terminal transferase (400 u/µl)
ad 20 µl	H_2O

The reaction was incubated at 37°C for 30 min and stopped by adding 2 µl 0.2 M EDTA and chilling on ice. Labeled probes were purified with mini Quick Spin Oligo Columns following manufacturer's instructions and activity was measured with a liquid scintillation counter.

- Hybridization

Before hybridization paraffin sections were dewaxed and pretreated as follows:

step	time	solution	remarks
dewaxing	2 x 15 min	RotiHistol	
rehydration	2 x 5 min	100% Ethanol	
rehydration	5 min	70% Ethanol	
rehydration	3 min	H_2O	
fixation	20 min	4% PFA in PBS	on ice
wash	5 min	1x PBS	
wash	2 x 5 min	2x SSC	
dehydration	1 min	60% Ethanol	

step	time	solution	remarks
dehydration	1 min	70% Ethanol	
dehydration	1 min	95% Ethanol	
dehydration	1 min	100% Ethanol	

Slides were air dried and prehybridized for at least 1 hour at 57°C with hybridization mix. For hybridization, the labeled probe was used at a concentration of approximately 6,000 cpm/µl in hybridization mix, whereas 100 µl of solution were used per slide. The probe in the hybridization mix was denatured at 90°C for 2 min, chilled on ice and pipetted on the prehybridized slides. Slides were covered with coverslips and kept in a humid chamber with chamber fluid during hybridization at 57°C o/n.

After hybridization, cover slips were removed and slides were washed according to the following protocol:

step	time	solution	temp.
wash	4 x 15 min	1x SSC / 0.05% Tween / 0.5µM DTT	55°C
wash	2 x 15 min	0.2x SSC / 0.05% Tween / 0.5µM DTT	55°C
wash	30 min	0.2x SSC / 0.05% Tween / 0.5µM DTT	55°C, cooling down to RT
wash	2 x 5 min	0.1x SSC	RT
wash	30 sec	H_2O	RT
dehydration	2 min	70% Ethanol	RT
dehydration	2 min	95% Ethanol	RT
dehydration	2 min	100% Ethanol	RT

Slides were air dried and exposed to an autoradiography film (BioMax MR) for 1-3 days. For a detailed analysis slides were dipped with a photo emulsion (diluted 1:1 with H_20) and stored at 4°C in the dark for an appropriate time depending on the signal intensity (estimated by the results from the film; in general 2-4 weeks). For developing, slides were equilibrated to RT, developed for 5 min, rinsed in H_20 and fixed for 7 min. After rinsing the slides for 25 min in floating tap water, remaining emulsion on the backside was scratch with a razor blade and slides were counterstained with cresyl violet.

6.4.6 Nissl staining (cresyl violet)

Nissl staining of dried sections was performed according to the following protocol:

step	time	solution	remarks
staining	1-5 min	cresyl violet staining solution	
rinse		H_2O	
clearing	1 min	70% Ethanol	until slide is clear
clearing	10-60 sec	96% Ethanol + 0.5% acetic acid	
dehydration	2 x 1 min	96% Ethanol	
dehydration	2 x 2 min	100% Ethanol	
	2 x 10 min	xylol	

Slides were lidded immediately with DPX and dried o/n under the hood.

6.4.7 Immunhistochemistry on frozen sections (free floating)

Free-floating sections (30 µm in thickness) were first washed in 1x TBS, 3x 10 min for freshly cut tissue and 12x 30 min or overnight for slices stored in cryoprotection solution. Further steps were performed gently shaking at RT according to the following protocol:

step	time	solution	remarks
quenching peroxidase	5 min	10% methanol, 3% H_2O_2 in TBS	
wash	3 x 10 min	1x TBS	
membrane permeabilization	15 min	0.5% Triton X-100 in TBS	
wash	3 x 5 min	1x TBS	
1st antibody	o/n	1st antibody in TBS	4°C
wash	3 x 10 min	1x TBS	
2nd antibody	2 h	biotinylated 2nd antibody in TBS	
wash	3 x 10 min	1x TBS	
ABC incubation	75 min	1:300 in TBS	preparation 30 min before use
wash	10 min	1x TBS	
wash	2 x 10 min	1x TB	

step	time	solution	remarks
development	30 min	0.1% DAB, 0.005% H_2O_2 in TB	
wash	3 x 10 min	1x TB	

Sections were mounted on slides, air dried and dehydrated as follows:

step	time	solution
wash	2 x 2 min	H2O
dehydration	2 x 2 min	70% Ethanol
dehydration	2 x 2 min	96% Ethanol
dehydration	2 x 2 min	100% Ethanol
	2 x 5 min	RotiHistol

Slides were lidded immediately with RotiHistokitt and dried o/n under the hood.

6.5 Behavioral testing

All behavioral tests were performed in the GMC. Mice were transferred at the age of 8-10 weeks from the breeding facility to the GMC. First tests started after two weeks of accommodation for the animals. The test battery was divided into two batches, so that each batch of animals was subjected to a maximum of five of the eight single tests. The tests applied on each batch and the order of the tests are listed in the following:

batch I	batch II
Light-Dark box test	modified Hole Board
social discrimination test	elevated plus maze
tail suspension test	social interaction test
	accelerating rotarod
	forced swim test

Each batch of animals consisted of 10-15 mice for each sex and genotype (mutant / control) with a maximal difference in age of two weeks.

Data were statistically analyzed using SPSS software. The chosen level of significance was $p < 0.05$.

6.5.1 Light-Dark box test

The test box was made of PVC and divided into two compartments, connected by a small tunnel (4 x 6 x 9 cm high). The lit compartment (29 x 19 x 24 cm high) was made of white PVC and was illuminated by cold light with an intensity in the center of 650 lux. The dark compartment (14 x 19 x 24 cm high) was made of black PVC and not directly illuminated (approx. 20 lux in the center). The mouse was placed in the center of the dark compartment and allowed to freely explore the apparatus for 5 min. Behaviors were observed by a trained observer sitting next to the box using a hand-held computer. Data were analyzed with respect to (1) the number of entries, latency to first entry, and time spent in both compartments and the tunnel; and (2) the number of rearings in both compartments and the tunnel. An entry into a compartment was defined as placement of all four paws into the compartment. Additionally, a camera was mounted above the center of the test arena to videotape the trial, and the animal's locomotor path in the lit compartment was analyzed with a video-tracking system. The box was cleaned before each trial with a disinfectant.

6.5.2 Social discrimination test

Social memory was assessed using the social discrimination procedure described previously (Engelmann et al., 1995). As stimulus adult ovariectomized 129S1/SvlmJ female mice were used. Briefly, test animals were separated by transferring them to fresh cages 2 h before starting the session. The social discrimination procedure consisted of two 4 min exposures of stimulus animals to the test animal in the test animal's home cage. During the first exposure ("sampling") one stimulus animal was exposed to the test animal, and after a retention interval of 2 h, this stimulus animal was re-exposed to the test animal together with an additional, previously not presented stimulus animal during the second ("test") exposure. During each exposure the duration of investigatory behavior of the test animal towards the stimulus animal(s) was recorded by a trained observer blind to the genotype with a hand-held computer. A significantly longer investigation duration of the unfamiliar stimulus animal compared to the familiar one (i.e., the conspecific previously presented during the sampling phase) was taken as an evidence for an intact recognition memory.

6.5.3 Tail suspension test

For testing tail suspension, the animal's tail tip was fixed with adhesive tape on the edge of a table. For 6 min, activity and immobility behavior was observed by a trained observer using a hand-held computer. Data were analyzed with respect to (1)

duration and frequency of activity or immobility periods; (2) total duration of each behavior; and (3) latency to the first immobility period.

6.5.4 Modified Hole Board

The modified Hole Board (mHB) test was carried out in a improved version of the procedures described by Ohl et al. (2001). The test apparatus consisted of a box (150 x 50 x 50 cm) which was divided into a test arena (100 x 50 cm) and a group compartment (50 x 50 cm) by a transparent PVC partition (50 x 50 x 0.5 cm) with 111 holes (1 cm diameter) staggered in twelve lines to allow group contact. A board (60 x 20 x 2 cm) with 23 holes (1.5 x 0.5 cm) staggered in three lines with all holes covered by movable lids was placed in the middle of the test arena, thus representing the central area of the test arena as an open field. The area around the board was divided into twelve similarly sized quadrants by lines taped onto the floor of the box (see Ohl et al., 2001). Both, box and board, were made of dark grey PVC. All lids were closed before the start of a trial. For each trial, an unfamiliar object (a blue plastic tube lid) and a familiar object (a metal cube, which was placed into the home cage three days before testing and removed again one day before testing; similar in size to the unfamiliar object) were placed into the test arena with a distance of 2 cm between them. The illumination levels were set at approximately 150 lux in the corners and 200 lux in the middle of the test arena.

At the beginning of the experiment, all animals of one cage were allowed to habituate to the test environment together in the group compartment for 20 min. Then each animal was placed individually into the test arena and allowed to explore it freely for 5 min, during which the cage mates stayed present in the group compartment. The animals were always placed into the test arena in the same corner next to the partition, facing the board diagonally. The two objects were placed in the corner quadrant diametrically to the starting point. During the 5 min trial, the animal's behavior was recorded by a trained observer with a hand-held computer. Additionally, a camera was mounted 1.2 m above the center of the test arena, and the animal's track was videotaped and its locomotor path was analyzed with a video-tracking system. After each trial, the test arena was cleaned carefully with a disinfectant.

6.5.5 Elevated plus maze

The test arena was made of light grey PVC and consisted of two open arms (30 x 5 x 0.3 cm) and two closed arms of the same size with 15 cm high walls. The open arms and accordingly the closed arms were facing each other connected via a central

square (5 x 5 cm). The apparatus was elevated 75 cm above the floor by a pole fixed underneath the central square. The illumination level was set at approx. 100 lux in the center of the maze. For testing, each mouse was placed at the end of a closed arm (distal to the center) facing the wall and was allowed to explore the maze for 5 min. A camera was mounted above the center of the maze to video-monitor each trial by a trained observer in an adjacent room. The number of entries into each type of arm (placement of all four paws into an arm defining an entry), latency to enter the open arms as well as the time spent in the open and closed arms were recorded by the observer with a hand-held computer. After each trial, the test arena was cleaned carefully with a disinfectant.

6.5.6 Social interaction test

On two subsequent days before testing, mice were habituated separately to the test area (fresh cage with floor covered with bedding) for 10 min in moderate lighting conditions (40 lux) to enhance active interaction during testing (File and Hyde, 1978). For testing, two unfamiliar, weight-matched mice of the same sex and genotype were placed for 10 min into the known test area. The total time spent in active (grooming, sniffing the partner, crawling under and over) and passive social behavior (sitting next to each other in physical contact) was recorded by a trained observer. As social interaction time of one individual depends on the partner's social activity, one dataset was recorded for each pair expressing the behavior of both animals (Tonissaar et al., 2004).

6.5.7 Accelerating rotarod

Motor coordination and balance was assessed using a rotating rod apparatus. The rod diameter was approx. 4.5 cm made of hard plastic material covered by soft black rubber foam with lane widths of 5 cm. The test phase consisted of three trials separated by 15 min intertrial intervals (ITI). Per each trial, three mice were placed on the rod leaving an empty lane between two mice. The rod was initially rotating at constant speed (4 rpm) to allow positioning of all mice in their respective lanes. Once all mice were positioned, the trial was started and the rod accelerated from 4 rpm to 40 rpm in 300 sec. The latency and the speed at which each mouse fell off the rod was measured. Passive rotations were counted as a fall off and the mouse was removed from the rod carefully. After each trail the apparatus was disinfected and dried.

6.5.8 Forced swim test

The forced swimming procedure was adapted from Ebner et al. (2002). The forced swimming apparatus consisted of a cylindrical 10 l glass tank (24.5 cm in diameter) filled with water (25 ± 1°C) to a depth of 20 cm. A trained observer recorded the animal's behavior in moderate lighting conditions (30 lux) for 6 min with a handheld computer according to one of the following behaviors: (1) struggling, defined as movements during which the forelimbs broke the water's surface; (2) swimming, defined as movement of the animal induced by movements of the fore and hind limbs without breaking the water surface; and (3) floating, defined as the behavior during which the animal used limb movement just to keep its equilibrium without any movement of the trunk. After each trial, first the mouse was dried with a tissue and put in a new cage, second the water was renewed before continuing with testing.

7 Literature

Arendt T. 2003. Synaptic plasticity and cell cycle activation in neurons are alternative effector pathways: the 'Dr. Jekyll and Mr. Hyde concept' of Alzheimer's disease or the yin and yang of neuroplasticity. *Prog Neurobiol* **71**(2-3):83-248.

Arendt T, Gartner U, Seeger G, Barmashenko G, Palm K, Mittmann T, Yan L, Hummeke M, Behrbohm J, Bruckner MK, Holzer M, Wahle P, Heumann R. 2004. Neuronal activation of Ras regulates synaptic connectivity. *Eur J Neurosci* **19**(11):2953-2966.

Ariyasu H, Takaya K, Iwakura H, Hosoda H, Akamizu T, Arai Y, Kangawa K, Nakao K. 2005. Transgenic mice overexpressing des-acyl ghrelin show small phenotype. *Endocrinology* **146**(1):355-364.

Association AP. 2000. Diagnostic and Statistical Manual of Mental Disorders - DSM-IV-TR Washington, DC: American Psychiatric Association.

Atack JR. 2005. The benzodiazepine binding site of GABA(A) receptors as a target for the development of novel anxiolytics. *Expert Opin Investig Drugs* **14**(5):601-618.

Atkins CM, Selcher JC, Petraitis JJ, Trzaskos JM, Sweatt JD. 1998. The MAPK cascade is required for mammalian associative learning. *Nat Neurosci* **1**(7):602-609.

Bardwell AJ, Flatauer LJ, Matsukuma K, Thorner J, Bardwell L. 2001. A conserved docking site in MEKs mediates high-affinity binding to MAP kinases and cooperates with a scaffold protein to enhance signal transmission. *J Biol Chem* **276**(13):10374-10386.

Barnier JV, Papin C, Eychene A, Lecoq O, Calothy G. 1995. The mouse B-raf gene encodes multiple protein isoforms with tissue-specific expression. *J Biol Chem* **270**(40):23381-23389.

Bauer EP, Schafe GE, LeDoux JE. 2002. NMDA receptors and L-type voltage-gated calcium channels contribute to long-term potentiation and different components of fear memory formation in the lateral amygdala. *J Neurosci* **22**(12):5239-5249.

Belanger LF, Roy S, Tremblay M, Brott B, Steff AM, Mourad W, Hugo P, Erikson R, Charron J. 2003. Mek2 is dispensable for mouse growth and development. *Mol Cell Biol* **23**(14):4778-4787.

Bell-Horner CL, Dohi A, Nguyen Q, Dillon GH, Singh M. 2006. ERK/MAPK pathway regulates GABAA receptors. *J Neurobiol* **66**(13):1467-1474.

Beom S, Cheong D, Torres G, Caron MG, Kim KM. 2004. Comparative studies of molecular mechanisms of dopamine D2 and D3 receptors for the activation of extracellular signal-regulated kinase. *J Biol Chem* **279**(27):28304-28314.

Bichler Z, Manns M, Stegemann B, Heumann R. 2004. Does neuronal stabilization of granule cells in adult hippocampus regulate neurogenesis and behaviour? *FENS Forum Abstracts* vol. **2**, A145-1, 2004.

Blair HT, Schafe GE, Bauer EP, Rodrigues SM, LeDoux JE. 2001. Synaptic plasticity in the lateral amygdala: a cellular hypothesis of fear conditioning. *Learn Mem* **8**(5):229-242.

Bogoyevitch MA, Court NW. 2004. Counting on mitogen-activated protein kinases--ERKs 3, 4, 5, 6, 7 and 8. *Cell Signal* **16**(12):1345-1354.

Brott BK, Alessandrini A, Largaespada DA, Copeland NG, Jenkins NA, Crews CM, Erikson RL. 1993. MEK2 is a kinase related to MEK1 and is differentially expressed in murine tissues. *Cell Growth Differ* **4**(11):921-929.

Brummelkamp TR, Bernards R, Agami R. 2002. A system for stable expression of short interfering RNAs in mammalian cells. *Science* **296**(5567):550-553.

Cade J. 1949. Lithium salts in the treatment of psychotic excitement. *Med J Aust* **2**:349- 352.

Cammalleri M, Cervia D, Dal Monte M, Martini D, Langenegger D, Fehlmann D, Feuerbach D, Pavan B, Hoyer D, Bagnoli P. 2006. Compensatory changes in the hippocampus of somatostatin knockout mice: upregulation of somatostatin receptor 2 and its function in the control of bursting activity and synaptic transmission. *Eur J Neurosci* **23**(9):2404-2422.

Cammarota M, Bevilaqua LR, Ardenghi P, Paratcha G, Levi de Stein M, Izquierdo I, Medina JH. 2000. Learning-associated activation of nuclear MAPK, CREB and Elk-1, along with Fos production, in the rat hippocampus after a one-trial avoidance learning: abolition by NMDA receptor blockade. *Brain Res Mol Brain Res* **76**(1):36-46.

Carmell MA, Zhang L, Conklin DS, Hannon GJ, Rosenquist TA. 2003. Germline transmission of RNAi in mice. *Nat Struct Biol* **10**(2):91-92.

Casu MA, Sanna A, Spada GP, Falzoi M, Mongeau R, Pani L. 2007. Effects of acute and chronic valproate treatments on p-CREB levels in the rat amygdala and nucleus accumbens. *Brain Res* **1141**:15-24.

Catling AD, Reuter CW, Cox ME, Parsons SJ, Weber MJ. 1994. Partial purification of a mitogen-activated protein kinase kinase activator from bovine brain. Identification as B-Raf or a B-Raf-associated activity. *J Biol Chem* **269**(47):30014-30021.

Cavanaugh JE, Ham J, Hetman M, Poser S, Yan C, Xia Z. 2001. Differential regulation of mitogen-activated protein kinases ERK1/2 and ERK5 by neurotrophins, neuronal activity, and cAMP in neurons. *J Neurosci* **21**(2):434-443.

Cavanaugh JE, Jaumotte JD, Lakoski JM, Zigmond MJ. 2006. Neuroprotective role of ERK1/2 and ERK5 in a dopaminergic cell line under basal conditions and in response to oxidative stress. *J Neurosci Res* **84**(6):1367-1375.

Chen AP, Ohno M, Giese KP, Kuhn R, Chen RL, Silva AJ. 2006. Forebrain-specific knockout of B-raf kinase leads to deficits in hippocampal long-term potentiation, learning, and memory. *J Neurosci Res* **83**(1):28-38.

Consortium CeS. 1998. Genome sequence of the nematode C. elegans: a platform for investigating biology. *Science* **282**(5396):2012-2018.

Consortium IHGS. 2004. Finishing the euchromatic sequence of the human genome. *Nature* **431**(7011):931-945.

Constantine-Paton M, Cline HT, Debski E. 1990. Patterned activity, synaptic convergence, and the NMDA receptor in developing visual pathways. *Annu Rev Neurosci* **13**:129-154.

Coumoul X, Shukla V, Li C, Wang RH, Deng CX. 2005. Conditional knockdown of Fgfr2 in mice using Cre-LoxP induced RNA interference. *Nucleic Acids Res* **33**(11):e102.

Coyle JT, Duman RS. 2003. Finding the intracellular signaling pathways affected by mood disorder treatments. *Neuron* **38**(2):157-160.

Cryan JF, Holmes A. 2005. The ascent of mouse: advances in modelling human depression and anxiety. *Nat Rev Drug Discov* **4**(9):775-790.

Cryan JF, Mombereau C, Vassout A. 2005. The tail suspension test as a model for assessing antidepressant activity: review of pharmacological and genetic studies in mice. *Neurosci Biobehav Rev* **29**(4-5):571-625.

Dalvi A, Rodgers RJ. 1996. GABAergic influences on plus-maze behaviour in mice. *Psychopharmacology (Berl)* **128**(4):380-397.

Das G, Henning D, Wright D, Reddy R. 1988. Upstream regulatory elements are necessary and sufficient for transcription of a U6 RNA gene by RNA polymerase III. *Embo J* **7**(2):503-512.

Davids E, Lesch KP. 1996. [The 5-HT1A receptor: a new effective principle in psychopharmacologic therapy?]. *Fortschr Neurol Psychiatr* **64**(11):460-472.

D'Hooge R, De Deyn PP. 2001. Applications of the Morris water maze in the study of learning and memory. *Brain Res Brain Res Rev* **36**(1):60-90.

Di Benedetto B, Hitz C, Holter SM, Kuhn R, Vogt Weisenhorn DM, Wurst W. 2007. Differential mRNA distribution of components of the ERK/MAPK signalling cascade in the adult mouse brain. *J Comp Neurol* **500**(3):542-556.

Dugan LL, Kim JS, Zhang Y, Bart RD, Sun Y, Holtzman DM, Gutmann DH. 1999. Differential effects of cAMP in neurons and astrocytes. Role of B-raf. *J Biol Chem* **274**(36):25842-25848.

Duman CH, Schlesinger L, Kodama M, Russell DS, Duman RS. 2007. A Role for MAP Kinase Signaling in Behavioral Models of Depression and Antidepressant Treatment. *Biol Psychiatry* **61**(5):661-670.

Dwivedi Y, Rizavi HS, Conley RR, Pandey GN. 2006. ERK MAP kinase signaling in post-mortem brain of suicide subjects: differential regulation of upstream Raf kinases Raf-1 and B-Raf. *Mol Psychiatry* **11**(1):86-98.

Dykxhoorn DM, Novina CD, Sharp PA. 2003. Killing the messenger: short RNAs that silence gene expression. *Nat Rev Mol Cell Biol* **4**(6):457-467.

Ebner K, Wotjak CT, Landgraf R, Engelmann M. 2002. Forced swimming triggers vasopressin release within the amygdala to modulate stress-coping strategies in rats. *Eur J Neurosci* **15**(2):384-388.

Einat H, Manji HK, Gould TD, Du J, Chen G. 2003. Possible involvement of the ERK signaling cascade in bipolar disorder: behavioral leads from the study of mutant mice. *Drug News Perspect* **16**(7):453-463.

Einat H, Yuan P, Gould TD, Li J, Du J, Zhang L, Manji HK, Chen G. 2003. The role of the extracellular signal-regulated kinase signaling pathway in mood modulation. *J Neurosci* **23**(19):7311-7316.

Elbashir SM, Harborth J, Lendeckel W, Yalcin A, Weber K, Tuschl T. 2001. Duplexes of 21-nucleotide RNAs mediate RNA interference in cultured mammalian cells. *Nature* **411**(6836):494-498.

Engelmann M, Wotjak CT, Landgraf R. 1995. Social discrimination procedure: an alternative method to investigate juvenile recognition abilities in rats. *Physiol Behav* **58**(2):315-321.

English JD, Sweatt JD. 1997. A requirement for the mitogen-activated protein kinase cascade in hippocampal long term potentiation. *J Biol Chem* **272**(31):19103-19106.

File SE, Hyde JR. 1978. Can social interaction be used to measure anxiety? *Br J Pharmacol* **62**(1):19-24.

File SE, Cheeta S, Akanezi C. 2001. Diazepam and nicotine increase social interaction in gerbils: a test for anxiolytic action. *Brain Res* **888**(2):311-313.

Fire A, Xu S, Montgomery MK, Kostas SA, Driver SE, Mello CC. 1998. Potent and specific genetic interference by double-stranded RNA in Caenorhabditis elegans. *Nature* **391**(6669):806-811.

Fountaine TM, Wood MJ, Wade-Martins R. 2005. Delivering RNA interference to the mammalian brain. *Curr Gene Ther* **5**(4):399-410.

Franklin KBJ, Paxinos G. 1997. The mouse brain in stereotaxic coordinates. San Diego, CA, USA: Academic Press.

Gegelashvili G, Schousboe A. 1997. High affinity glutamate transporters: regulation of expression and activity. *Mol Pharmacol* **52**(1):6-15.

Giroux S, Tremblay M, Bernard D, Cardin-Girard JF, Aubry S, Larouche L, Rousseau S, Huot J, Landry J, Jeannotte L, Charron J. 1999. Embryonic death of Mek1-deficient mice reveals a role for this kinase in angiogenesis in the labyrinthine region of the placenta. *Curr Biol* **9**(7):369-372.

Gordon JW. 1993. Production of transgenic mice. *Methods Enzymol* **225**:747-771.

Gorman JM. 2006. Gender differences in depression and response to psychotropic medication. *Gend Med* **3**(2):93-109.

Gossen M, Freundlieb S, Bender G, Muller G, Hillen W, Bujard H. 1995. Transcriptional activation by tetracyclines in mammalian cells. *Science* **268**(5218):1766-1769.

Grady RM, Teng H, Nichol MC, Cunningham JC, Wilkinson RS, Sanes JR. 1997. Skeletal and cardiac myopathies in mice lacking utrophin and dystrophin: a model for Duchenne muscular dystrophy. *Cell* **90**(4):729-738.

Gurvich N, Klein PS. 2002. Lithium and valproic acid: parallels and contrasts in diverse signaling contexts. *Pharmacol Ther* **96**(1):45-66.

Hao Y, Creson T, Zhang L, Li P, Du F, Yuan P, Gould TD, Manji HK, Chen G. 2004. Mood stabilizer valproate promotes ERK pathway-dependent cortical neuronal growth and neurogenesis. *J Neurosci* **24**(29):6590-6599.

Hasler G, Drevets WC, Manji HK, Charney DS. 2004. Discovering endophenotypes for major depression. *Neuropsychopharmacology* **29**(10):1765-1781.

Hasuwa H, Kaseda K, Einarsdottir T, Okabe M. 2002. Small interfering RNA and gene silencing in transgenic mice and rats. *FEBS Lett* **532**(1-2):227-230.

He L, Hannon GJ. 2004. MicroRNAs: small RNAs with a big role in gene regulation. *Nat Rev Genet* **5**(7):522-531.

Hemann MT, Fridman JS, Zilfou JT, Hernando E, Paddison PJ, Cordon-Cardo C, Hannon GJ, Lowe SW. 2003. An epi-allelic series of p53 hypomorphs created by stable RNAi produces distinct tumor phenotypes in vivo. *Nat Genet* **33**(3):396-400.

Hettema JM, Neale MC, Kendler KS. 2001. A review and meta-analysis of the genetic epidemiology of anxiety disorders. *Am J Psychiatry* **158**(10):1568-1578.

Hitz C, Wurst W, Kühn R. 2007. Conditional brain-specific knockdown of MAPK using Cre/loxP regulated RNA interference. *Nucleic Acids Res* **35**(12):e90.

Holmes A, Heilig M, Rupniak NM, Steckler T, Griebel G. 2003. Neuropeptide systems as novel therapeutic targets for depression and anxiety disorders. *Trends Pharmacol Sci* **24**(11):580-588.

Huang TY, Lin CH. 2006. Role of amygdala MAPK activation on immobility behavior of forced swim rats. *Behav Brain Res* **173**(1):104-111.

Impey S, Obrietan K, Wong ST, Poser S, Yano S, Wayman G, Deloulme JC, Chan G, Storm DR. 1998. Cross talk between ERK and PKA is required for Ca2+ stimulation of CREB-dependent transcription and ERK nuclear translocation. *Neuron* **21**(4):869-883.

Impey S, Obrietan K, Storm DR. 1999. Making new connections: role of ERK/MAP kinase signaling in neuronal plasticity. *Neuron* **23**(1):11-14.

Initiative AG. 2000. Analysis of the genome sequence of the flowering plant Arabidopsis thaliana. *Nature* **408**(6814):796-815.

Ivanov A, Pellegrino C, Rama S, Dumalska I, Salyha Y, Ben-Ari Y, Medina I. 2006. Opposing role of synaptic and extrasynaptic NMDA receptors in regulation of the extracellular signal-regulated kinases (ERK) activity in cultured rat hippocampal neurons. *J Physiol* **572**(Pt 3):789-798.

Kamakura S, Moriguchi T, Nishida E. 1999. Activation of the protein kinase ERK5/BMK1 by receptor tyrosine kinases. Identification and characterization of a signaling pathway to the nucleus. *J Biol Chem* **274**(37):26563-26571.

Kanai Y. 1997. Family of neutral and acidic amino acid transporters: molecular biology, physiology and medical implications. *Curr Opin Cell Biol* **9**(4):565-572.

Kanehisa M, Akiyoshi J, Kitaichi T, Matsushita H, Tanaka E, Kodama K, Hanada H, Isogawa K. 2006. Administration of antisense DNA for ghrelin causes an antidepressant and anxiolytic response in rats. *Prog Neuropsychopharmacol Biol Psychiatry* **30**(8):1403-1407.

Kasim V, Miyagishi M, Taira K. 2004. Control of siRNA expression using the Cre-loxP recombination system. *Nucleic Acids Res* **32**(7):e66.

Kim SH, Yang YC. 1996. A specific association of ERK3 with B-Raf in rat hippocampus. *Biochem Biophys Res Commun* **229**(2):577-581.

Knippers R. 2001. Molekulare Genetik. Stuttgart: Georg Thieme Verlag.

Kunath T, Gish G, Lickert H, Jones N, Pawson T, Rossant J. 2003. Transgenic RNA interference in ES cell-derived embryos recapitulates a genetic null phenotype. *Nat Biotechnol* **21**(5):559-561.

Kunkel GR, Maser RL, Calvet JP, Pederson T. 1986. U6 small nuclear RNA is transcribed by RNA polymerase III. *Proc Natl Acad Sci U S A* **83**(22):8575-8579.

Kwon MS, Seo YJ, Shim EJ, Choi SS, Lee JY, Suh HW. 2006. The effect of single or repeated restraint stress on several signal molecules in paraventricular nucleus, arcuate nucleus and locus coeruleus. *Neuroscience* **142**(4):1281-1292.

Kyriakis JM, App H, Zhang XF, Banerjee P, Brautigan DL, Rapp UR, Avruch J. 1992. Raf-1 activates MAP kinase-kinase. *Nature* **358**(6385):417-421.

Kyriakis JM, Avruch J. 1996. Sounding the alarm: protein kinase cascades activated by stress and inflammation. *J Biol Chem* **271**(40):24313-24316.

Lepicard EM, Joubert C, Hagneau I, Perez-Diaz F, Chapouthier G. 2000. Differences in anxiety-related behavior and response to diazepam in BALB/cByJ and C57BL/6J strains of mice. *Pharmacol Biochem Behav* **67**(4):739-748.

Lie DC, Colamarino SA, Song HJ, Desire L, Mira H, Consiglio A, Lein ES, Jessberger S, Lansford H, Dearie AR, Gage FH. 2005. Wnt signalling regulates adult hippocampal neurogenesis. *Nature* **437**(7063):1370-1375.

Lieberman J, Song E, Lee SK, Shankar P. 2003. Interfering with disease: opportunities and roadblocks to harnessing RNA interference. *Trends Mol Med* **9**(9):397-403.

Linnarsson S, Willson CA, Ernfors P. 2000. Cell death in regenerating populations of neurons in BDNF mutant mice. *Brain Res Mol Brain Res* **75**(1):61-69.

Mackay-Sim A, Chuah MI. 2000. Neurotrophic factors in the primary olfactory pathway. *Prog Neurobiol* **62**(5):527-559.

MacLennan AJ, Brecha N, Khrestchatisky M, Sternini C, Tillakaratne NJ, Chiang MY, Anderson K, Lai M, Tobin AJ. 1991. Independent cellular and ontogenetic expression of mRNAs encoding three alpha polypeptides of the rat GABAA receptor. *Neuroscience* **43**(2-3):369-380.

Manji HK, Potter WZ, Lenox RH. 1995. Signal transduction pathways. Molecular targets for lithium's actions. *Arch Gen Psychiatry* **52**(7):531-543.

Mazzucchelli C, Vantaggiato C, Ciamei A, Fasano S, Pakhotin P, Krezel W, Welzl H, Wolfer DP, Pages G, Valverde O, Marowsky A, Porrazzo A, Orban PC, Maldonado R, Ehrengruber MU, Cestari V, Lipp HP, Chapman PF, Pouyssegur J, Brambilla R. 2002. Knockout of ERK1 MAP kinase enhances synaptic plasticity in the striatum and facilitates striatal-mediated learning and memory. *Neuron* **34**(5):807-820.

Metzlaff M, O'Dell M, Cluster PD, Flavell RB. 1997. RNA-mediated RNA degradation and chalcone synthase A silencing in petunia. *Cell* **88**(6):845-854.

Millan MJ. 2003. The neurobiology and control of anxious states. *Prog Neurobiol* **70**(2):83-244.

Minichiello L, Korte M, Wolfer D, Kuhn R, Unsicker K, Cestari V, Rossi-Arnaud C, Lipp HP, Bonhoeffer T, Klein R. 1999. Essential role for TrkB receptors in hippocampus-mediated learning. *Neuron* **24**(2):401-414.

Mombereau C, Kaupmann K, Froestl W, Sansig G, van der Putten H, Cryan JF. 2004. Genetic and pharmacological evidence of a role for GABA(B) receptors in the modulation of anxiety- and antidepressant-like behavior. *Neuropsychopharmacology* **29**(6):1050-1062.

Morice C, Nothias F, Konig S, Vernier P, Baccarini M, Vincent JD, Barnier JV. 1999. Raf-1 and B-Raf proteins have similar regional distributions but differential subcellular localization in adult rat brain. *Eur J Neurosci* **11**(6):1995-2006.

Mousseaux D, Le Gallic L, Ryan J, Oiry C, Gagne D, Fehrentz JA, Galleyrand JC, Martinez J. 2006. Regulation of ERK1/2 activity by ghrelin-activated growth hormone secretagogue receptor 1A involves a PLC/PKCvarepsilon pathway. *Br J Pharmacol* **148**(3):350-365.

Mozid AM, Tringali G, Forsling ML, Hendricks MS, Ajodha S, Edwards R, Navarra P, Grossman AB, Korbonits M. 2003. Ghrelin is released from rat hypothalamic explants and stimulates corticotrophin-releasing hormone and arginine-vasopressin. *Horm Metab Res* **35**(8):455-459.

Muller MB, Zimmermann S, Sillaber I, Hagemeyer TP, Deussing JM, Timpl P, Kormann MS, Droste SK, Kuhn R, Reul JM, Holsboer F, Wurst W. 2003. Limbic corticotropin-releasing hormone receptor 1 mediates anxiety-related behavior and hormonal adaptation to stress. *Nat Neurosci* **6**(10):1100-1107.

Muller MB, Wurst W. 2004. Getting closer to affective disorders: the role of CRH receptor systems. *Trends Mol Med* **10**(8):409-415.

Nagy A, Mar L. 2001. Creation and use of a Cre recombinase transgenic database. *Methods Mol Biol* **158**:95-106.

Nicholls D, Attwell D. 1990. The release and uptake of excitatory amino acids. *Trends Pharmacol Sci* **11**(11):462-468.

Oberdoerffer P, Kanellopoulou C, Heissmeyer V, Paeper C, Borowski C, Aifantis I, Rao A, Rajewsky K. 2005. Efficiency of RNA interference in the mouse hematopoietic system varies between cell types and developmental stages. *Mol Cell Biol* **25**(10):3896-3905.

Ohl F, Sillaber I, Binder E, Keck ME, Holsboer F. 2001. Differential analysis of behavior and diazepam-induced alterations in C57BL/6N and BALB/c mice using the modified hole board test. *J Psychiatr Res* **35**(3):147-154.

Ortiz J, Harris HW, Guitart X, Terwilliger RZ, Haycock JW, Nestler EJ. 1995. Extracellular signal-regulated protein kinases (ERKs) and ERK kinase (MEK) in brain: regional distribution and regulation by chronic morphine. *J Neurosci* **15**(2):1285-1297.

Paddison PJ, Cleary M, Silva JM, Chang K, Sheth N, Sachidanandam R, Hannon GJ. 2004. Cloning of short hairpin RNAs for gene knockdown in mammalian cells. *Nat Methods* **1**(2):163-167.

Pages G, Lenormand P, L'Allemain G, Chambard JC, Meloche S, Pouyssegur J. 1993. Mitogen-activated protein kinases p42mapk and p44mapk are required for fibroblast proliferation. *Proc Natl Acad Sci U S A* **90**(18):8319-8323.

Papin C, Denouel A, Calothy G, Eychene A. 1996. Identification of signalling proteins interacting with B-Raf in the yeast two-hybrid system. *Oncogene* **12**(10):2213-2221.

Phiel CJ, Klein PS. 2001. Molecular targets of lithium action. *Annu Rev Pharmacol Toxicol* **41**:789-813.

Racz Z, Hamar P. 2006. Can siRNA technology provide the tools for gene therapy of the future? *Curr Med Chem* **13**(19):2299-2307.

Refojo D, Echenique C, Muller MB, Reul JM, Deussing JM, Wurst W, Sillaber I, Paez-Pereda M, Holsboer F, Arzt E. 2005. Corticotropin-releasing hormone activates ERK1/2 MAPK in specific brain areas. *Proc Natl Acad Sci U S A* **102**(17):6183-6188.

Robinson FL, Whitehurst AW, Raman M, Cobb MH. 2002. Identification of novel point mutations in ERK2 that selectively disrupt binding to MEK1. *J Biol Chem* **277**(17):14844-14852.

Rothstein JD, Dykes-Hoberg M, Pardo CA, Bristol LA, Jin L, Kuncl RW, Kanai Y, Hediger MA, Wang Y, Schielke JP, Welty DF. 1996. Knockout of glutamate transporters reveals a major role for astroglial transport in excitotoxicity and clearance of glutamate. *Neuron* **16**(3):675-686.

Rudolph U, Crestani F, Benke D, Brunig I, Benson JA, Fritschy JM, Martin JR, Bluethmann H, Mohler H. 1999. Benzodiazepine actions mediated by specific gamma-aminobutyric acid(A) receptor subtypes. *Nature* **401**(6755):796-800.

Rudolph U, Mohler H. 2004. Analysis of GABAA receptor function and dissection of the pharmacology of benzodiazepines and general anesthetics through mouse genetics. *Annu Rev Pharmacol Toxicol* **44**:475-498.

Ruter J, Kobelt P, Tebbe JJ, Avsar Y, Veh R, Wang L, Klapp BF, Wiedenmann B, Tache Y, Monnikes H. 2003. Intraperitoneal injection of ghrelin induces Fos expression in the paraventricular nucleus of the hypothalamus in rats. *Brain Res* **991**(1-2):26-33.

Schafe GE, Nadel NV, Sullivan GM, Harris A, LeDoux JE. 1999. Memory consolidation for contextual and auditory fear conditioning is dependent on protein synthesis, PKA, and MAP kinase. *Learn Mem* **6**(2):97-110.

Schafe GE, Atkins CM, Swank MW, Bauer EP, Sweatt JD, LeDoux JE. 2000. Activation of ERK/MAP kinase in the amygdala is required for memory consolidation of pavlovian fear conditioning. *J Neurosci* **20**(21):8177-8187.

Schafe GE, Nader K, Blair HT, LeDoux JE. 2001. Memory consolidation of Pavlovian fear conditioning: a cellular and molecular perspective. *Trends Neurosci* **24**(9):540-546.

Schwarz DS, Hutvagner G, Du T, Xu Z, Aronin N, Zamore PD. 2003. Asymmetry in the assembly of the RNAi enzyme complex. *Cell* **115**(2):199-208.

Seibler J, Kuter-Luks B, Kern H, Streu S, Plum L, Mauer J, Kuhn R, Bruning JC, Schwenk F. 2005. Single copy shRNA configuration for ubiquitous gene knockdown in mice. *Nucleic Acids Res* **33**(7):e67.

Setalo G, Jr., Singh M, Nethrapalli IS, Toran-Allerand CD. 2005. Protein kinase C activity is necessary for estrogen-induced Erk phosphorylation in neocortical explants. *Neurochem Res* **30**(6-7):779-790.

Shalin SC, Zirrgiebel U, Honsa KJ, Julien JP, Miller FD, Kaplan DR, Sweatt JD. 2004. Neuronal MEK is important for normal fear conditioning in mice. *J Neurosci Res* **75**(6):760-770.

Shatz CJ. 1990. Impulse activity and the patterning of connections during CNS development. *Neuron* **5**(6):745-756.

Simpson PJ, Wang E, Moon C, Matarazzo V, Cohen DR, Liebl DJ, Ronnett GV. 2003. Neurotrophin-3 signaling maintains maturational homeostasis between neuronal populations in the olfactory epithelium. *Mol Cell Neurosci* **24**(4):858-874.

Sklar P. 2002. Linkage analysis in psychiatric disorders: the emerging picture. *Annu Rev Genomics Hum Genet* **3**:371-413.

Smith AG, Heath JK, Donaldson DD, Wong GG, Moreau J, Stahl M, Rogers D. 1988. Inhibition of pluripotential embryonic stem cell differentiation by purified polypeptides. *Nature* **336**(6200):688-690.

Soriano P. 1999. Generalized lacZ expression with the ROSA26 Cre reporter strain. *Nat Genet* **21**(1):70-71.

Sternberg N, Sauer B, Hoess R, Abremski K. 1986. Bacteriophage P1 cre gene and its regulatory region. Evidence for multiple promoters and for regulation by DNA methylation. *J Mol Biol* **187**(2):197-212.

Storm SM, Cleveland JL, Rapp UR. 1990. Expression of raf family proto-oncogenes in normal mouse tissues. *Oncogene* **5**(3):345-351.

Tabara H, Grishok A, Mello CC. 1998. RNAi in C. elegans: soaking in the genome sequence. *Science* **282**(5388):430-431.

Tanaka K, Watase K, Manabe T, Yamada K, Watanabe M, Takahashi K, Iwama H, Nishikawa T, Ichihara N, Kikuchi T, Okuyama S, Kawashima N, Hori S, Takimoto M, Wada K. 1997. Epilepsy and exacerbation of brain injury in mice lacking the glutamate transporter GLT-1. *Science* **276**(5319):1699-1702.

Timmons L, Fire A. 1998. Specific interference by ingested dsRNA. *Nature* **395**(6705):854.

Timpl P, Spanagel R, Sillaber I, Kresse A, Reul JM, Stalla GK, Blanquet V, Steckler T, Holsboer F, Wurst W. 1998. Impaired stress response and reduced anxiety in mice lacking a functional corticotropin-releasing hormone receptor 1. *Nat Genet* **19**(2):162-166.

Tiscornia G, Tergaonkar V, Galimi F, Verma IM. 2004. CRE recombinase-inducible RNA interference mediated by lentiviral vectors. *Proc Natl Acad Sci U S A* **101**(19):7347-7351.

Tonissaar M, Philips MA, Eller M, Harro J. 2004. Sociability trait and serotonin metabolism in the rat social interaction test. *Neurosci Lett* **367**(3):309-312.

Tronche F, Kellendonk C, Kretz O, Gass P, Anlag K, Orban PC, Bock R, Klein R, Schutz G. 1999. Disruption of the glucocorticoid receptor gene in the nervous system results in reduced anxiety. *Nat Genet* **23**(1):99-103.

Vanhoose AM, Emery M, Jimenez L, Winder DG. 2002. ERK activation by G-protein-coupled receptors in mouse brain is receptor identity-specific. *J Biol Chem* **277**(11):9049-9053.

Ventura A, Meissner A, Dillon CP, McManus M, Sharp PA, Van Parijs L, Jaenisch R, Jacks T. 2004. Cre-lox-regulated conditional RNA interference from transgenes. *Proc Natl Acad Sci U S A* **101**(28):10380-10385.

Vermeulen A, Behlen L, Reynolds A, Wolfson A, Marshall WS, Karpilow J, Khvorova A. 2005. The contributions of dsRNA structure to Dicer specificity and efficiency. *Rna* **11**(5):674-682.

Wang RM, Zhang QG, Li CH, Zhang GY. 2005. Activation of extracellular signal-regulated kinase 5 may play a neuroprotective role in hippocampal CA3/DG region after cerebral ischemia. *J Neurosci Res* **80**(3):391-399.

Waterhouse PM, Wang MB, Lough T. 2001. Gene silencing as an adaptive defence against viruses. *Nature* **411**(6839):834-842.

Weber JD, Raben DM, Phillips PJ, Baldassare JJ. 1997. Sustained activation of extracellular-signal-regulated kinase 1 (ERK1) is required for the continued expression of cyclin D1 in G1 phase. *Biochem J* **326** (Pt 1):61-68.

Wellbrock C, Karasarides M, Marais R. 2004. The RAF proteins take centre stage. *Nat Rev Mol Cell Biol* **5**(11):875-885.

Werry TD, Gregory KJ, Sexton PM, Christopoulos A. 2005. Characterization of serotonin 5-HT2C receptor signaling to extracellular signal-regulated kinases 1 and 2. *J Neurochem* **93**(6):1603-1615.

Williams RL, Hilton DJ, Pease S, Willson TA, Stewart CL, Gearing DP, Wagner EF, Metcalf D, Nicola NA, Gough NM. 1988. Myeloid leukaemia inhibitory factor maintains the developmental potential of embryonic stem cells. *Nature* **336**(6200):684-687.

Williamson DE, Forbes EE, Dahl RE, Ryan ND. 2005. A genetic epidemiologic perspective on comorbidity of depression and anxiety. *Child Adolesc Psychiatr Clin N Am* **14**(4):707-726, viii.

Williams-Simons L, Westphal H. 1999. EIIaCre -- utility of a general deleter strain. *Transgenic Res* **8**(4):53-54.

Wittchen H-U, Jacobi F. 2001. Die Versorgungssituation psychischer Störungen in Deutschland. *Bundesgesundheitsblatt - Gesundheitsforschung - Gesundheitsschutz* **44**(10):993-1000.

Wojnowski L, Zimmer AM, Beck TW, Hahn H, Bernal R, Rapp UR, Zimmer A. 1997. Endothelial apoptosis in Braf-deficient mice. *Nat Genet* **16**(3):293-297.

Xu B, Wilsbacher JL, Collisson T, Cobb MH. 1999. The N-terminal ERK-binding site of MEK1 is required for efficient feedback phosphorylation by ERK2 in vitro and ERK activation in vivo. *J Biol Chem* **274**(48):34029-34035.

Yu J, McMahon AP. 2006. Reproducible and inducible knockdown of gene expression in mice. *Genesis* **44**(5):252-261.

Yuan PX, Huang LD, Jiang YM, Gutkind JS, Manji HK, Chen G. 2001. The mood stabilizer valproic acid activates mitogen-activated protein kinases and promotes neurite growth. *J Biol Chem* **276**(34):31674-31683.

Zhou G, Bao ZQ, Dixon JE. 1995. Components of a new human protein kinase signal transduction pathway. *J Biol Chem* **270**(21):12665-12669.

Zimmerman L, Parr B, Lendahl U, Cunningham M, McKay R, Gavin B, Mann J, Vassileva G, McMahon A. 1994. Independent regulatory elements in the nestin gene direct transgene expression to neural stem cells or muscle precursors. *Neuron* **12**(1):11-24.

8 Appendix

8.1 Abbreviations

8.1.1 General abbreviatons

°C	degree Celsius
µ	micro (10-6)
5-HT	5-hydroxytryptamine, serotonin
A	purine base adenine
A	ampere
Ac	acetate
ACTH	adrenocortocotropic hormone
ATP	adenosine triphosphate
attB	attachment site in the donor vector (RMCE)
attP	attachment site in the acceptor sequence (RMCE)
BDZ	benzodiazepine
b-Gal	β-Galactosidase
bp	basepair
BSA	bovine serum albumin
c	centi (10-2)
C	pyrimidine base cytosine
C.elegans	Caenorhabditis elegans
C31Int	integrase from phage fC31
cDNA	copyDNA
Ci	Curie; 1 Ci = 3.7 x 10^{10} Bq
CNS	central nervous system
CORT	corticosterone
cpm	counts per minute
CREB	cAMP responsive element binding protein
CRH(R)	corticotropin releasing hormone (receptor)
c-terminus	carboxy terminus
CTP	cytosine triphosphate
Da	Dalton
DAB	3,3'-diaminobenzidine
DEPC	diethylpyrocarbonate
DMSO	dimethylsulfoxide
DNA	desoxyribonucleic acid
dNTP	desoxyribonucleotide triphosphate
dsRNA	double stranded RNA
DTT	1,4-dithiothreitol
E.coli	Escherichia coli
e.g.	exempli gratia, for example

EDTA	ethylendiamintetraacetate
EGTA	ethylenglycol-bis-(b-aminoethylether)-N,N,N´,N´-tetraacetate
ES cells	embryonic stem cells
EtBr	ethydiumbromide
EtOH	ethanol
F	Farad
FCS	fetal calf serum
Fig.	figure
g	acceleration of gravity (9.81 m/s2)
g	gramme
G	purinbase guanine
GABA	g-aminobutyric acid
GMC	German mouse clinic
GSK3	glycogen synthase kinase 3
h	hour(s)
hCG	human chorion gonadotropin
HDAC	histone deacetylase
HPRT	hypoxanthine phosphoribosyltransferase
IHC	immunhistochemistry
IMP	inositol monophosphatase
ISH	in situ hybridization
ITI	intertrial interval
IVC	indivudally ventilated cages
k.o.	knock-out; organism, in which one gene is completely switched off
kb	kilobasepairs
kD	kilodalton
l	liter
lacZ	ß-Galactosidase
LB	Luria Broth
Li	lithium
LIF	leukemia inhibiting factor
LNA	locked nucleic acid
Luc	firefly-luciferase
m	milli (10-3)
M	molar
M	molar (mol/l)
mA	milli-ampere
MAPK	mitogen activated protein kinase
mHB	modified Holeboard
mHB	modified Holeboard
min	minute(s)
miRNA	micro RNA
mRNA	messenger ribonucleic acid

mut	mutant
n	nano (10-9)
n	sample size
neo	neomycin
NMDA	N-methyl-D-aspartate
NP-40	Nonidet P-40
nt	nucleotides
n-terminus	ammino terminus
o/n	over night
OD	optical density
ORF	open reading frame
p	pico (10-12)
p	p-value for statistical analysis
PBS	phosphate buffered saline
PCR	polymerase chain reaction
PFA	paraformaldehyde
PMSG	pregnant mare's serum gonadotropin
PTGS	post-transcriptional gene silencing
RISC	RNA-inducing silencing complex
RMCE	recombinase mediated cassette exchange
RNA	ribonucleic acid
RNAi	RNA interference
rpm	rounds per minute
RT	room temperature
RT-PCR	reverse transcription PCR
SDS	sodium dodecyl sulfate
sec or s	second(s)
shRNA	short hairpin RNA
siRNA	short interfering RNA
SSC	sodium saline citrate
SSRI	selective serotonin reuptake inhibitor
T	pyrimidine base thymine
Tab.	table
TAE	tris acetate with EDTA
TB	tris buffer
TBE	tris borate with EDTA
TBS	tris buffered saline
TBS(T)	tris buffered saline (with Tween)
TE	tris-EDTA
temp.	temperature
Tris	trishydroxymethyl-aminoethane
tRNA	tranfer ribonucleic acid
u	unit(s)

UTP	uracil triphosphate
UV	ultraviolet
V	volt
Vol.	volume or volumetric content
VPA	valproic acid
Wnt	wingless-type MMTV integration site family
wt	wildtype

8.1.2 Anatomical abbreviations

5	trigeminal nucleus
Acb	nucleus accumbens
Amy	amygdala
BA	basolateral nuclei, amygdala
C	cochlear nucleus
CA	field of Ammon's horn, hippocampus
CA1	CA1 region, hippocampus
CA2	CA2 region, hippocampus
CA3	CA3 region, hippocampus
CeA	central nucleus, amygdala
Cl	claustrum
Co	cerebral cortex
CPu	caudate putamen
DB	diagonal band
DG	dentate gyrus
En	endopiriform nucleus
EPl	external plexiform layer, olfactory bulb
Ge	lateral geniculate nucleus
GL	granule cell layer, cerebellum
Gl	periglomerular cell layer
Gr	granule cells, olfactory bulb
Hb	habenula (medial and lateral part)
Hy	hypothalamus
IC	inferior colliculus
LA	lateral nucleus, amygdala
LC	locus coeruleus
LS	lateral septum
LSt	lateral striatal stripe
Mi	mitral cell layer, olfactory bulb
ML	molecular cell layer, cerebellum
MM	mammillary nuclei
MS	medial septum
O	oculomotor nucleus

OB	olfactory bulb
PC	purkinje cell layer, cerebellum
PG	periaqueductal grey
Pir	piriform cortex
Pn	pontine nuclei
PnR	pontine reticular nucleus
PT	pretectal nucleus
R	red nucleus
Ra	raphe nuclei
Rt	formatio reticularis
SN	substantia nigra
SNC	substantia nigra pars compacta
SNR	substantia nigra pars reticulata
SO	superior olive
Su	superior colliculus
Tg	tegmental nuclei
Th	thalamus
Tu	olfactory tubercle
Tz	trapezoid body
VT	ventral tegmental area
ZI	zona incerta

8.2 Supplementary data from behavior analyses

8.2.1 Data sheet from mHB analysis of Braf mice

	control		mutant		male + female		ANOVA		
Parameter	**male** (n=11)	**female** (n=15)	**male** (n=16)	**female** (n=11)	**control** (n=26)	**mutant** (n=27)	**sex**	**genotype**	**sex x genotype**
Absolute meander (degrees/sec)	17.77 ± 0.99	17.03 ± 1.32	15.93 ± 1.32	14.85 ± 1.88	17.35 ± 0.84	15.47 ± 1.09	ns	ns	ns
Angular velocity (degrees/sec)	181.27 ± 11.35	176.72 ± 23.04	151.46 ± 6.4	141.74 ± 5.12	178.72 ± 13.59	147.3 ± 4.29	ns	p<0.05	ns
Board entry (frequency)	6.18 ± 1.3	7.6 ± 0.97	9.33 ± 1.53	8.27 ± 2.1	7 ± 0.78	8.88 ± 1.23	ns	ns	ns
Board entry (latency)	96.93 ± 26.89	53.85 ± 9.08	39.13 ± 6.29	46.43 ± 8.96	72.08 ± 12.93	42.22 ± 5.18	ns	p<0.05	ns
Board entry (maximum duration, sec)	9.24 ± 1.3	8.95 ± 1.05	11.74 ± 3.1	9.94 ± 2.39	9.08 ± 0.8	10.97 ± 2.02	ns	ns	ns
Board entry (total duration, %)	8.71 ± 1.58	9.91 ± 1.55	9.29 ± 1.95	7.16 ± 1.51	9.4 ± 1.1	8.39 ± 1.29	ns	ns	ns
Defecation (frequency)	0.36 ± 0.28	0.2 ± 0.14	0.8 ± 0.24	0.82 ± 0.4	0.27 ± 0.14	0.81 ± 0.21	ns	p<0.05	ns
Defecation (latency)	279.79 ± 13.93	279.52 ± 15.93	198.15 ± 29.62	214.53 ± 37.17	279.63 ± 10.72	205.08 ± 22.8	ns	p<0.01	ns
Grooming (frequency)	1.36 ± 0.41	2.4 ± 0.83	1.93 ± 0.41	4.45 ± 1.34	1.96 ± 0.51	3 ± 0.65	p=0.05	p=0.08	ns
Grooming (latency)	176.86 ± 27.95	191.48 ± 26.27	126.79 ± 25.71	116.4 ± 24.21	185.3 ± 18.9	122.39 ± 17.71	ns	p<0.05	ns
Grooming (total duration, %)	0.59 ± 0.27	2.81 ± 1.44	8.98 ± 3.18	9.08 ± 3.97	1.87 ± 0.86	9.02 ± 2.44	ns	p<0.01	ns
Group contact (frequency)	20.09 ± 2.52	19.27 ± 2.4	27.27 ± 3.19	29.18 ± 3.7	19.62 ± 1.72	28.08 ± 2.37	ns	p<0.01	ns

	control		mutant		male + female		ANOVA		
Parameter	**male** (n=11)	**female** (n=15)	**male** (n=16)	**female** (n=11)	**control** (n=26)	**mutant** (n=27)	**sex**	**genotype**	**sex x genotype**
Group contact (latency)	15.65 ± 3.12	20.17 ± 3.09	27.37 ± 7.62	38.22 ± 14.33	18.26 ± 2.22	31.96 ± 7.39	ns	p=0.07	ns
Group contact (total duration, %)	12.03 ± 2.48	10.73 ± 1.5	17.71 ± 3.1	10.33 ± 1.1	11.28 ± 1.33	14.59 ± 1.96	ns	ns	ns
Hole exploration (frequency)	44.64 ± 6.3	45.73 ± 4.92	41.13 ± 4.52	26 ± 3.84	45.27 ± 3.81	34.73 ± 3.37	ns	p=0.07	ns
Hole exploration (latency)	16.02 ± 8.48	12.25 ± 2.62	14.63 ± 4.17	13.4 ± 2.82	13.85 ± 3.81	14.11 ± 2.64	ns	ns	ns
Line crossing (frequency)	127.45 ± 8.83	127.4 ± 6.45	131.2 ± 20.48	192.09 ± 46.22	127.42 ± 5.16	156.96 ± 23.09	ns	ns	ns
Line crossing (latency)	0.84 ± 0.06	1.7 ± 0.67	3.69 ± 1.2	2.77 ± 0.88	1.33 ± 0.39	3.3 ± 0.78	ns	p<0.05	ns
Maximum velocity (cm/sec)	57.86 ± 3.57	60.94 ± 2.37	74.52 ± 3.92	83.32 ± 5.65	59.58 ± 2.03	78.29 ± 3.34	ns	p<0.001	ns
Mean distance to board (cm)	8.03 ± 0.25	7.86 ± 0.2	9.59 ± 0.29	10.22 ± 0.41	7.93 ± 0.15	9.86 ± 0.25	ns	p<0.001	ns
Mean distance to wall (cm)	7.56 ± 0.33	7.88 ± 0.3	6.49 ± 0.38	5.56 ± 0.57	7.74 ± 0.22	6.09 ± 0.33	ns	p<0.001	ns
Mean turn angle (degrees)	27.02 ± 1.54	26.01 ± 2.19	24.46 ± 1.55	23.61 ± 2.16	26.46 ± 1.38	24.1 ± 1.26	ns	ns	ns
Mean velocity (cm/sec)	18.77 ± 0.68	19.52 ± 0.51	24.64 ± 1.71	29.95 ± 3.42	19.19 ± 0.41	26.92 ± 1.8	ns	p<0.001	ns
Rearing on board (frequency)	0.64 ± 0.24	0.67 ± 0.25	0 ± 0	0 ± 0	0.65 ± 0.17	0 ± 0	ns	p<0.001	ns
Rearing on board (latency)	272.77 ± 10.15	260.29 ± 16.33	300 ± 0	300 ± 0	265.57 ± 10.25	300 ± 0	ns	p<0.01	ns
Rearings in box (frequency)	32.18 ± 3.28	29.93 ± 2.11	14.4 ± 2.14	10 ± 1.59	30.88 ± 1.82	12.54 ± 1.45	ns	p<0.001	ns

	control		mutant		male + female		ANOVA		
Parameter	**male** (n=11)	**female** (n=15)	**male** (n=16)	**female** (n=11)	**control** (n=26)	**mutant** (n=27)	**sex**	**genotype**	**sex x genotype**
Rearings in box (latency)	31.03 ± 5.33	29.25 ± 2.79	59.23 ± 13.43	44.3 ± 8.25	30 ± 2.71	52.91 ± 8.48	ns	p<0.05	ns
Total distance moved (cm)	3097.96 ± 181.11	3159.45 ± 148.95	3296.44 ± 430.41	4503.44 ± 933.93	3132.39 ± 113.06	3813.73 ± 473.62	ns	ns	ns
Turns (frequency)	1633.82 ± 64.59	1635.07 ± 61.42	1341.13 ± 124.46	1489.58 ± 186.46	1634.52 ± 43.69	1404.75 ± 105.77	ns	p=0.08	ns
Familiar object exploration (frequency)	8.73 ± 1.05	7.73 ± 0.62	4.33 ± 0.71	3.45 ± 0.43	8.15 ± 0.57	3.96 ± 0.45	ns	p<0.001	ns
Familiar object exploration (latency)	16.6 ± 2.37	30.63 ± 8.31	109.23 ± 22.39	115.29 ± 26.8	24.7 ± 5.02	111.79 ± 16.85	ns	p<0.001	ns
Familiar object exploration (total duration, %)	0.78 ± 0.1	1.22 ± 0.21	1.3 ± 0.38	1.42 ± 0.47	1.03 ± 0.13	1.35 ± 0.29	ns	ns	ns
Unfamiliar object exploration (frequency)	7.45 ± 0.85	6.33 ± 0.47	2.27 ± 0.4	1.91 ± 0.58	6.81 ± 0.45	2.12 ± 0.33	ns	p<0.001	ns
Unfamiliar object exploration (latency)	21.45 ± 4.56	34.76 ± 14.67	111.75 ± 27.74	145.1 ± 32.63	29.13 ± 8.65	125.86 ± 20.97	ns	p<0.001	ns
Unfamiliar object exploration (total duration, %)	1.24 ± 0.19	1.66 ± 0.3	0.55 ± 0.14	0.36 ± 0.14	1.48 ± 0.19	0.47 ± 0.1	ns	p<0.001	ns
Object index	0.2 ± 0.06	0.12 ± 0.09	-0.38 ± 0.1	-0.49 ± 0.14	0.16 ± 0.06	-0.42 ± 0.08	ns	p<0.001	ns

8.2.2 Data sheet from mHB analysis of shMek1/2 mice

Parameter	control		mutant		male + female		ANOVA		
	male (n=7)	female (n=8)	male (n=13)	female (n=14)	control (n=15)	mutant (n=27)	sex	genotype	sex x genotype
Absolute meander (degrees/sec)	34.66 ± 5.85	24.52 ± 2.52	28.08 ± 3.07	25 ± 1.32	29.25 ± 3.22	26.48 ± 1.62	p=0.07	ns	ns
Angular velocity (degrees/sec)	315.02 ± 43.61	224.49 ± 29.8	192.95 ± 14.09	208.93 ± 14.39	266.74 ± 27.62	201.23 ± 10.01	ns	p<0.05	p<0.05
Board entry (frequency)	2.57 ± 1.09	5.75 ± 3.92	4.54 ± 1.34	6.29 ± 1.03	4.27 ± 2.12	5.44 ± 0.84	ns	ns	ns
Board entry (latency)	186.57 ± 41.67	164.9 ± 36.56	160.31 ± 32.25	96.64 ± 22.44	175.01 ± 26.69	127.29 ± 20.02	ns	ns	ns
Board entry (maximum duration, sec)	4.66 ± 1.76	3.69 ± 0.93	7.82 ± 1.58	11.25 ± 1.53	4.14 ± 0.93	9.6 ± 1.13	ns	p<0.01	ns
Board entry (total duration, %)	3.35 ± 1.17	4.03 ± 2.33	5.17 ± 1.19	9.38 ± 1.49	3.71 ± 1.31	7.35 ± 1.03	ns	p<0.05	ns
Defecation (frequency)	0.43 ± 0.3	1 ± 0.42	1 ± 0.32	1.07 ± 0.43	0.73 ± 0.27	1.04 ± 0.26	ns	ns	ns
Defecation (latency)	266.86 ± 23.59	251.65 ± 24.22	190.21 ± 32.8	222.77 ± 26.52	258.75 ± 16.49	207.09 ± 20.77	ns	ns	ns
Grooming (frequency)	5 ± 1.11	4.38 ± 0.89	3.92 ± 1.22	3.57 ± 0.42	4.67 ± 0.68	3.74 ± 0.61	ns	ns	ns
Grooming (latency)	113 ± 27.82	80.59 ± 3.65	97.18 ± 14.97	84.13 ± 9.37	95.71 ± 13.3	90.41 ± 8.61	ns	ns	ns
Grooming (total duration %)	3.57 ± 0.61	3.43 ± 0.6	2.8 ± 0.47	2.97 ± 0.44	3.5 ± 0.42	2.89 ± 0.32	ns	ns	ns
Hole exploration (frequency)	28 ± 6.32	38.25 ± 14.72	36.23 ± 6.67	51.29 ± 6.34	33.47 ± 8.22	44.04 ± 4.74	ns	ns	ns
Hole exploration (latency)	28.6 ± 8.94	22.78 ± 4.68	60.21 ± 28.91	29.79 ± 12.29	25.49 ± 4.73	44.44 ± 15.29	ns	ns	ns

Parameter	control		mutant		male + female		ANOVA		
	male (n=7)	female (n=8)	male (n=13)	female (n=14)	control (n=15)	mutant (n=27)	sex	genotype	sex x genotype
Line crossing (frequency)	74.57 ± 9.9	92.5 ± 11.12	72.54 ± 10.49	79.57 ± 6.7	84.13 ± 7.63	76.19 ± 6.05	ns	ns	ns
Line crossing (latency)	11.19 ± 1.24	10.23 ± 1.72	55.55 ± 30.15	8.76 ± 1.68	10.67 ± 1.05	31.29 ± 14.96	ns	ns	ns
Maximum velocity (cm/sec)	65.74 ± 5.85	61.35 ± 4.08	49.32 ± 2.59	53.7 ± 2.56	63.4 ± 3.41	51.59 ± 1.84	ns	p<0.01	ns
Mean distance to board (cm)	10.15 ± 0.77	9.71 ± 0.65	9.73 ± 0.46	9.02 ± 0.31	9.91 ± 0.48	9.36 ± 0.28	ns	ns	ns
Mean distance to wall (cm)	5.42 ± 0.63	5.7 ± 0.78	5.98 ± 0.45	6.87 ± 0.39	5.57 ± 0.49	6.44 ± 0.3	ns	ns	ns
Mean turn angle (degrees)	49.8 ± 7.63	35.55 ± 3.86	38.17 ± 3.75	35.3 ± 1.9	42.2 ± 4.39	36.68 ± 2.04	ns	ns	ns
Mean velocity (cm/sec)	13.79 ± 1.15	16.89 ± 1.19	14.61 ± 0.97	15.3 ± 0.54	15.44 ± 0.9	14.97 ± 0.54	ns	ns	ns
Rearing on board (frequency)	0.43 ± 0.2	1.13 ± 0.99	1.62 ± 0.58	2.64 ± 0.6	0.8 ± 0.53	2.15 ± 0.42	ns	p=0.05	ns
Rearing on board (latency)	275.16 ± 14.1	259.45 ± 26.57	237.17 ± 25.72	199.47 ± 25.66	266.78 ± 15.24	217.62 ± 18.2	ns	p=0.07	ns
Rearings in box (frequency)	37.86 ± 4.93	43.75 ± 8.29	49.62 ± 6.57	61.86 ± 4.97	41 ± 4.88	55.96 ± 4.18	ns	p<0.05	ns
Rearings in box (latency)	29.59 ± 6.09	18.65 ± 3.2	23.07 ± 3.96	15.67 ± 1.98	23.75 ± 3.5	19.23 ± 2.24	p<0.05	ns	ns
Risk assessment (frequency)	0.29 ± 0.18	0.13 ± 0.13	0.4 ± 0.39	0.07 ± 0.07	0.2 ± 0.11	0.26 ± 0.19	ns	ns	ns
Risk assessment (latency)	218.09 ± 52.88	264.84 ± 35.16	258.14 ± 28.42	279.04 ± 20.96	243.02 ± 30.46	268.97 ± 17.25	ns	ns	ns
Total distance moved (cm)	1933.17 ± 334.29	2442.82 ± 342.76	2018.18 ± 190.48	2241.9 ± 145.38	2204.98 ± 241.45	2134.18 ± 118.42	ns	ns	ns

Parameter	control		mutant		male + female		ANOVA		
	male (n=7)	**female** (n=8)	**male** (n=13)	**female** (n=14)	**control** (n=15)	**mutant** (n=27)	**sex**	**genotype**	**sex x genotype**
Turns (frequency)	1134 ± 194.36	1329.5 ± 135.4	1194.54 ± 96.21	1308.79 ± 71.71	1238.27 ± 114.56	1253.78 ± 59.29	ns	ns	ns
Familiar object exploration (frequency)	8 ± 1.7	5.75 ± 0.92	6 ± 0.96	6.79 ± 0.82	6.8 ± 0.95	6.41 ± 0.62	ns	ns	ns
Familiar object exploration (latency)	59.76 ± 12.77	67.49 ± 14.84	115.44 ± 30.59	64.09 ± 11.1	63.88 ± 9.61	88.8 ± 16.29	ns	ns	ns
Familiar object exploration (total duration, %)	1.27 ± 0.28	1.05 ± 0.19	1.06 ± 0.19	1.17 ± 0.14	1.15 ± 0.16	1.12 ± 0.11	ns	ns	ns
Unfamiliar object exploration (frequency)	5.14 ± 1.34	6.63 ± 1.46	5.69 ± 1.36	6.57 ± 0.71	5.93 ± 0.98	6.15 ± 0.74	ns	ns	ns
Unfamiliar object exploration (latency)	69.31 ± 9.19	76.58 ± 34.36	112.32 ± 30.97	58.2 ± 13.01	73.19 ± 18.24	84.26 ± 16.88	ns	ns	ns
Unfamiliar object exploration (total duration, %)	1.21 ± 0.27	1.27 ± 0.32	1.44 ± 0.38	1.4 ± 0.16	1.24 ± 0.21	1.42 ± 0.2	ns	ns	ns
Object index	-0.01 ± 0.11	-0.06 ± 0.19	0.02 ± 0.13	0.09 ± 0.07	-0.03 ± 0.11	0.06 ± 0.07	ns	ns	ns